

# Flood protection and marine power in the Wash Estuary, United Kingdom

*Technical and economical feasibility study*

Appendices



Delft University of Technology  
Faculty of Civil Engineering and Geosciences  
Department of Hydraulic Engineering  
In association with  
Royal Haskoning Rotterdam  
Department Coastal & Rivers



Bram Hofschreuder  
Delft, May 23<sup>th</sup> 2012

Courtesy cover photo: John Watson.

# Flood protection and marine power in the Wash Estuary, United Kingdom

*Technical and economical feasibility study*

Appendices

Graduation student: Bram Hofschreuder  
Student number 1401661  
b.hofschreuder@student.tudelft.nl

Graduation Committee:  
Prof. dr.ir. J.K. Vrijling TU Delft, Department of Hydraulic Engineering  
Ir. W.F. Molenaar TU Delft, Department of Hydraulic Engineering  
Dr. ir. R. J. Labeur TU Delft, Department of Hydraulic Engineering  
Ir. L.F. Mooyaart Royal Haskoning Rotterdam, Coastal & Rivers

Delft University of Technology  
Faculty of Civil Engineering and Geosciences  
Department of Hydraulic Engineering  
In association with  
Royal Haskoning Rotterdam  
Department Coastal & Rivers



Version 2  
Delft, May 23<sup>th</sup> 2012



## TABLE OF CONTENTS

Appendix 1: geology and bottom sediments

Appendix 2: land reclamation areas bordering the Wash estuary

Appendix 3: locations of mussel and cockle beds in the Wash estuary through the years

Appendix 4: nature protection areas

Appendix 5: astronomical tide and shallow water tides

Appendix 6: predicted tidal signals in the Wash estuary

Appendix 7: asymmetry of the vertical tide in the Wash estuary

Appendix 8: analysis of extremes

Appendix 9: extreme offshore wave and wind conditions

*9.1: monthly distribution of significant wave height*

*9.2: monthly distribution of wind speed*

Appendix 10: analysis of the UK's energy market

Appendix 11: top views and longitudinal cross-sections navigation locks

*11.1: commercial navigation lock*

*11.2: recreational navigation lock*

Appendix 12: preliminary design tidal power plant

*12.1: determination of the discharge coefficient for a single turbine*

Appendix 13: determination of the discharge coefficient for a single sluice

Appendix 14: estimation construction costs

*14.1: embankment dam*

*14.2: caisson dam*

*14.3: final conceptual design*

Appendix 15: storage basin approach

## Appendix 16: final conceptual design

*16.1: Boston Deeps*

*16.2: Lynn Deeps*

## Appendix 17: economic analysis

*17.1: credit estimate Wash barrier and tidal power plant*

*17.2: discounted value of the expenses*

*17.3: discounted value of the revenues of energy*

*17.4: discounted value of the revenues of improved flood protection*

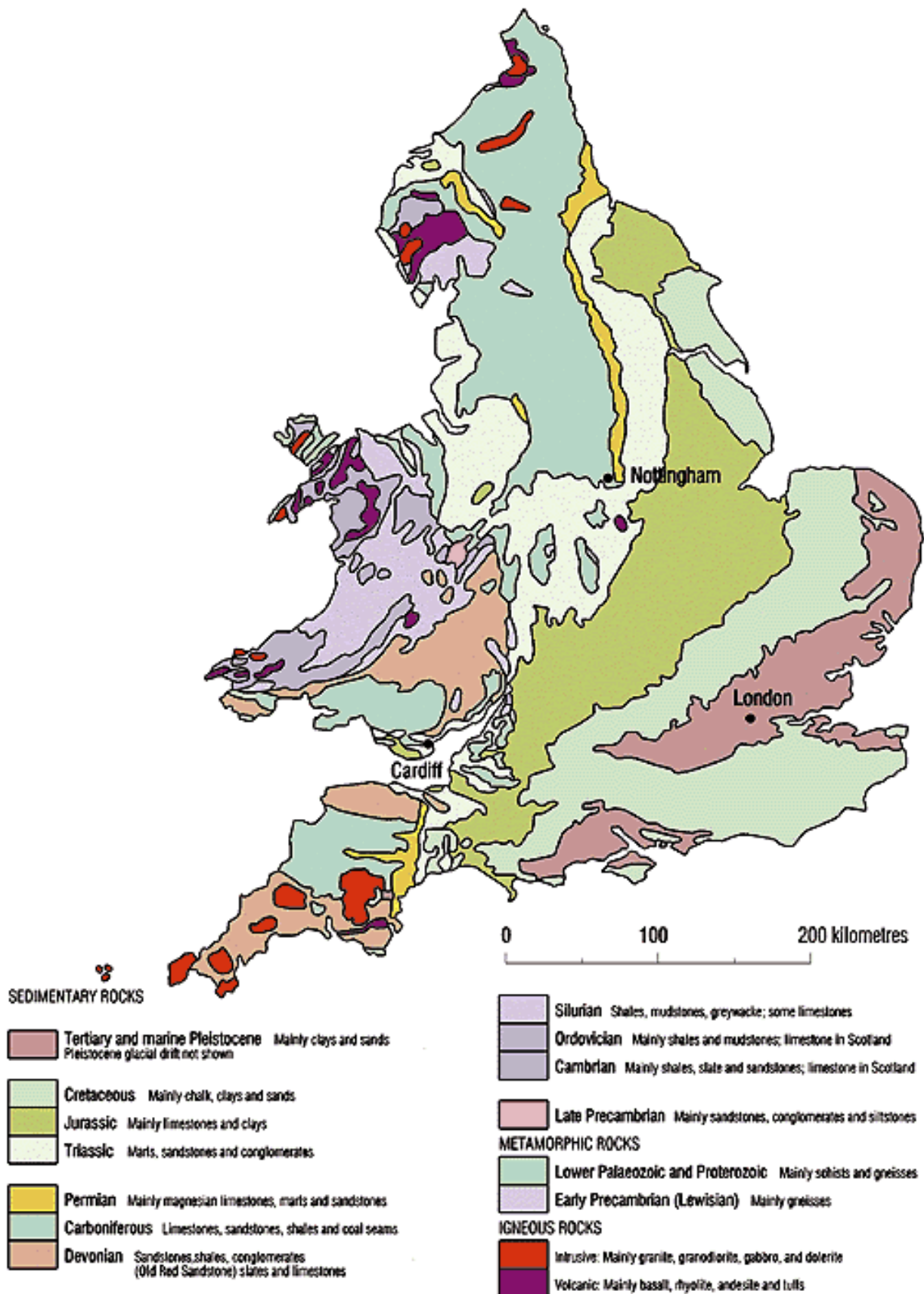
## APPENDICES



# **Appendix 1**

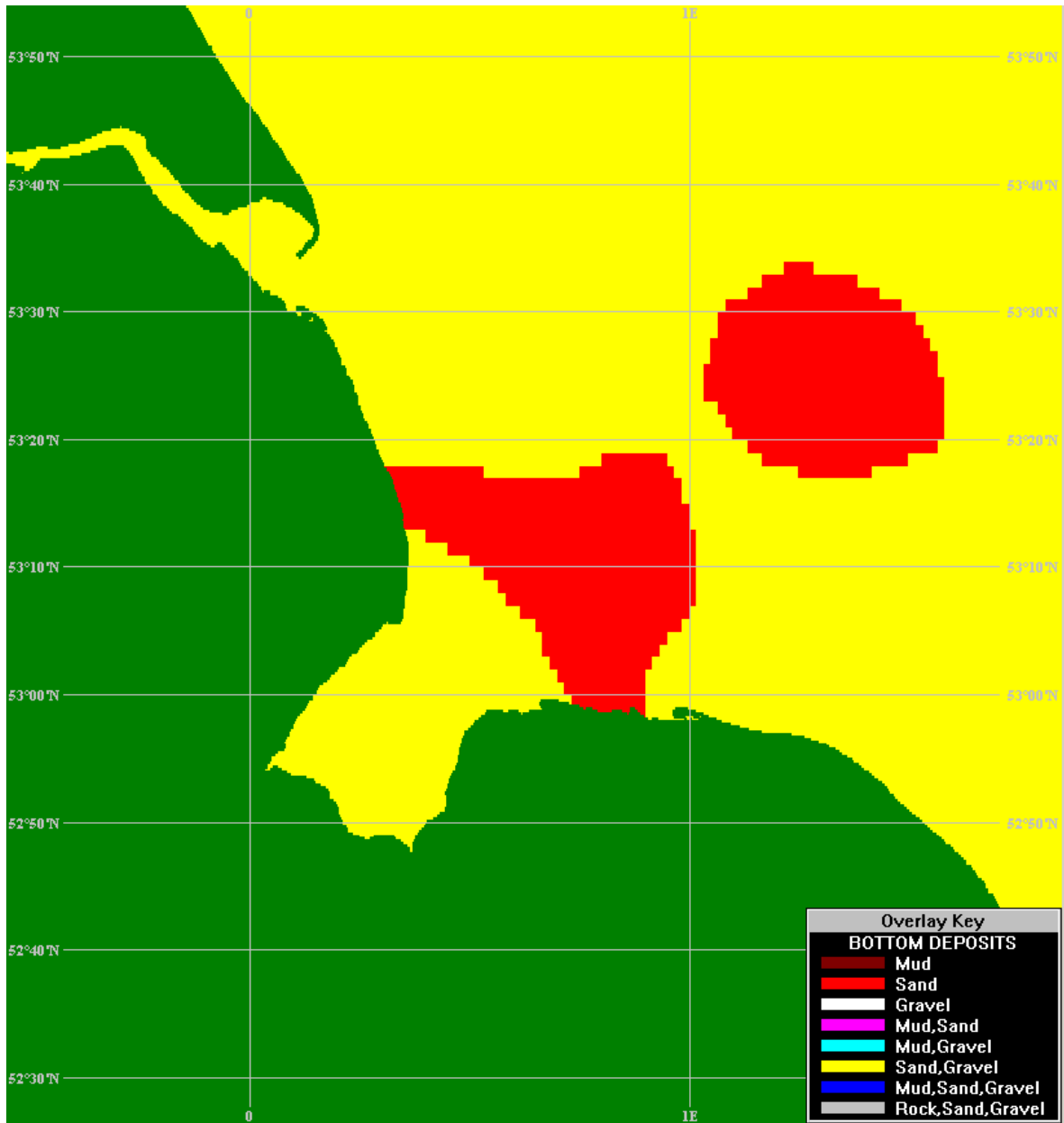
## *Geology and bottom sediments*





Geological structure of England and Wales  
(Courtesy: the British Geological Survey ©NERC 1995. All rights reserved)





Bottom deposits within the Wash estuary.

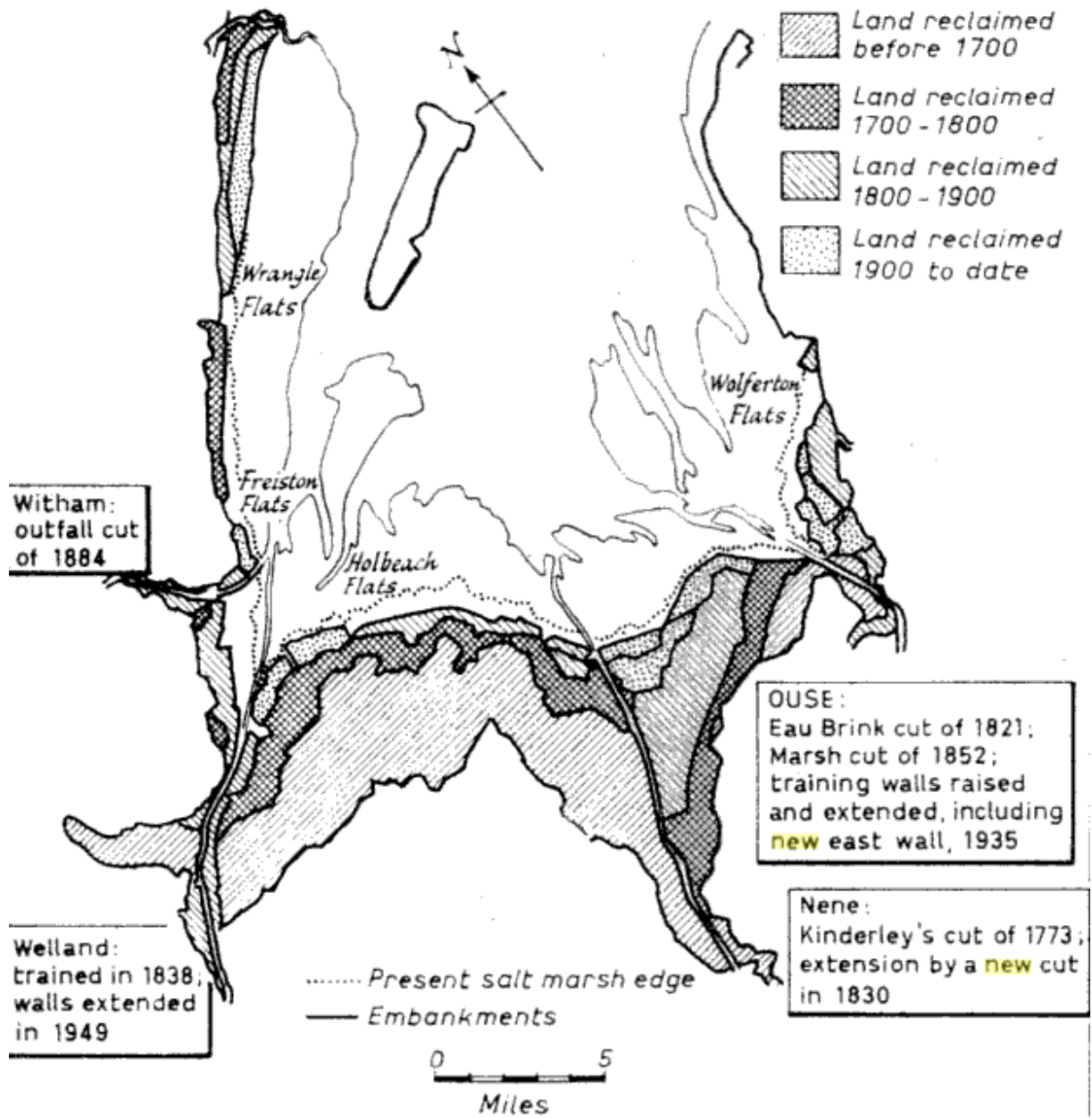
(Courtesy: *United Kingdom Digital Marine Atlas, Natural Environmental Research Council, 1998*)



## **Appendix 2**

*Land reclamations bordering the Wash estuary*





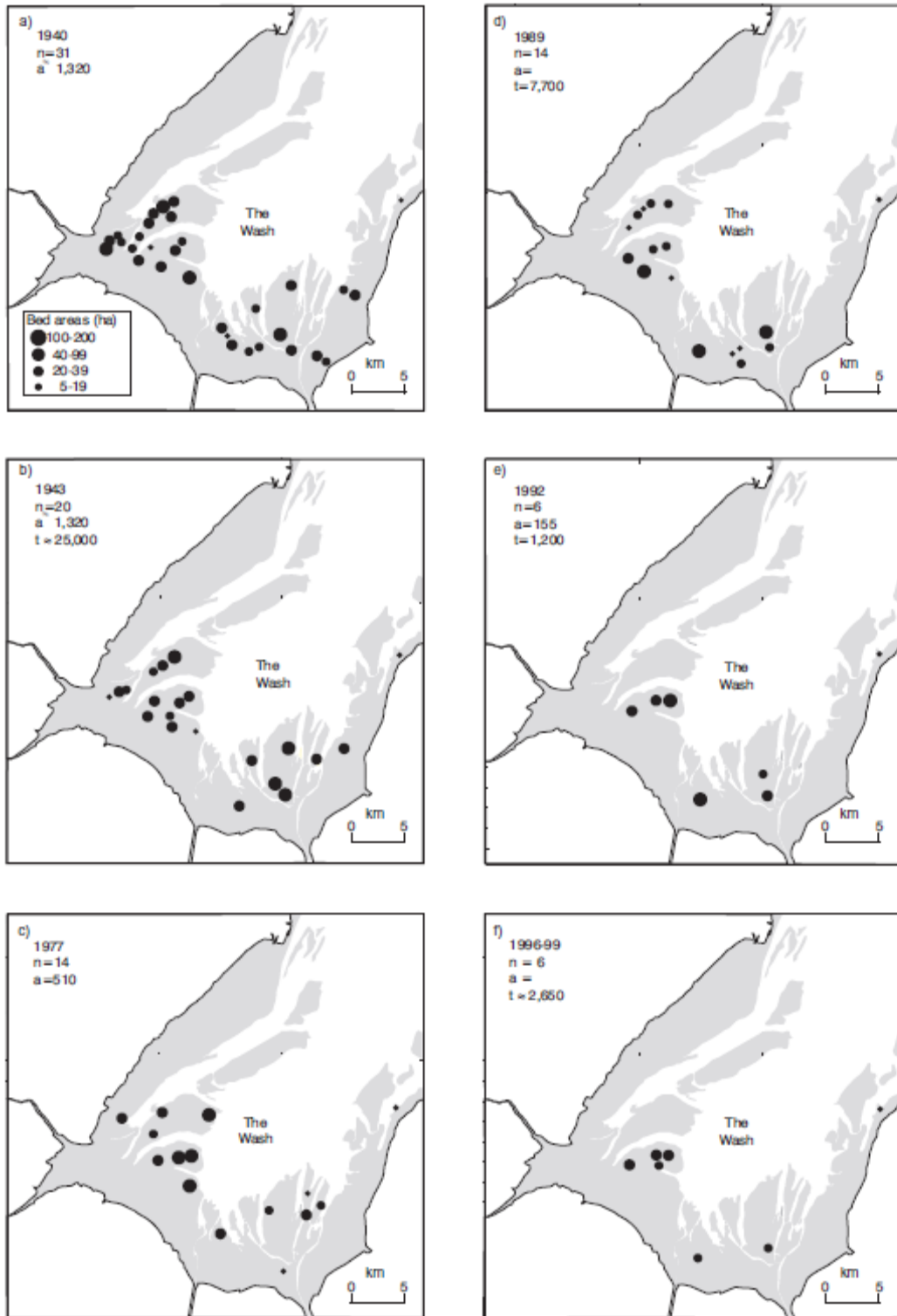
Source: *New Scientist*, edition 6-9-1962, article "The old coastline of the Wash" by F.T.J. Kestner, Hydraulic research station, Department of Scientific and Industrial Research.



## **Appendix 3**

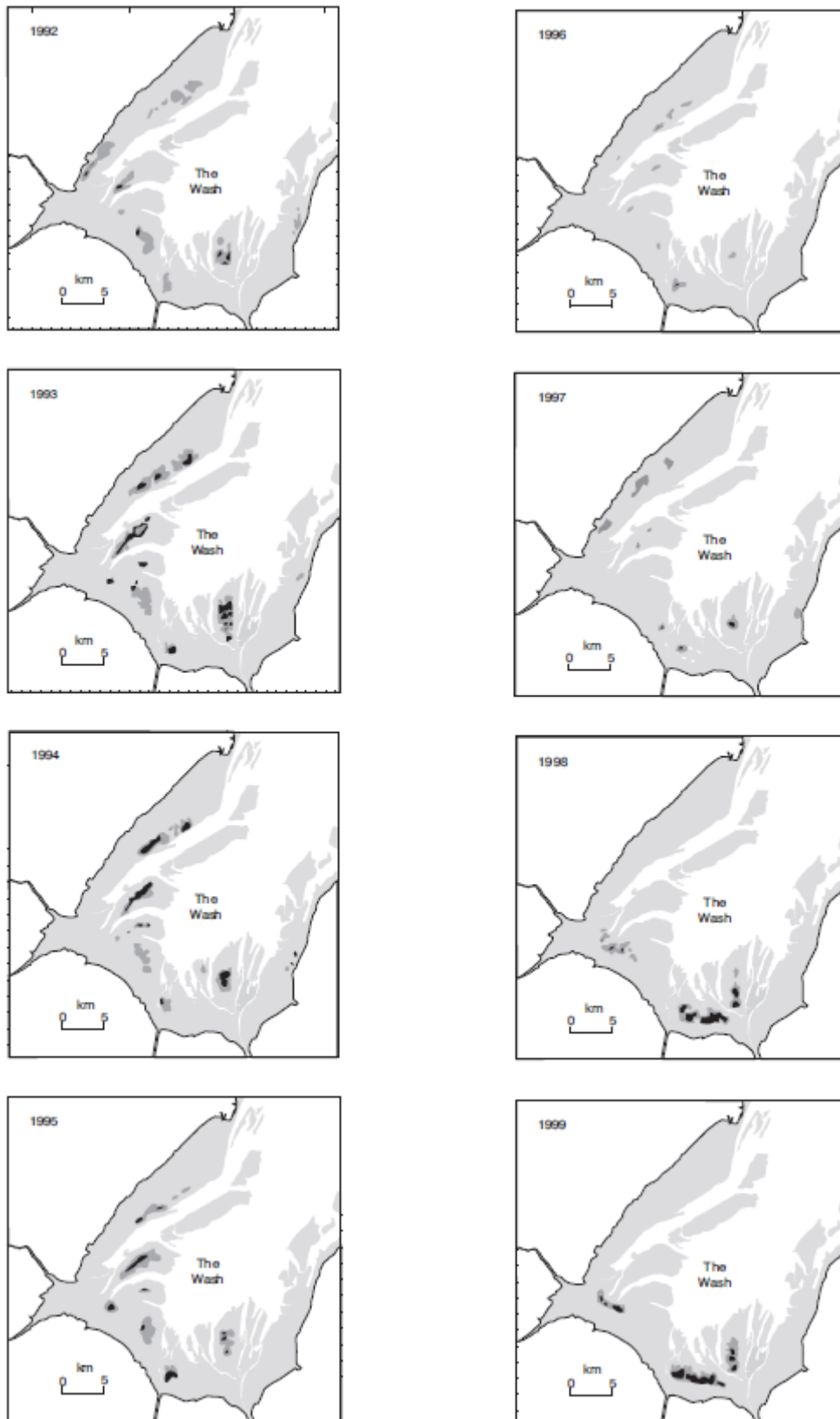
*Locations of mussel and cockle beds in the Wash estuary  
through the years*





Location of mussel beds in the Wash estuary through the years [Dare, 2004].





Location of cockle beds in the Wash estuary through the years [Dare, 2004].  
Black shading :  $> 100$  cockles/m<sup>2</sup>; grey shading: 10-99 cockles/m<sup>2</sup>.



## **Appendix 4**

### *Nature protection areas*





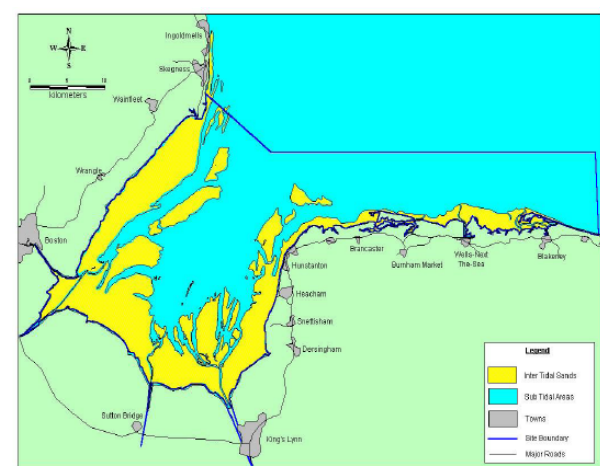
Ramsar sites in Norfolk and Lincolnshire.  
(Courtesy: Environmental resources Management)



SPA sites in Norfolk and Lincolnshire.  
(Courtesy: Environmental resources Management)

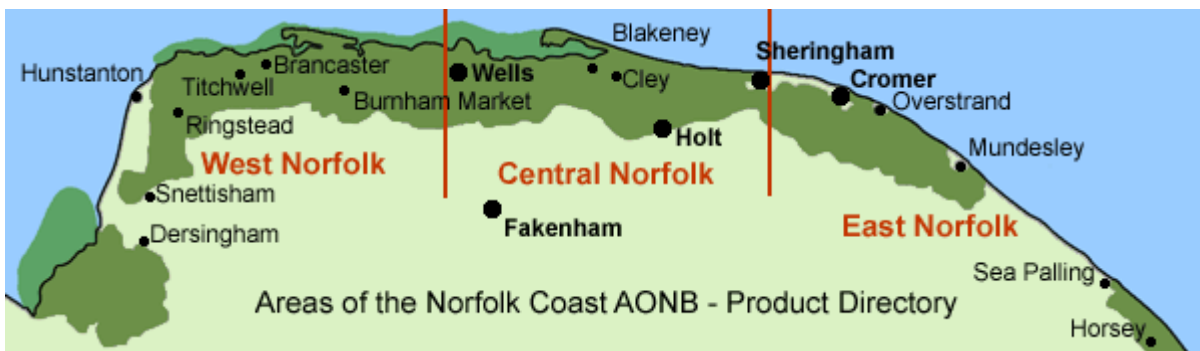


SAC sites in Norfolk and Lincolnshire.  
(Courtesy: Environmental resources Management)



EMS site in Norfolk and Lincolnshire.  
(Courtesy: The Wash and North Norfolk Coast Site Plan, November 2010)

- SPA : Special Protection Area
- SAC : Special Area of Conservation
- EMS : European Marine Sites



Areas of Outstanding Natural Beauty in Wash estuary and along the North Norfolk Coast.  
(Courtesy: Norfolk Coast Partnership)



## **Appendix 5**

*Astronomical tide and shallow water tides*



## 5.1 Astronomical tide

The forces involved in the generation of the astronomical tide originate from the gravitational pull caused by the rotation of the earth-moon system around a common centre of gravity *and* the rotation of the sun-earth system around their common centre of gravity. The astronomical tides or ocean tides are generated as a result of the differences between the gravitational pull on the ocean water masses located at different distances from both moon and sun. In box 1 the derivation of this tide generating force, or differential pull, is presented. Newton's equilibrium theory of tides<sup>1</sup> will be used to explain some tidal phenomena, namely the daily inequality, the spring and neap tide cycle and the main tidal constituents.

### Box 1: tide generating force or differential pull.

Newton's Law of gravitation states: 
$$F = G \cdot \frac{m_1 \cdot m_2}{r^2} \quad (5.1)$$

Where F is the force between the masses [N], G is the gravitational constant [Nm<sup>2</sup>/kg<sup>2</sup>], m<sub>1</sub> is the first mass [kg], m<sub>2</sub> is the second mass [kg] and r is the distance between the masses [m].

The gravitational pull of the moon on 1 kg of mass on earth, using the distance between the centres of gravity of both earth and moon, is:

$$F_{E-M} = M_E \cdot a_{E-M} = G \cdot \frac{M_E \cdot M_M}{r_M^2} \quad (5.2)$$

and hence 
$$a_{E-M} = G \cdot \frac{M_M}{r_M^2} = 6.67 \cdot 10^{-11} \cdot \frac{7.35 \cdot 10^{22}}{(3.84 \cdot 10^8)^2} = 3.32 \cdot 10^{-5} = 3.38 \cdot 10^{-6} \cdot g \quad (5.3)$$

Where: F<sub>E-M</sub> is the gravitational pull of the moon on 1 kg of mass on earth [N], M<sub>E</sub> is the mass on earth [1 kg], a<sub>E-M</sub> is the gravitational acceleration of the centre of the earth in the earth-moon system [m/s<sup>2</sup>], M<sub>M</sub> is the mass of the moon [kg], r<sub>M</sub> is the distance between the centres of earth and moon [m] and g is the gravitational acceleration of earth itself at the earth's surface [m/s<sup>2</sup>].

Similarly for the sun:

$$a_{E-S} = G \cdot \frac{M_S}{r_S^2} = 6.67 \cdot 10^{-11} \cdot \frac{1.99 \cdot 10^{30}}{(1.5 \cdot 10^{11})^2} = 5.90 \cdot 10^{-3} = 6.01 \cdot 10^{-4} \cdot g \quad (5.4)$$

Where: F<sub>E-S</sub> is the gravitational pull of the sun on 1 kg of mass on earth [N], a<sub>E-M</sub> is the gravitational acceleration of the centre of the earth in the earth-sun system [m/s<sup>2</sup>], M<sub>S</sub> is the mass of the sun [kg] and r<sub>S</sub> is the distance between the centres of earth and sun [m].

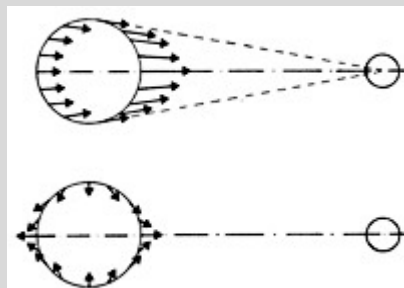


Figure 5.1: tidal forcing.

The upper image of figure 5.1 shows the gravitational pull of the moon on the earth. As can be seen the distance between the centre of the attracting body (moon or sun) varies slightly for different locations at the earth's surface, hence nowhere on earth is the gravitational acceleration exactly equal to the gravitational acceleration of the centre of gravity of the earth in respectively the earth- moon or earth- sun system. These differences in gravitational pull along earth's surface is known as the differential pull (see lower image in figure 5.1) and this phenomenon is responsible for the generation of the astrological tides.

<sup>1</sup> Newton made the following assumptions in his theory: 1) the Earth is entirely covered by water, 2) the water surface responds immediately to the forcing, 3) the presence of the continents is neglected.

Computing this differential pull ( $\Delta a_{E-M}$ ) on 1 kg of mass situated on the earth's near side of the moon can be done as follows:

$$\Delta a_{E-M} = a_{E-M_{ns}} - a_{E-M} = G \cdot \frac{M_M}{(r_M - R_E)^2} - G \cdot \frac{M_M}{r_M^2} \approx 2 \cdot G \cdot \frac{M_M \cdot R_E}{r_M^3} = 1.13 \cdot 10^{-7} \cdot g \quad (5.5)$$

Similarly for the sun:

$$\Delta a_{E-S} = a_{E-S_{ns}} - a_{E-S} = G \cdot \frac{M_S}{(r_S - R_E)^2} - G \cdot \frac{M_S}{r_S^2} \approx 2 \cdot G \cdot \frac{M_S \cdot R_E}{r_S^3} = 0.515 \cdot 10^{-7} \cdot g \quad (5.6)$$

Where:  $\Delta a_{E-M}$  is the differential pull of the moon on 1kg of mass on the near side of earth [ $m/s^2$ ],  $\Delta a_{E-S}$  is the differential pull of the sun on 1 kg of mass on the near side of earth [ $m/s^2$ ] and  $R_E$  is the radius of the earth [m].

From the above can be concluded that the differential pull caused by the moon is the most influential regarding

the generation of the earth's astrological tides:  $\frac{\Delta a_{E-M}}{\Delta a_{E-S} + \Delta a_{E-M}} \cdot 100\% = 69\% \quad (5.7)$

The resulting differential pull as presented in the lower image of figure 5.1 can be decomposed into components normal and parallel to the earth's surface. The normal components have a size negligible compared to the earth's own gravitational acceleration ( $g$ ). Although the components parallel to the earth's surface are of the same order of magnitude as  $g$ , they are perpendicular to the earth's gravity field and therefore shift the water mass both to the side facing the celestial body and the side opposing it, see figure 5.2. Without some opposing force all the water would pile up at either side of the earth, which is obviously not the case. The shift of the water mass is compensated for by a pressure gradient in the opposite direction that is the result of the sloping water surface, resulting in the typical ellipsoid as described in Newton's equilibrium theory of tides.

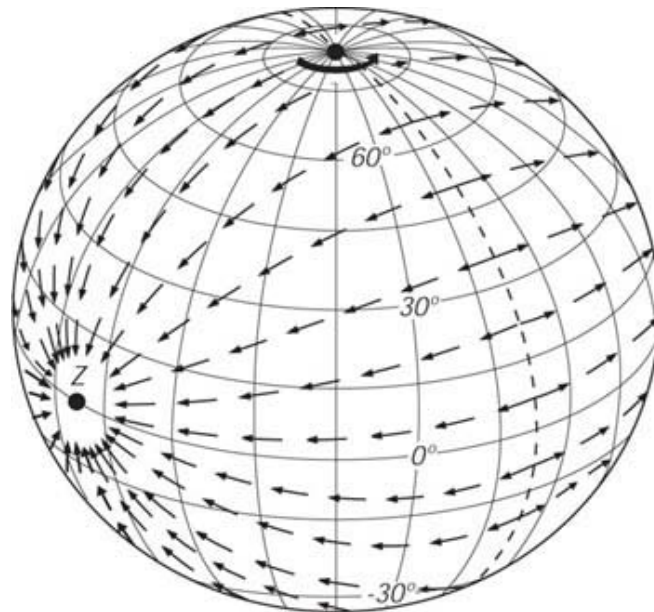


**Figure 5.2:** components of the tidal force perpendicular to the earth's gravity field, in case the celestial body is above the equator at point Z. (Courtesy: Dietrich, 1980)

### 5.1.1 Daily inequality

Until now it was implicitly assumed that the astronomical tide generating bodies stayed over the equator all the time. However in reality the orbits of the moon around the earth and the earth around the sun are not situated within the equatorial plane. This is caused by the fact that the earth axis is not perpendicular to both the earth-moon and sun-earth connection lines. The angle between the equatorial plane and these connection lines is called declination. As a result of the declination a daily inequality occurs between the two consecutive high water's and low water's, this means that the two high and low waters are not equal (except on the equator). The daily inequality increases with latitude and becomes so large at the higher latitudes that there occurs only one high and one low water per day.

But the daily inequality itself also varies with the planetary motions. The earth rotates around the sun, but its tilted axis stays in the same position. Hence the line were the sun induced tidal force is largest changes throughout one year between  $23.5^\circ$  S and  $23.5^\circ$  N, as a result the daily inequality is largest when the sun's position is furthest north or south. Therefore the sun induced astrological tide is largest in early January and early July. Within the moon's cycle around the earth, which takes 29.53 days, the daily inequality is also largest when the moon's position is furthest north or south<sup>2</sup>.

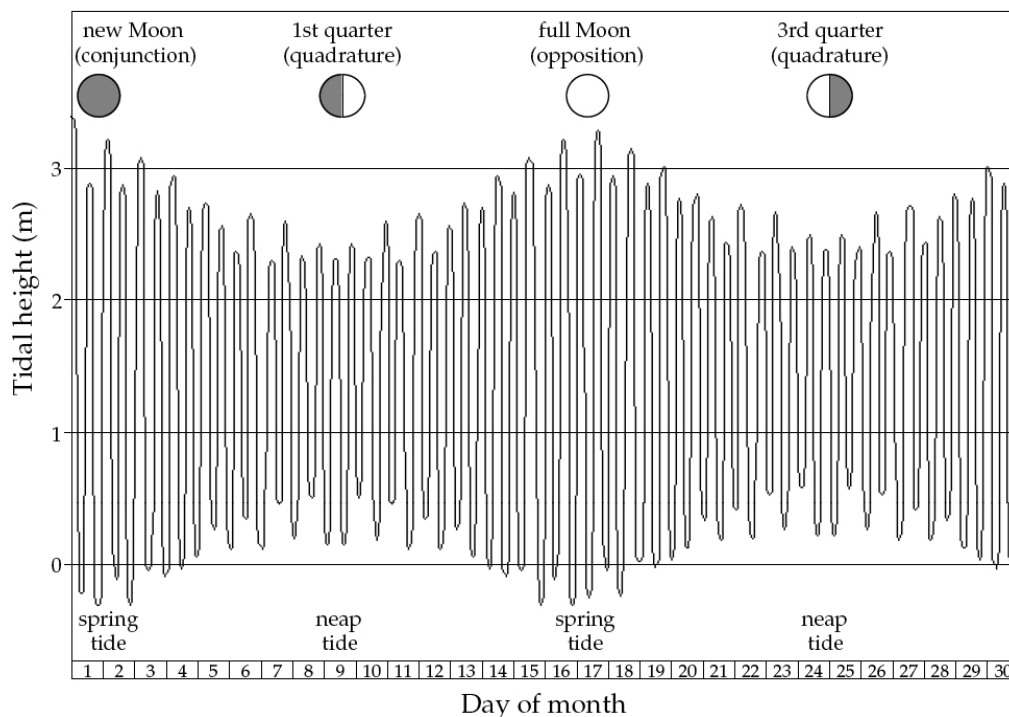


Figure 5.3: signal of spring-neap cycles during one month.

### 5.1.2 Spring and neap tide

As the earth revolves around its own axis, it rotates underneath the ellipsoid resulting in a semidiurnal tide on the earth's surface (except on the poles) that is constant for the same point every day. However both moon and sun create an ellipsoid, and their relative position changes

<sup>2</sup> The moon's declination varies between  $23.5^\circ$  S  $\pm 5^\circ$  and  $23.5^\circ$  N  $\pm 5^\circ$  in a 18.6 year cycle. The deviation of  $5^\circ$  is caused by the fact that earth's and moon's orbit are approximately in the same plane, but not quite.

in time. If moon and sun are in the same line their ellipsoids enhance each other and the tidal amplitude is increased, this is called spring tide and occurs both at new moon and full moon. When the position of moon and sun is  $90^\circ$  out of phase the combined effect of their ellipsoids approaches a circle and the amplitude of the astronomical tide is reduced, this is called neap tide and occurs both in the first and last quarter of the moon. In figure 5.3 the signal of the tidal amplitude variation during one month is depicted, the signal shows clearly the two spring-neap tide cycles. Also the daily inequality can be recognized.

During the year the amplitude of the astronomical spring-neap cycle does not remain constant, it varies as a result of the elliptic orbit of the earth-moon system around the sun *and* the elliptic orbit of the moon around the earth. First the effect of the orbit of the moon will be considered as the moon has the most influence on the generation of the astronomical tides. When the moon is in apogee the exerted gravitational pull is smallest and hence the amplitude of the lunar tide will be smallest, when the moon is at perigee the gravitational pull is largest as is the amplitude of the lunar tide. Regarding the sun a similar effect occurs, only the duration of the cycle is one year instead of one lunar month. When the earth is at aphelion the gravitational pull exerted by the sun is smallest and when at perihelion it is largest.

### 5.1.3 Tidal constituents

In the idealized situation the differential pull of moon and sun only generates the two main tidal constituents, the principal lunar and solar tides. All deviations from this idealized situation, e.g. a elliptic orbit instead of a circular orbit, the declination of the earth axis, etc., result in additional astronomical tidal constituents to the aforementioned main constituents. The eleven most dominant tidal constituents are listed in table 5.1.

Tidal constituent	Nomenclature	Equilibrium amplitude $A_i$ [m]	Period $T_i$ [h]	Radian frequency $\omega_i$ [ $10^{-4}$ /s]
<b>Semidiurnal</b>				
Principal lunar	$M_2$	0.242334	12.421	1.40519
Principal solar	$S_2$	0.112841	12.000	1.45444
Lunar elliptic	$N_2$	0.046398	12.658	1.37880
Lunisolar	$K_2$	0.030704	11.967	1.45842
<b>Diurnal</b>				
Lunisolar	$K_1$	0.141565	23.935	0.72921
Principal lunar	$O_1$	0.100514	25.819	0.67598
Principal solar	$P_1$	0.046843	24.066	0.72523
Lunar elliptic	$Q_1$	0.019256	26.868	0.64959
<b>Long period</b>				
Fortnightly	$M_f$	0.041742	327.86	0.053234
Monthly	$M_m$	0.022026	661.31	0.026392
Semi-annual	$S_{sa}$	0.019446	4383.05	0.003982

Table 5.1: principal tidal constituents [Apel, 1987].

In contrast to wind and short waves, tidal constituents have their own precise frequencies. Hence the spectrum consists of discrete lines. This characteristic of the tide makes it possible to decompose a measured tidal signal into its separate tidal constituents, its building blocks so

to speak. In paragraph 5.2 this property will be used to determine the characteristic of the tide in the North Sea offshore of the Wash estuary.

In section 5.3 physical processes causing non-linear deviations from the astronomical equilibrium tides will be discussed, resulting in the so called overtides or shallow water tides.

#### 5.1.4 Harmonic analysis

Since the harmonic constituents of the astronomical tide are the result of regular astronomical phenomena it is possible to predict the tide accurately at every location on earth, as their frequencies are known and fixed. Performing a Fourier analysis on a measured time series of water levels will result in the amplitudes and phases of the main tidal constituents on that specific location. In principle it boils down to determining amplitudes and phases.

$$\eta(t) = a_0 + \sum_{n=1}^N a_n \cdot \cos(\omega_n \cdot t - \alpha_n) \quad (5.8)$$

Were:

$\eta(t)$	: measured tidal level with reference to ordnance level	[m]
$a_0$	: mean level	[m]
$a_n$	: amplitude of constituent number n	[m]
$\omega_n$	: angular velocity of constituent number n	[rad/s]
$\alpha_n$	: phase angle of constituent number n	[rad]
$t$	: time	[s]

When the tidal constituents are known the character of the tide (diurnal, semidiurnal or mixed) at a certain location can be determined. The tidal character is defined by means of the form factor  $F$ , which is defined as the ratio of amplitudes of the sum of the two main diurnal components over the main two main semidiurnal components.

$$F = \frac{K_1 + O_1}{M_2 + S_2} \quad (5.9)$$

Were:

$F$	: form factor	[-]
$K_1$	: amplitude of the lunar-solar declinational diurnal tidal constituent	[m]
$O_1$	: amplitude of the principal lunar diurnal tidal constituent	[m]
$M_2$	: amplitude of the principal lunar semidiurnal tidal constituent	[m]
$S_2$	: amplitude of the principal solar semidiurnal tidal constituent	[m]

In table 5.2 the four tidal categories that are distinguished are shown:

Tidal category	Value for F [-]
Semidiurnal tide	0.00-0.25
Mixed tide, mainly semidiurnal	0.25-1.50
Mixed tide, mainly diurnal	1.50-3.00
Diurnal tide	> 3.00

Source: *Bosboom, 2011*.

**Table 5.2:** tidal character expressed by the form factor.

The amplitudes of the main tidal diurnal and semidiurnal components from the two closest measuring stations of the UK Tide Gauge Network are presented in table 5.3, as is the form factor.

Tidal category	M <sub>2</sub> [m]	S <sub>2</sub> [m]	K <sub>1</sub> [m]	O <sub>1</sub> [m]	F [-]
Cromer	1.568	0.533	0.145	0.158	0.14
Immingham	2.260	0.741	0.155	0.171	0.11

Source: British Oceanographic Data Centre & Proudman Oceanographic Laboratory.

Table 5.3: harmonic constants along the English east coast.

As was to be expected the tide on the North Sea in front of the Wash estuary is characterized as a semidiurnal tide. Since the mean spring tidal range is approximately 6.25 m, which is larger than 4 m, the tidal environment is characterized as a macro-tidal regime.

### 5.3 Shallow water tides

In the previous section Newton's equilibrium theory of tides has been used to explain several important concepts regarding the generation of the astronomical tide. But in reality the presence of the continents and the limited water depth in the open oceans prevent the generation of the equilibrium tide. The only place on earth where the equilibrium tide can more or less develop is in the Southern Hemisphere (65° S), because here are no land masses present. From 65° S the tidal wave propagates into the ocean basins on the Northern Hemisphere and from there into the marginal seas.

Due to differences in water depth and width restrictions caused by land masses the tidal wave becomes distorted during its journey north. However the wave period remains always the same, but the wave length changes as a result of the change in wave celerity, which in turn depends on the water depth, see equations 5.10 and 5.11. Thus as the tidal wave propagates into shallower water the wave length becomes shorter resulting in energy bunching, which causes an increase in amplitude of the tidal wave. This explains why the amplitudes of the tidal constituents along a coastline are much larger than the amplitudes of the ocean equilibrium tide stated in table 5.1.

$$L = c \cdot T \quad (5.10)$$

And

$$c = \sqrt{g \cdot d} \quad (5.11)$$

Were:

$L$	: wave length	[m]
$c$	: wave celerity	[m/s]
$T$	: wave period	[s]
$g$	: gravitational acceleration	[m/s <sup>2</sup> ]
$d$	: water depth	[m]

The shape of the North Sea basin is such that in North-South direction its length corresponds more or less with half the wave period of the tidal wave entering the basin, thus creating a standing wave pattern [Pietrzak, 2010]. As a result of earth's rotation the Coriolis acceleration

transforms the standing wave pattern into a rotary wave propagating around an amphidromic point. The vertical tide is zero in the amphidromic point and maximum along the coastline of the North Sea basin. As can be seen in figure 5.4, amplification of the tidal range along the UK coastline is particular large.

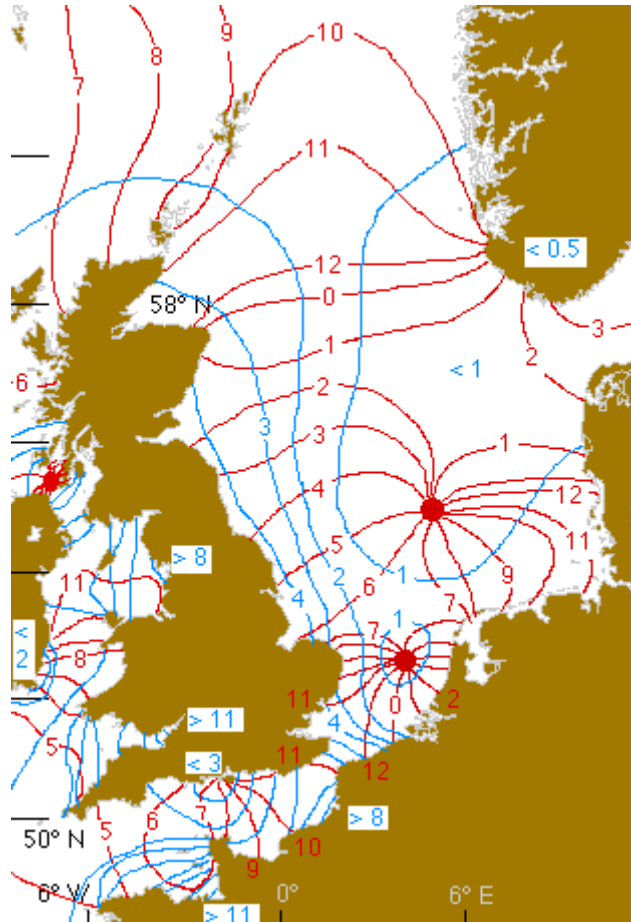


**Figure 5.4:** amphidromic systems in the North Sea basin.  
(Courtesy: M. Tomczak, Flinders university, 1996)

The red lines represent the co-phase lines (in hrs) of the  $M_2$  tidal constituent, the blue lines represent the mean tidal range at spring tide in metres (co-range lines of the sum of  $M_2$  and  $S_2$  tidal constituents).

Furthermore non-linear effects are introduced in shallow water as bottom friction becomes important because the tidal amplitude is no longer small compared to the water depth. Also the effect on the propagation speed of the tidal wave due to the difference between wave crest and trough in combination with a finite depth results in non-linear effects. Besides resonance phenomena that are the result of the basin's geometry, additional non-linear effects are caused by interactions between tidal constituents. All these non-linear effects contribute to the tidal asymmetry that is observed in shallow water signals.

The higher harmonics resulting from the processes mentioned above are not a direct result from the tide generating forces and are therefore called overtides or shallow water tides. These tidal constituents have a period that is a integer fraction of the original tidal constituents. Bottom friction induced tides have a period that is 1/3 of that of the original

constituent, e.g.  $M_2 \Rightarrow M_6$  and  $K_1 \Rightarrow K_3$ . The difference in wave speed between the crest and trough results in overtides with a period that is 1/2 of the original astronomical period, e.g.  $M_2 \Rightarrow M_4 \Rightarrow M_8$  or  $S_2 \Rightarrow S_4 \Rightarrow S_8$ . The same holds for the interactions between tidal constituents, e.g.  $M_2 + S_2 \Rightarrow MS_4$ .

Although all higher harmonics contribute to the tidal distortion in shallow water, the most important are the  $M_4$  and  $M_6$  overtides, because these contribute most (together with the  $M_2$  astronomical tidal constituent) to the tidal amplitude. Also with respect to sediment transport the overtides also play a very important role.

#### 5.4 Propagation and deformation of the tidal wave within the Wash estuary

The sea-borne tidal asymmetry is transferred into the estuary where, as a result of the further decreasing depth, non-linear effects are being enhanced, resulting in an increasing tidal asymmetry.

Some amplitude amplification is to be expected as the tide propagates into the estuary. Due to the presence of bottom friction both the incoming and reflected wave are partly damped, resulting in a wave pattern with a partly standing character and a partly propagating character. As a result of the partly standing wave character a phase difference between water level and current velocity is to be expected (current velocity leads the water level variation). Apparently damping of the tidal wave due to bottom friction has a large effect in the Wash estuary as the amplitude of the tidal wave only increases approximately 0.10 m from the mouth of the estuary to the landward side of the basin (see section 2.1.3), despite a considerable decrease in water depth towards the end of the basin.

Also the wave celerity decreases in shallower water, resulting in a shortening of the wave length as the wave period remains constant, see equations 5.10 and 5.11.

Tidal constituent	Wave period [hr]	Wave length [km]	Amplitude <sup>1)</sup> [m]
$M_2$	12.42	443	2.260
$K_1$	23.93	853	0.155
$S_2$	12.00	428	0.741
$O_1$	25.82	256	0.171

Wave celerity of all constituents is 9.9 m/s.

<sup>1)</sup> Because no data with respect to the amplitudes of the four main tidal constituents is available at the time for the tide within the Wash estuary, the data of the Immingham measuring station of the UK Tide Gauge Network is used. This station was preferred over the Cromer station since the mean tidal amplitude is closer to that of the Wash estuary. Mean tidal amplitude Immingham 4.20 m; Cromer 2.92 m.

(Source: British Oceanographic Data Centre & Proudman Oceanographic Laboratory)

**Table 5.4:** wave length and amplitude of the four major tidal constituents.

From table 5.4 can be concluded that the basin length is in the order of 1/20 of the wave length of the  $M_2$  and  $S_2$  tidal constituents, being the main tidal constituents along the English eastern shoreline. Therefore a storage basin approach can be used to describe the change in time of the water level within the future basin and also assess the influence of the barrier on the tidal amplitude behind it.

### 5.4.1 Tidal asymmetry

As described in section 2.1.2 the amplitudes of both the horizontal and vertical tide are damped progressively as a result of bottom friction, the depth decreases considerably further into the basin and the partly standing wave pattern resulted in a phase difference between the horizontal and vertical tide ( $0 < \text{phase shift} < \pi/2$ ). As a result both the vertical and horizontal tide are deformed.

The vertical and horizontal deformation of the horizontal tide are very important factors in relation to the net sediment transport processes within the Wash estuary. The horizontal deformation of the horizontal tide results in a skewed velocity signal and relates to the transport of coarse sediment. In section 2.1.3 it was shown that the flood currents are larger than the ebb currents in the main channel. As a result the flood duration in the central part of the estuary is shorter than the ebb duration, thus causing net sediment transport into the estuary (flood dominance). According to theory flood dominance can be expected for a large ratio of tidal amplitude over water depth, shallow channels and limited intertidal storage area. On the other hand ebb dominance is expected to occur in case of the presence of deep channels and large intertidal storage area.

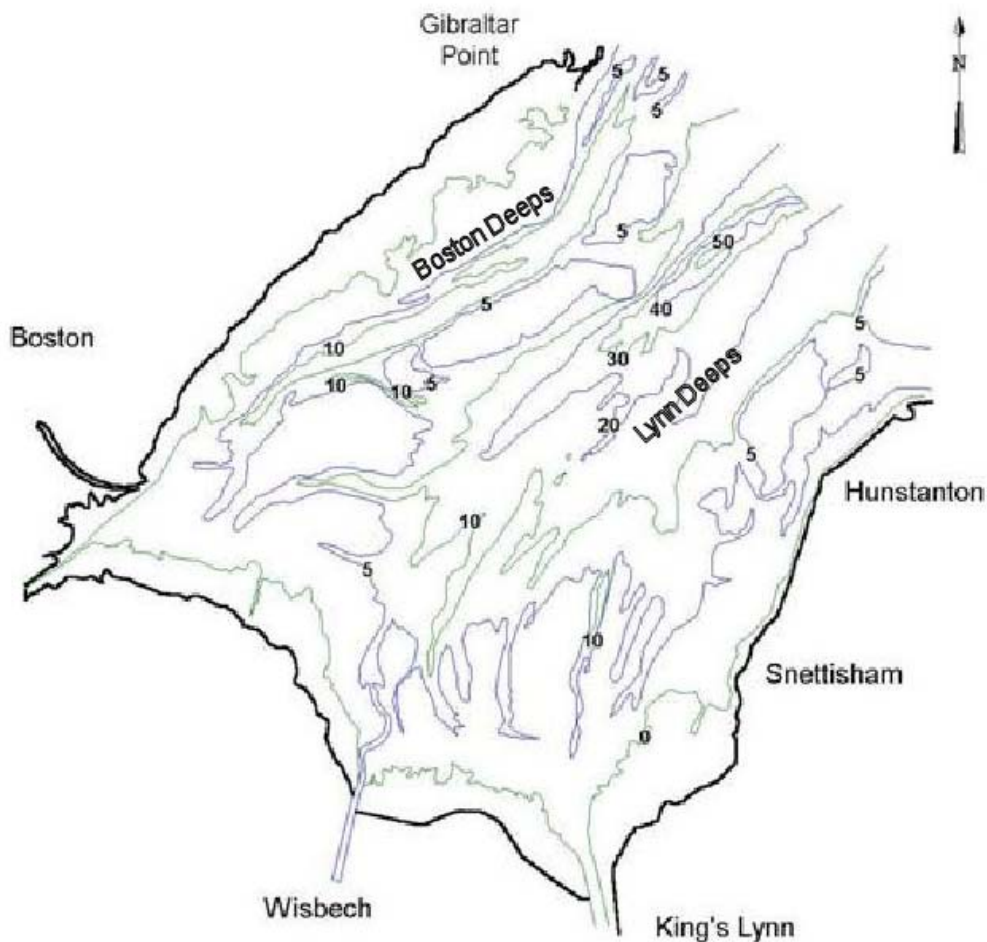


**Figure 5.5:** simplified bathymetry of the wash estuary, contour lines in m below ODN.  
(Courtesy: Royal Haskoning)

At first sight the fact that the central part of the estuary is characterized by flood dominance seems contradictory with theory, indeed the main channels are deep (see figure 5.5) and the intertidal storage area within the basin is approximately 290 km<sup>2</sup>. However most of these intertidal flats are located at the landward end of the estuary and here the residual flow, depicted in figure 5.6, clearly indicates ebb dominance. In the central part the width of the intertidal storage area is small compared to the width of the area permanently covered by water, which is consistent with flood dominance. Flood dominance results in a net transport of coarse sediment into the estuary, which is consistent with the situation depicted in figure 5.7.

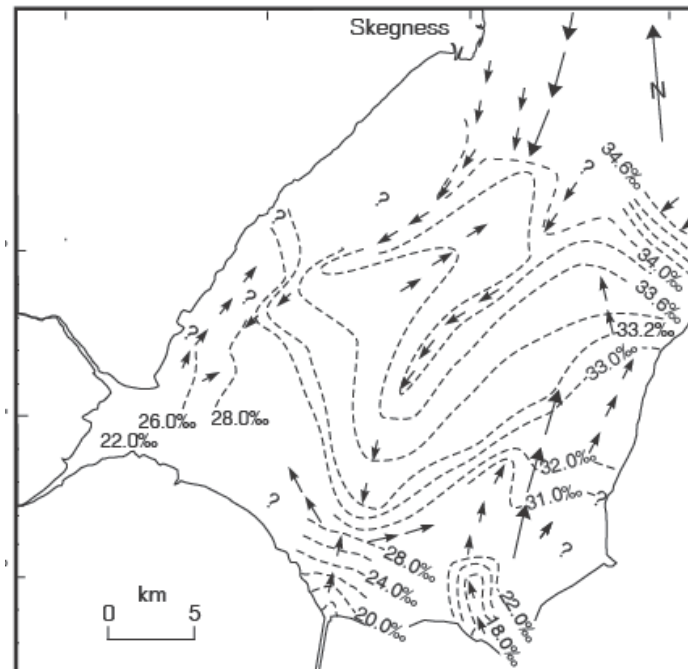


**Figure 5.6:** residual tidal flow direction.  
(Courtesy: Wingfield et al, 1978)

In contrast to the central part of the estuary both along the eastern and western boundary the residual flow direction is in ebb direction, which indicates ebb dominance and hence net sediment transport towards the North Sea. Here the channels are bordered by vast intertidal flats which is a typical configuration leading to ebb dominance. In these sections ebb dominance is further enhanced as a result of the rivers Witham, Welland, Nene and Great Ouse discharging into the estuary, thus contributing to a residual flow in ebb direction, see figure 5.6. However the net trend is the overall import of sediment in the estuary basin [The Wash SMP2, appendix C, 2010].

The vertical asymmetry of the horizontal tide relates to the transport of fine sediment and results in a saw-tooth velocity signal. The governing process with respect to the sediment transport of fines is the difference in duration between high-water slack and low-water slack. The location within the estuary where flood dominance occurs, Lynn Deeps, the high-water slack duration is longest and hence net transport of fines in landward direction occurs. This is consistent with the distribution of intertidal sediments as depicted in figure 5.6.

The margins of the estuary, where ebb dominance occurs, are characterized by a longer low-water slack duration. According to theory this will result in a net export of fines. This seems

not to be the situation, as mud is also present along the eastern and western shoreline. However because of the large intertidal area another mechanism plays a role. Due to the small water depth and large concentration fines in the water column strong settling occurs, apparently this process compensates for the short high-water slack duration.

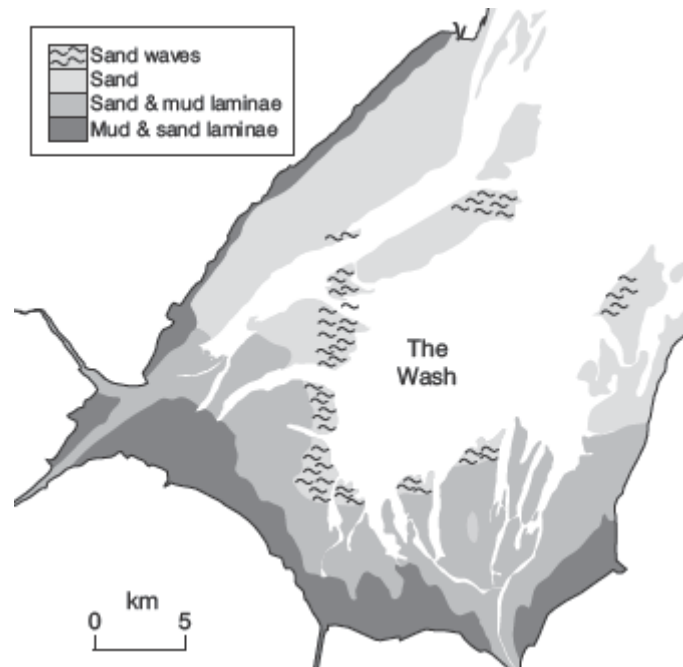


**Figure 5.7:** distribution of intertidal sediments in the Wash.  
(Courtesy: Ke et al, 1996, after Wingfield et al 1978)

Horizontal and vertical asymmetry of the vertical tide influence the water level within the estuary and are therefore of importance with respect to the energy potential. As is already shown in section 2.1.2, within the Wash estuary the main drivers are the tidal asymmetry already present at sea, the decreasing depth and the bottom friction.

Already at the mouth of the Wash estuary the falling period is longer than the rising period, this vertical asymmetry of the vertical tide increases slightly as the tidal wave progresses further into the estuary, see appendix 7. The asymmetry is most pronounced near the ports of Boston and King's Lynn that are located some distance upstream the tidal rivers Witham and Great Ouse respectively.

Keeping in mind the propagation speed of the tidal wave explains this vertical asymmetry. During rising tide the crest of the tidal wave propagates into the estuary, hence the water depth is larger and as a result the wave celerity is faster than during the falling tide.

From table 5.5 can be concluded that horizontal asymmetry of the vertical tide is barely present at the mouth of the Wash estuary. During spring tide the high waters are slightly higher above mean sea level than the low waters and during neap tide it is the other way around. This asymmetry progressively increases in landward direction.

	SK	BOS	HUN	KLY	TAHE	OWK	WES
MSL	3.93	3.56	4.10	3.77	4.08	3.75	4.06
MHWS - MSL	2.92	2.94	3.25	3.08	3.37	3.32	3.31
MSL - HLWS	2.93	2.16	3.12	2.47	3.28	3.17	3.01
MHWN - MSL	1.17	0.96	1.28	1.03	1.27	1.33	1.24
MSL - MLWN	1.26	1.84	1.43	1.77	1.50	1.58	1.64

MSL in m above CD (CD = -3.00 m ODN)

SK = Skegness

BOS = Boston

HUN = Hunstanton

KLY = King's Lynn

TAHE = Tabs Head

OWK = Outer Westmark Knock

WES = West Stones

MSL = Mean Sea Level

MHWS = Mean High Water Spring

MLWS = Mean Low Water Spring

MHWN = Mean High Water Neap

MLWN = Mean Low Water Neap

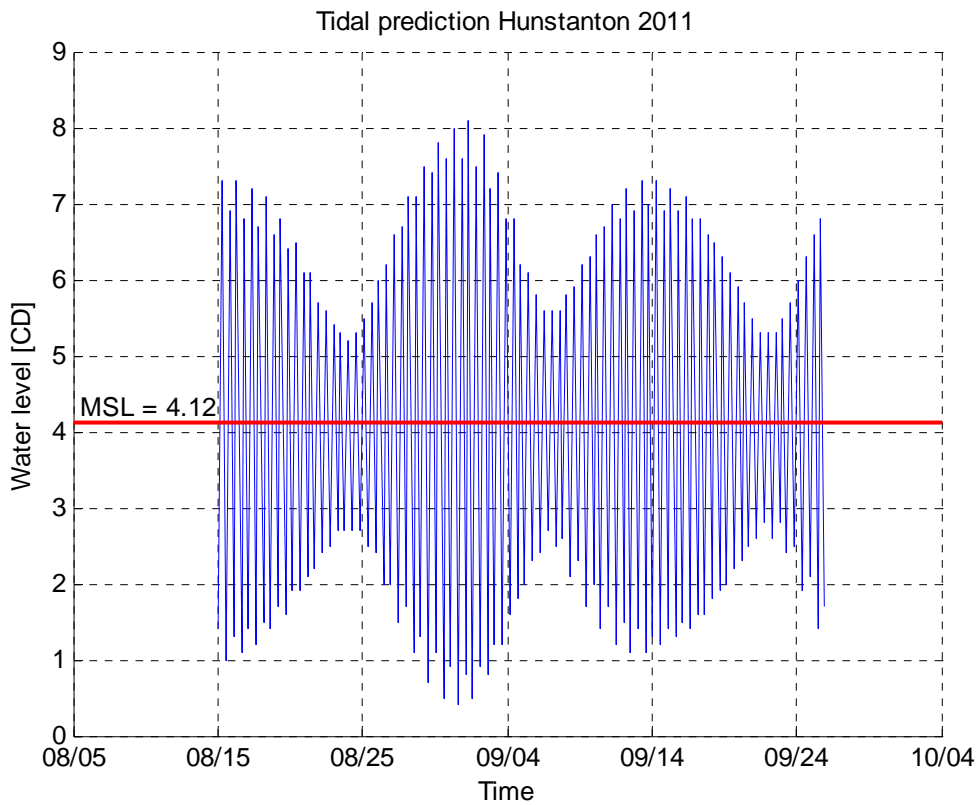
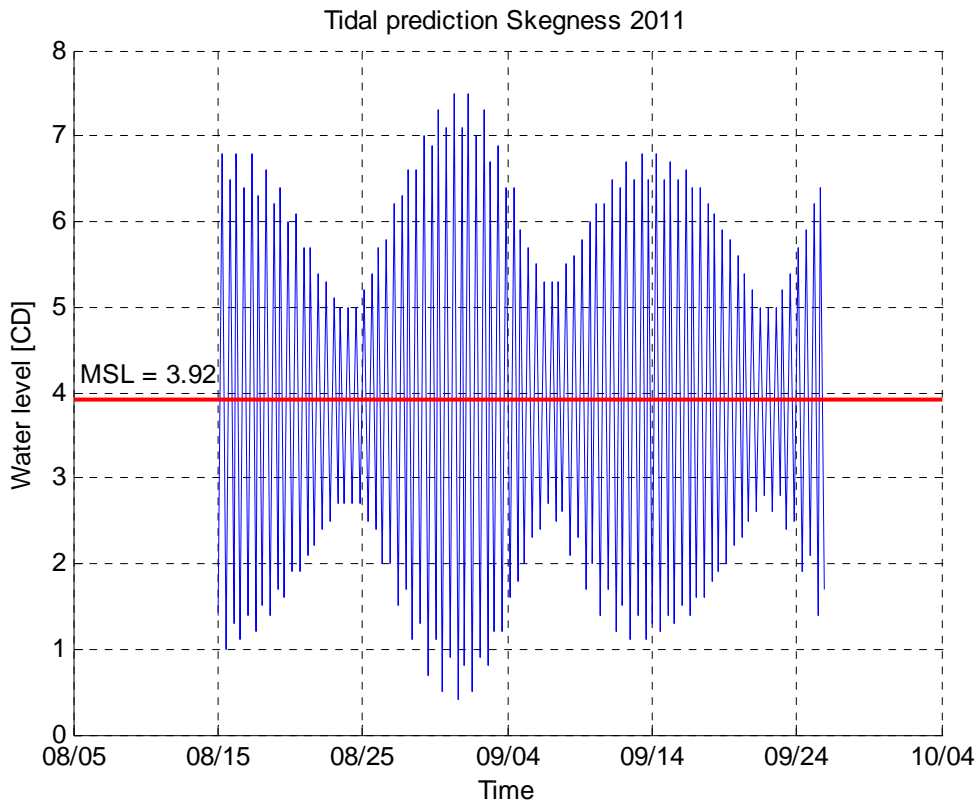
**Table 5.5:** water levels and tidal ranges.

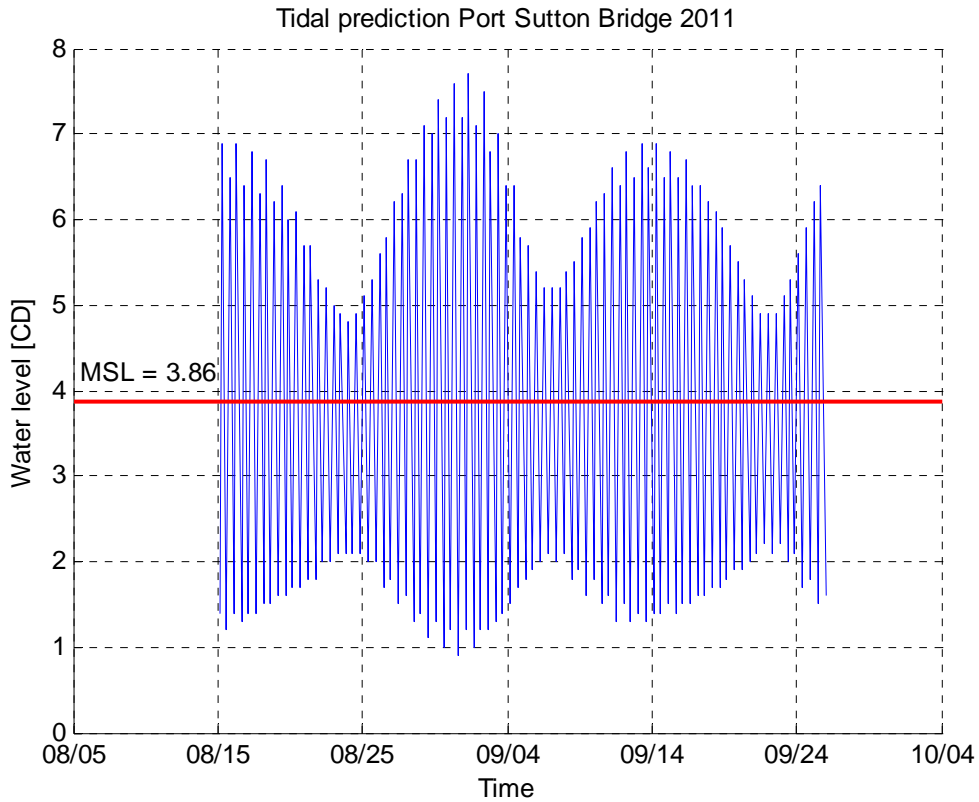
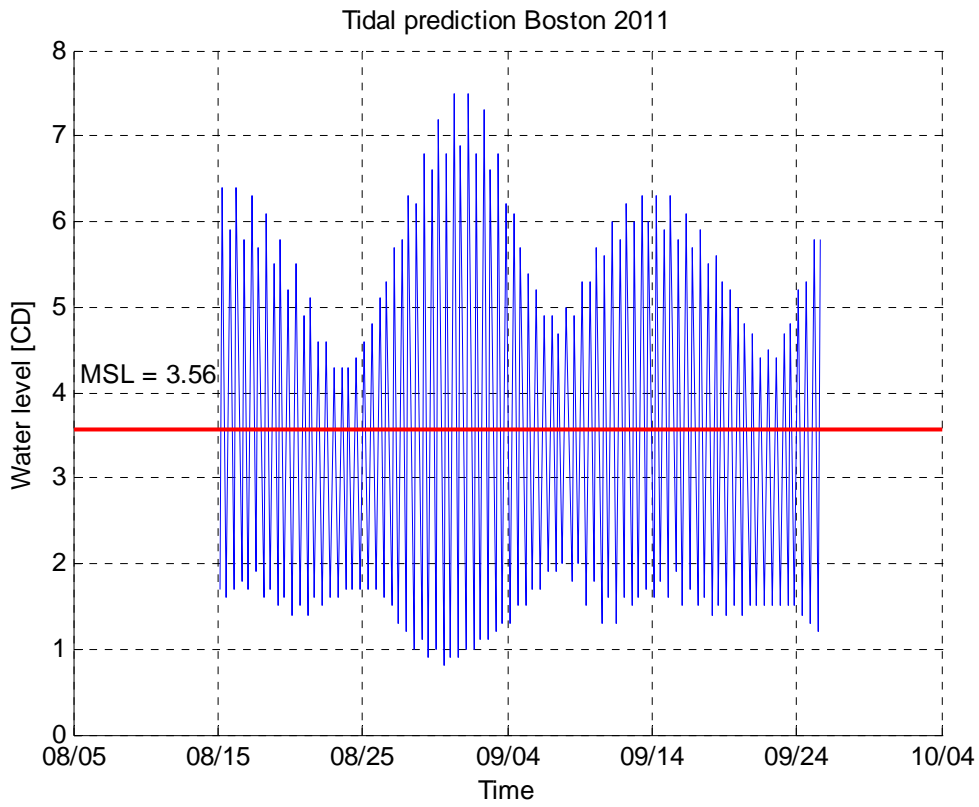
## **Appendix 6**

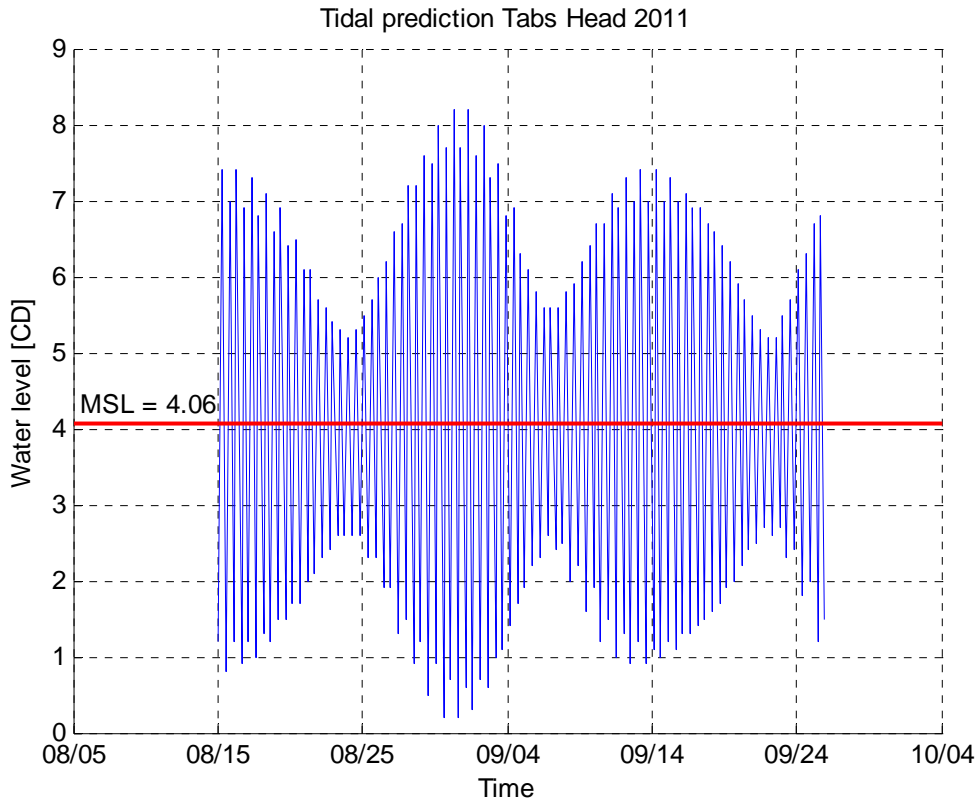
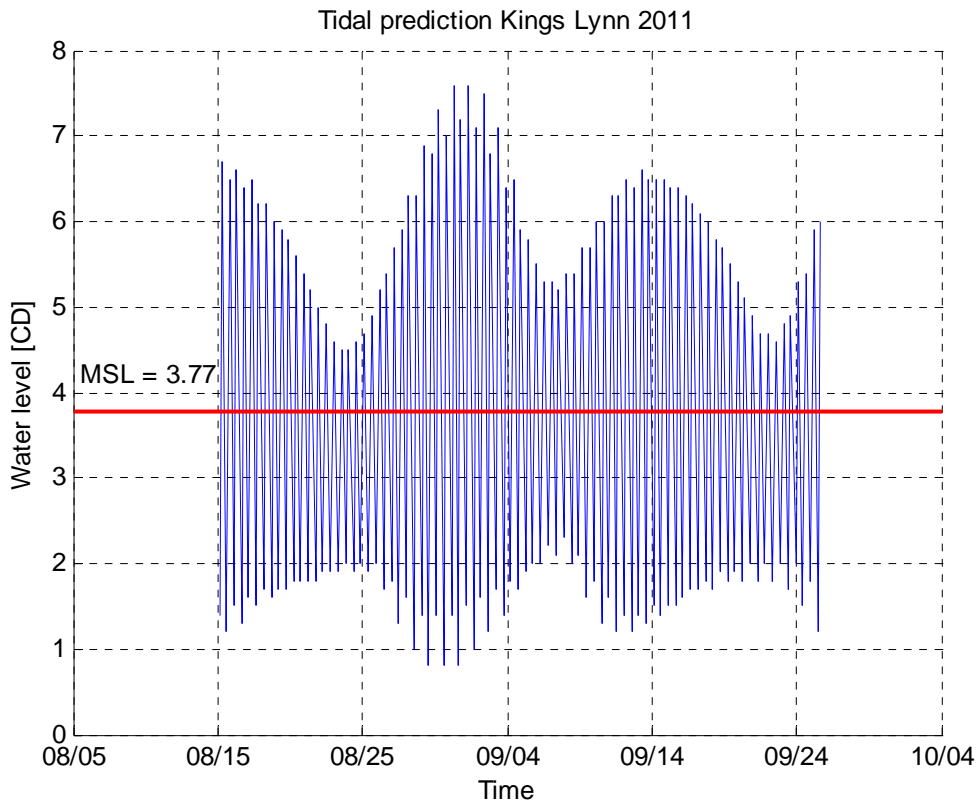
*Predicted tidal signals in the Wash estuary*

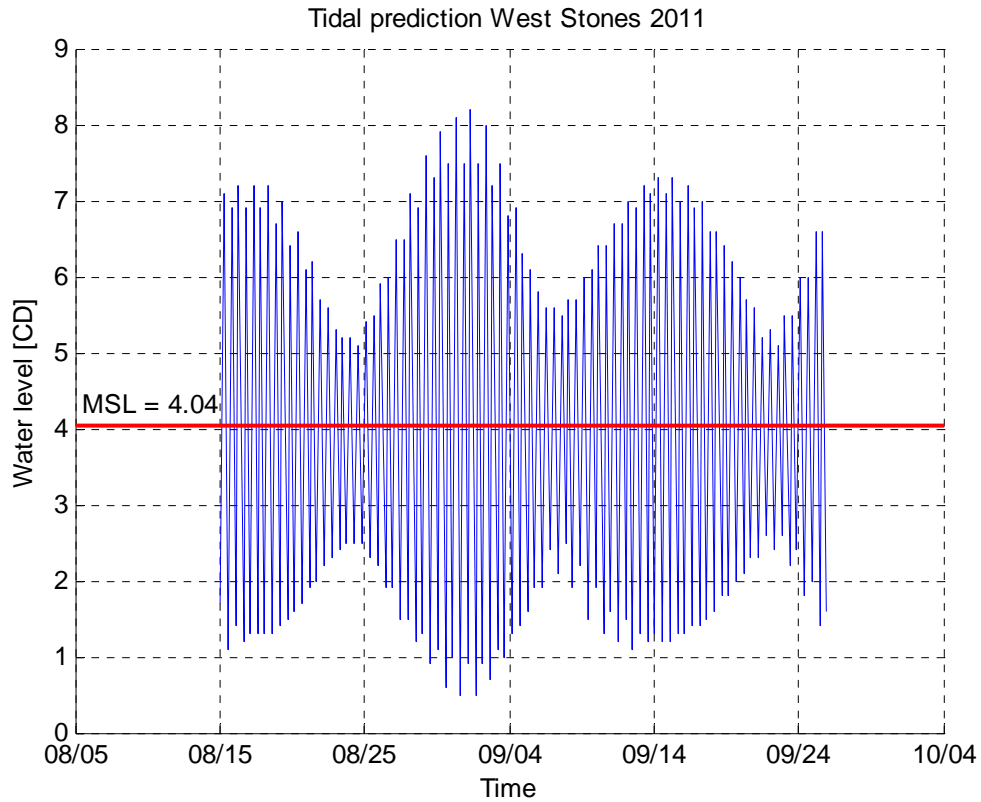
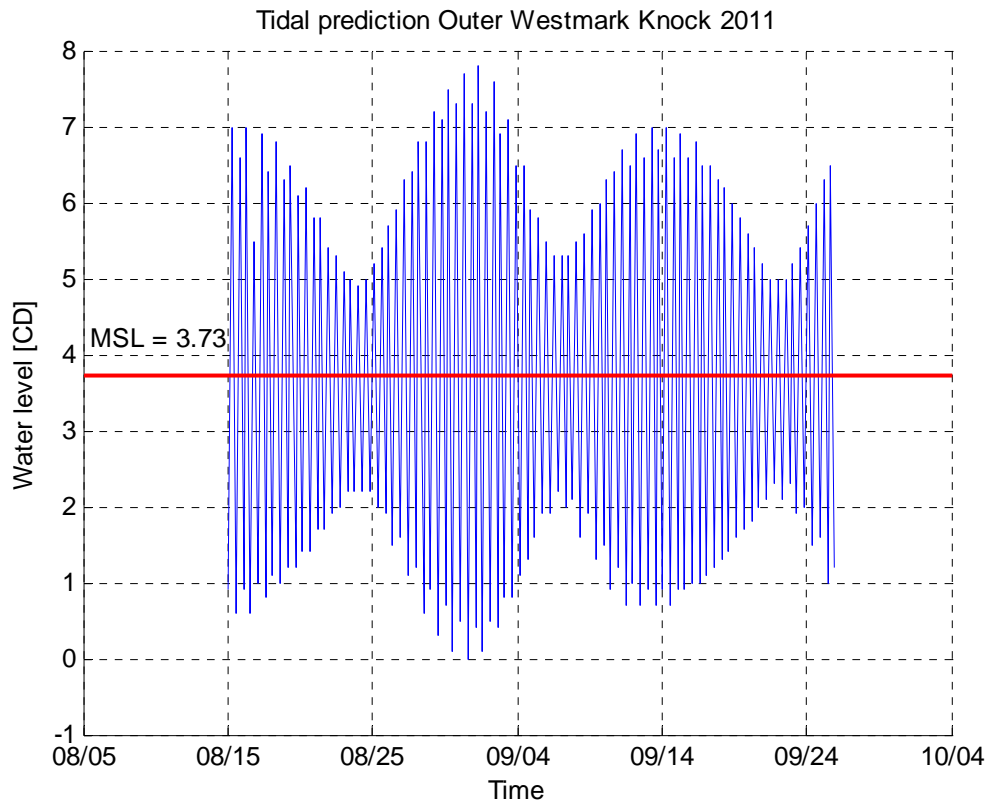


The figures below are plotted using data from the tidal prediction service provided by Admiralty EasyTide.









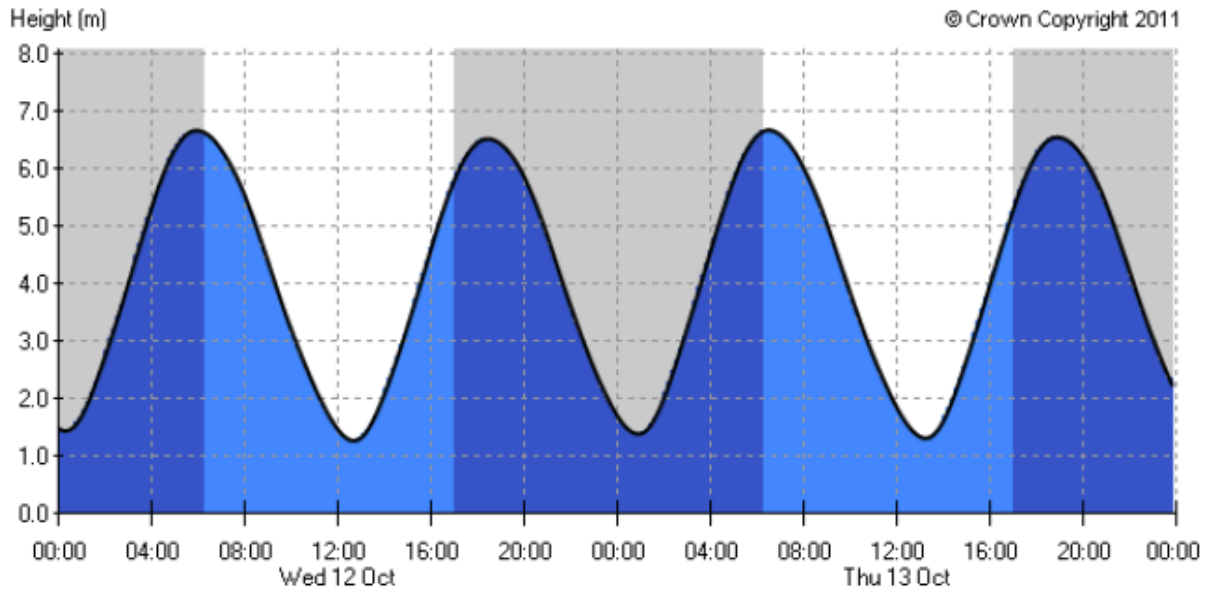
## **Appendix 7**

*Asymmetry of the vertical tide in the Wash estuary*

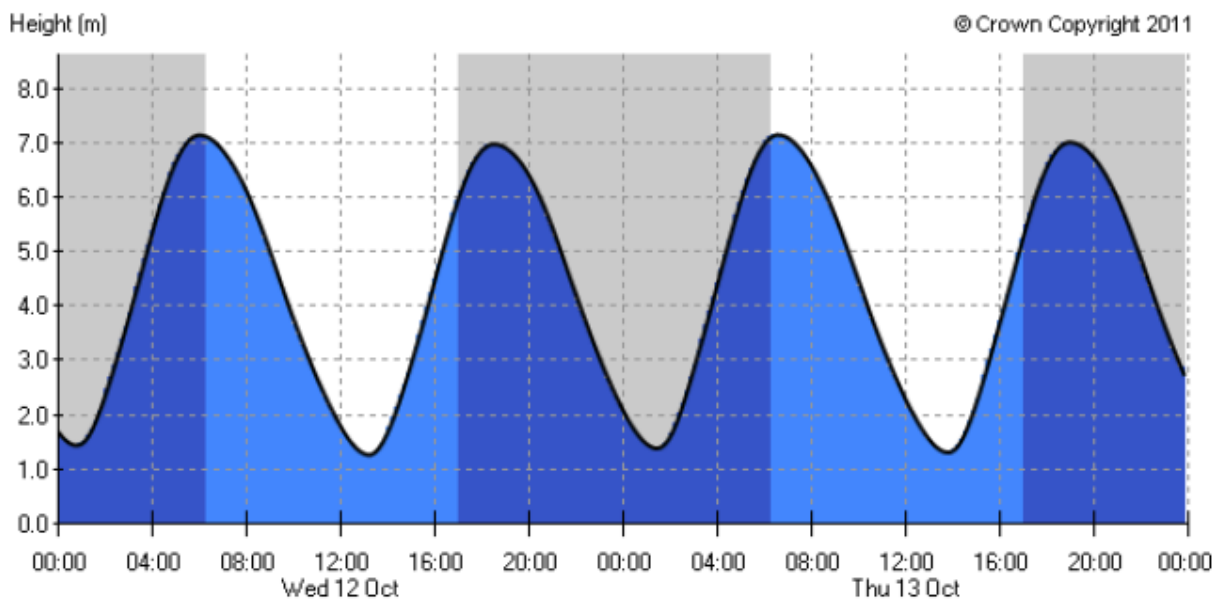


The figures below are copied from the website of the tidal prediction service provided by Admiralty EasyTide.

**Skegness:**



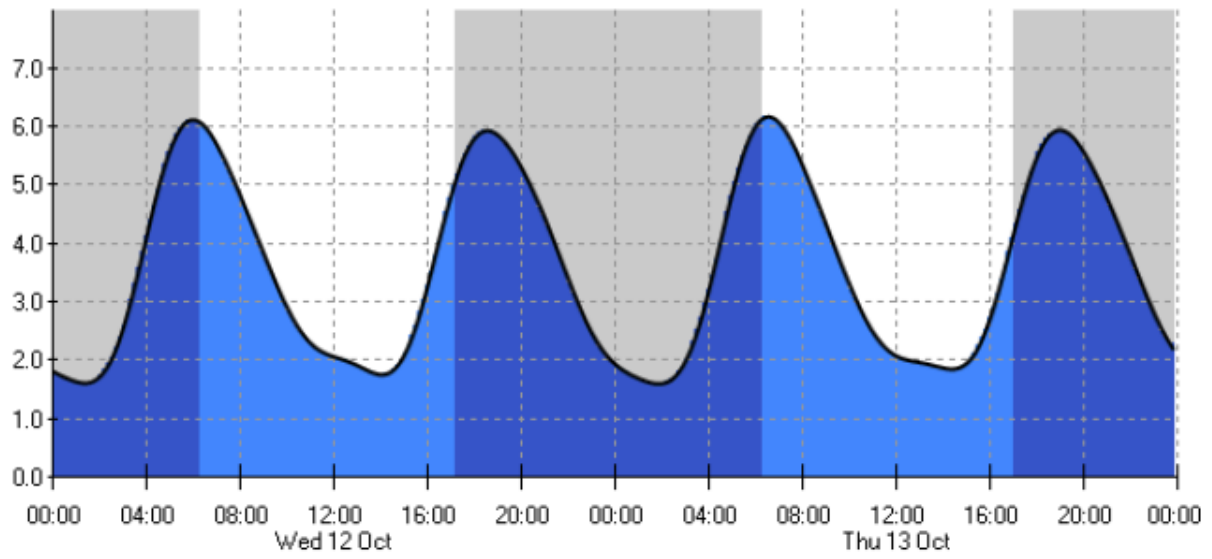
**Hunstanton:**



**Boston:**

Height (m)

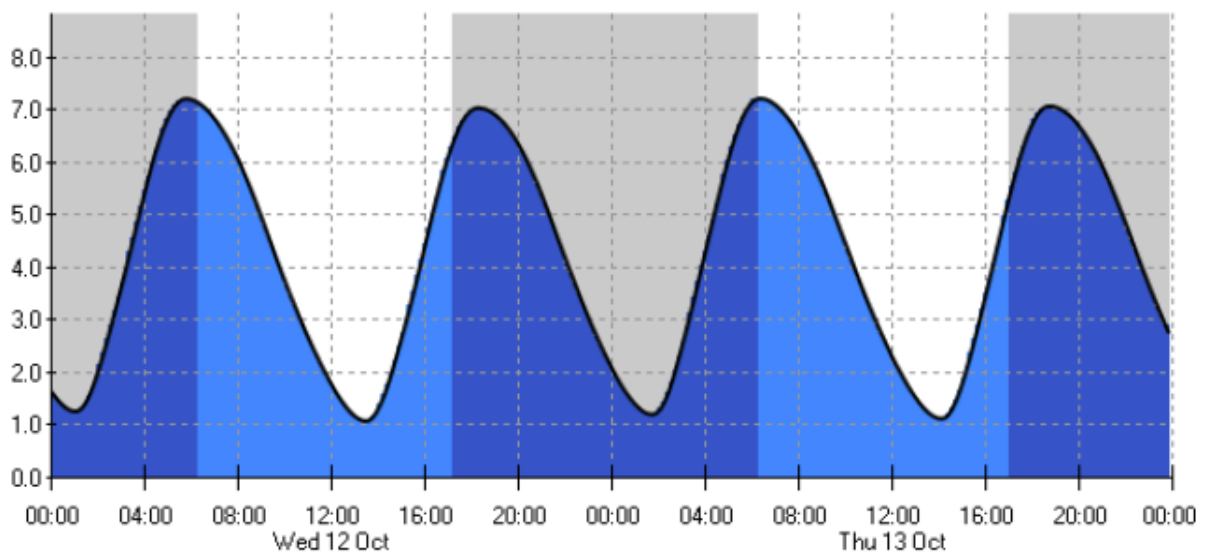
© Crown Copyright 2011



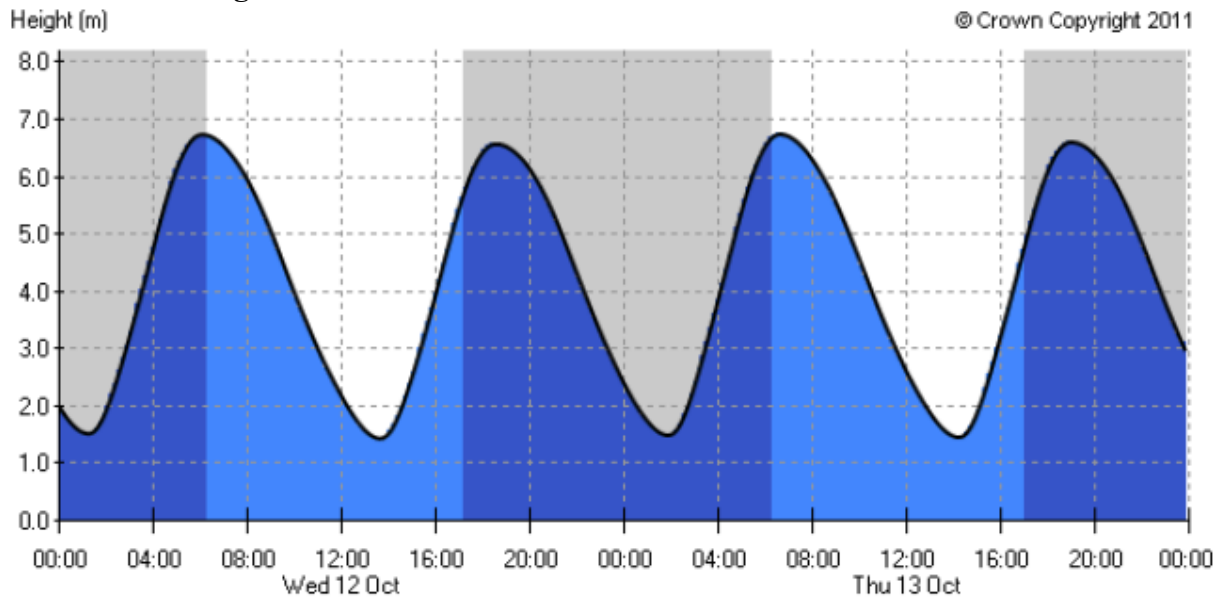
**Tabs Head:**

Height (m)

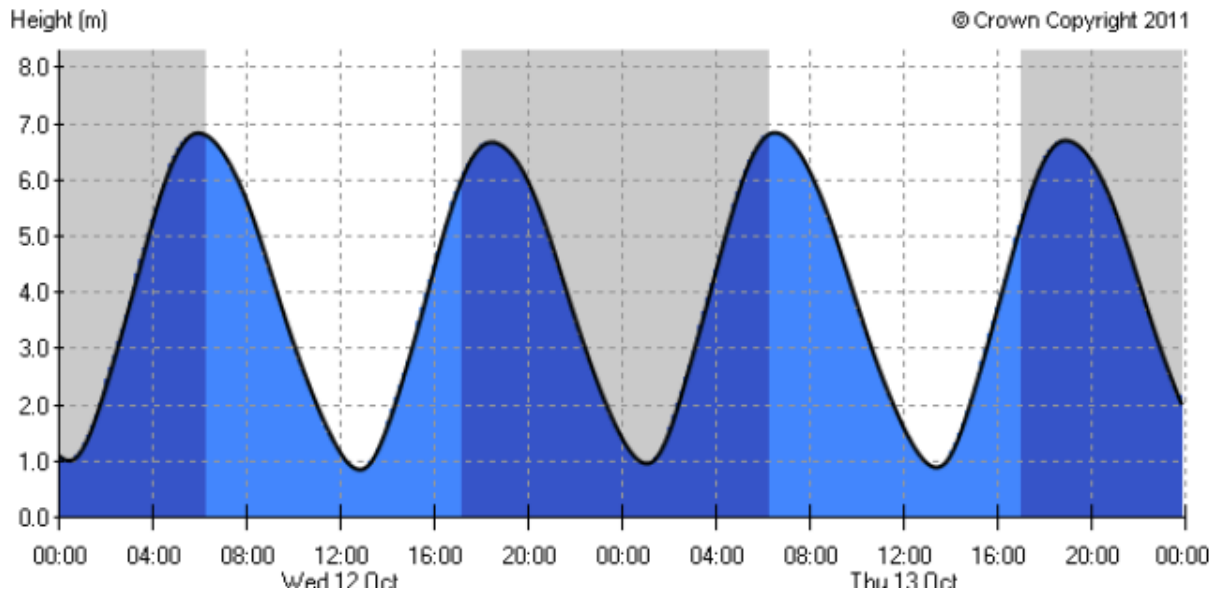
© Crown Copyright 2011



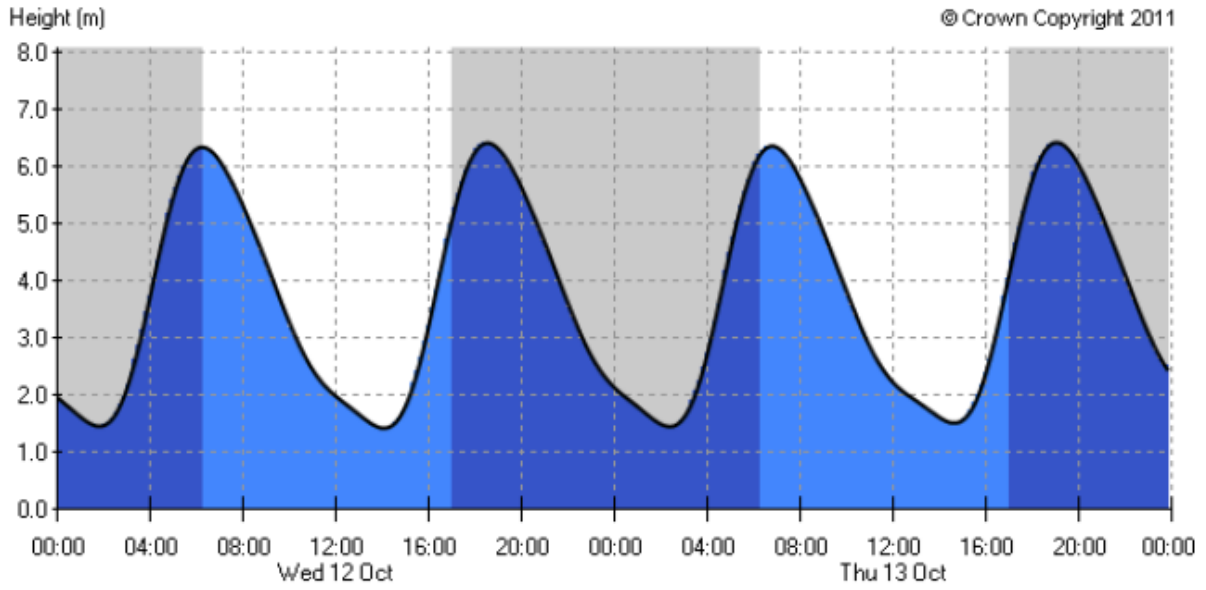
**Port Sutton Bridge:**



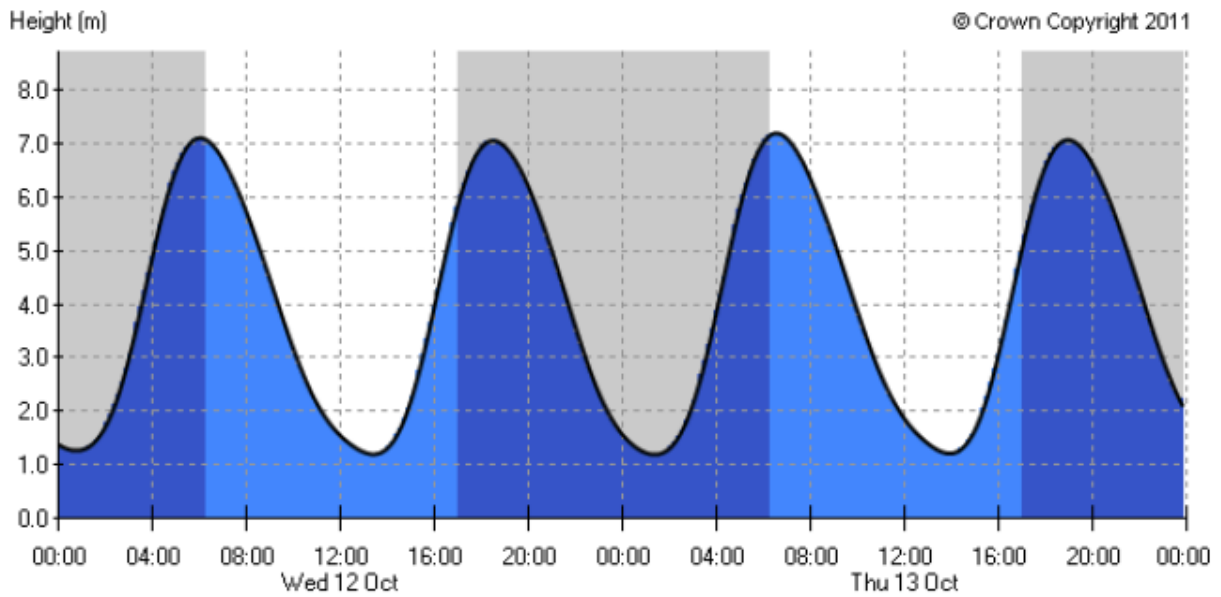
**Outer Westmark Knock:**



**King's Lynn:**



**West Stones:**



## **Appendix 8**

### *Analysis of extremes*



## 8.1 Introduction

In order to be able to design flood defence structures the extreme values of the significant wave height, peak period and wind speed have to be determined. Because usually extreme conditions fall outside the observed range, these conditions must be estimated. This can be done by fitting a curve through the observations and extrapolate this curve to the desired probability of occurrence. In this case two sources containing observations regarding significant wave height, peak period and wind speed are available, namely the wave atlas from Global Wave Statistics and the database from BMT ARGOSS<sup>3</sup>.

After comparing both data sets it was decided to use the database from BMT ARGOSS, since this database is more site-specific. The data set contains observations gathered from an area of 200·200 km<sup>2</sup> offshore from the Wash estuary, while the Global Wave Statistics data set contains observations gathered throughout the whole North Sea basin. Also the maximum significant wave height and wave period in the Global Wave Statistics database are slightly larger than in that of BMT ARGOSS. This is most probably the result of the larger area of observation, as the significant wave height and wave period are larger in other parts of the North Sea basin [Holthuisen et al, 1995].

The data provided by BMT ARGOSS consist of synthetic aperture radar (SAR) data. The data are grouped statistics of satellite observations, which means that the data are not sequential, in the sense that it is one continuous wave or wind record, also the number of storms per year is unknown. Therefore it is not possible to use the Peak-over-Threshold method to determine the extremes, instead a different approach is used. This initial distribution approach will be explained in this appendix, as is the interpretation of the end result, being design tables representing the probability of exceedance of significant wave height and wind speed corresponding to a certain design storm and return period.

## 8.2 Initial distribution approach for extreme wave height and period

In order to solve the problem of not knowing the number of storms per year, it is assumed that one year consists of a number of periods with a certain duration ( $t_{storm}$ ). It is also assumed that during those periods the significant wave height does not vary. The basic idea behind these assumptions is that, due to the persistence of winds, storm periods will have more or less the same duration. Next it is assumed that each random observation of a significant wave height describes an observation of one storm event. As a result such observation of a significant wave height represents the average significant wave height during that storm event ( $H_{s, storm}$ ). The storm event is defined by a predetermined storm duration [Verhagen, 2009].

Two distributions that are widely used for determining the long term distribution of the significant wave height are the log normal distribution and Weibull distribution [Holthuisen, 2008]. Although the choice of distribution is rather arbitrary, a distribution with more degrees of freedom will generally provide a better fit. As the log normal distribution has only two degrees of freedom and the Weibull distribution three, it was decided to use the latter in the performed analysis of extremes.

---

<sup>3</sup> [www.waveclimate.com](http://www.waveclimate.com)

The Weibull distribution is given by:

$$P(H_s > H_{s,storm}) = \left[ \exp\left(-\left(\frac{H_{s,storm} - \gamma}{\beta}\right)^\alpha\right) \right] \quad [8.1]$$

Were:

$\alpha$	: shape parameter	[-]
$\beta$	: location parameter, determines position of the distribution on the x-axis	[-]
$\gamma$	: scaling parameter, determines the width of the distribution	[-]

The degrees of freedom in this distribution,  $\alpha$ ,  $\beta$  and  $\gamma$ , can be determined by performing a linear regression analysis on the data. As a linear regression analysis will lead to only two constants,  $\beta$  and  $\gamma$ , the third coefficient,  $\alpha$ , is determined by trial-and-error. By assuming different values for  $\alpha$ , the curvature of the data and the correlation coefficient of the regression line will change. The value for  $\alpha$  that visually results in the straightest line and the highest possible correlation coefficient, will be chosen [Verhagen, 2009].

In order to be able to perform a linear regression analysis, equation 8.1 must be rewritten in the form:  $W = a \cdot H_{s,storm} + b$ , were  $W$  is called the Weibull reduced variable,  $a$  is the slope of the regression line and  $b$  the y-intercept. Rewriting equation 8.1 results finally in:

$$(-\ln Q)^\frac{1}{\alpha} = \frac{1}{\beta} H_{s,storm} - \frac{\gamma}{\beta} \quad [8.2]$$

And

$$W = (-\ln Q)^\frac{1}{\alpha} \quad [8.3]$$

The exceedance probability per year is found by using the relation presented in equation 8.4, were  $Q_s$  represents the probability of exceedance of a significant wave height in a storm per year in a random year, as long as  $Q_s < 1$ . If  $Q_s > 1$  the value has no statistical meaning, but physically the value indicates the expected number of storms that occurs in a year with a certain time averaged significant wave height.  $Q (= 1-P)$  indicates the probability of exceedance of a single storm and  $N_s$  is the number of occurring storms during a year, based on the storm duration set. The values for  $Q_s > 1$  are used to have sufficient basis for extrapolation.

$$Q_s = Q \cdot N_s \quad [8.4]$$

In order to compute the significant wave height belonging to the design storm, the Weibull reduced variable, equation 8.3, must be transformed by substituting equation 8.4, resulting in:

$$W = (-\ln Q_s)^\frac{1}{\alpha} \quad [8.5]$$

And

$$H_{s,storm} = \gamma + \beta \cdot (-\ln Q_s)^\frac{1}{\alpha} \quad [8.6]$$

Finally the design line is found by plotting the significant wave height against the Weibull reduced variable, while equation 8.6 can be used to compute the significant wave height corresponding to a certain probability of exceedance in a direct way.

All in all the initial distribution approach is a relative objective method as the fitting of the curve through the observation is done by using the least-squares technique<sup>4</sup>, which is an objective method. On the other hand however the choice of the distribution to be used is subjective.

### 8.2.1 Extreme significant wave height

In appendix 9.1 a table is included indicating the monthly distribution of significant wave height. Because the number of observations regarding the average significant wave heights is large the observations are grouped into 45° directional bins. The non-exceedance probability of a certain significant wave height is then defined as:

$$P(\overline{H_{s,i}} < H_{s,storm,i}) = \frac{n_i}{N} \quad [8.7]$$

Were:

- $n_i$  : number of observations in directional bin i [-]  
 $N$  : total number of observations [-]

The chosen duration of a storm event is very important in this method, as it determines the number of storms and consequently the probability of exceedance,  $Q_s$ , of a certain significant wave height. To establish the sensitivity of the method used, several storm durations were used. In table 8.1 a summary is presented of the results for the selected storm durations.

	Storm duration					
	3 hrs	6 hrs	8 hrs	9 hrs	12 hrs	15 hrs
$N_s$	2920	1460	1095	973	730	584
$H_s$	9.85	9.55	9.41	9.35	9.20	9.08
$N_s$ = number of storms per year			return period: 200 yrs			
$H_s$ = extreme significant wave height						

**Table 8.1:** summary of the initial distribution approach regarding  $H_s$ .

Note that the extreme significant wave height becomes lower as the storm duration increases. As can be seen in table 8.2 this trend is the same, independent from the return period chosen. This is strange because physically a longer storm will result in a higher significant wave height. Most probably this is a result of the combined effect of the fitting of the shape parameter  $\alpha$  by hand and the fact that the larger the data set the more accurate the Weibull distribution becomes. Hence the result of the performed analysis will only state the order of magnitude of the design wave condition. When the feasibility of the project depends solely on an one metre difference in design wave height, the project is by definition not feasible as in this stage only crude data are available and no local wave height measurements.

<sup>4</sup> This fitting technique is recommended by Goda for the Weibull distribution [Holthuijsen, 2008].

SoP		$H_s$ for storm duration [m]					
Return period [yr]	$Q_s$ [-]	3 hrs	6 hrs	8 hrs	9 hrs	12 hrs	15 hrs
50	0.02	8.74	8.40	8.25	8.19	8.02	7.89
200	0.005	9.85	9.55	9.41	9.35	9.20	9.08
500	0.002	10.62	10.35	10.23	10.17	10.03	9.91
1000	0.001	11.22	10.98	10.86	10.81	10.68	10.57
2000	0.0005	11.84	11.62	11.51	11.47	11.34	11.23
10,000	0.0001	13.33	13.17	13.08	13.04	12.94	12.84

SoP = standard of protection

$H_s$  = extreme significant wave height

**Table 8.2:**  $H_s$  for different return periods and storm durations.

Since the results of the fit may be unintentionally biased by the many observations of low values, more importance is assigned to the higher observations by ignoring all observations lower than one metre. The results are summarized in table 8.3.

	Storm duration					
	3 hrs	6 hrs	8 hrs	9 hrs	12 hrs	15 hrs
$N_s$	2920	1460	1095	973	730	584
$H_s$	9.79	9.50	9.36	9.30	9.15	9.02

$N_s$  = number of storms per year

return period: 200 yrs

$H_s$  = extreme significant wave height

**Table 8.3:** summary of the initial distribution approach regarding  $H_s$ , using censoring.

Comparing tables 8.2 and 8.4 learns that in this specific case the bias as a result of the lower wave heights is restricted to only a few centimetres, therefore the original data set will be used.

SoP		$H_s$ for storm duration [m]					
Return period [yr]	$Q_s$ [-]	3 hrs	6 hrs	8 hrs	9 hrs	12 hrs	15 hrs
50	0.02	8.70	8.36	8.21	8.15	7.98	7.85
200	0.005	9.79	9.50	9.36	9.30	9.15	9.02
500	0.002	10.55	10.29	10.16	10.10	9.96	9.84
1000	0.001	11.15	10.90	10.79	10.73	10.60	10.48
2000	0.0005	11.76	11.54	11.43	11.38	11.25	11.14
10,000	0.0001	13.23	13.07	12.98	12.93	12.82	12.72

SoP = standard of protection

$H_s$  = extreme significant wave height

**Table 8.4:**  $H_s$  for different return periods and storm durations, using censoring.

### 8.3 Initial distribution approach for extreme wind speed

For determining the extreme offshore wind speed the same approach is followed for the extreme significant wave height. For a more elaborate description the reader is referred to section 8.1 of this appendix. For the analysis of wind speed often a Rayleigh or Weibull distribution are used [Twidell, 2006]. Because the Weibull distribution has one degree of freedom more than the Rayleigh distribution and therefore tends to be more accurate, this distribution is used. A table containing the monthly distribution of the offshore wind speed is included in appendix 9.2.

The results of the performed analysis are summarized in table 8.5. Again the influence of the storm duration on the results is assessed.

	Storm duration					
	3 hrs	6 hrs	8 hrs	9 hrs	12 hrs	15 hrs
$N_s$	2920	1460	1095	973	730	584
$U_s$	25.1	25.4	26.1	26.1	26.0	25.9

$N_s$  = number of storms per year  
 $U_s$  = extreme wind speed  
return period: 200 yrs

**Table 8.5:** summary of the initial distribution approach regarding wind speed.

Note that there are no significant changes in wind speed for the different storm durations, this clearly shows the persistence of the wind. Table 8.6 shows that this trend is independent of the return period chosen.

SoP		$U_s$ for storm duration [m/s]					
Return period [yr]	$Q_s$ [-]	3 hrs	6 hrs	8 hrs	9 hrs	12 hrs	15 hrs
50	0.02	22.0	21.8	22.3	22.2	22.0	21.8
200	0.005	25.1	25.4	26.1	26.1	26.0	25.9
500	0.002	27.8	28.6	29.2	29.3	29.4	29.4
1000	0.001	30.2	30.2	31.9	32.0	32.2	32.2
2000	0.0005	32.9	23.9	34.9	35.0	35.4	35.7

SoP = standard of protection  
 $U_s$  = extreme wind speed

**Table 8.6:**  $U_s$  for different return periods and storm durations.

As can be seen from table 8.6, without censoring the extrapolated values of the extreme wind speed are unrealistic for long return periods (34-36 m/s), corresponding with wind force 12 on the Beaufort scale. However hurricanes are not likely to occur on the North Sea. This is the result of bias caused by the many observations of low wind speeds that are present in the dataset. Therefore all observations with a wind speed smaller than 4 m/s are discarded in the analysis. This wind speed corresponds with wind force 2 on the Beaufort scale. The results of the initial distribution approach using censoring are included in table 8.7.

SoP		$U_s$ for storm duration [m/s]					
Return period [yr]	$Q_s$ [-]	3 hrs	6 hrs	8 hrs	9 hrs	12 hrs	15 hrs
50	0.02	21.5	21.3	21.7	21.6	21.4	21.2
200	0.005	24.4	24.7	25.2	25.2	25.1	25.0
500	0.002	26.9	27.6	28.0	28.1	28.1	28.1
1000	0.001	29.1	30.2	30.5	30.6	30.8	30.8
2000	0.0005	31.6	33.1	33.2	33.4	33.7	33.8

SoP = standard of protection

$U_s$  = extreme wind speed

**Table 8.7:**  $U_s$  for different return periods and storm durations, using censoring.

Now the wind speed for longer return periods corresponds to wind force 11 on the Beaufort scale, which indicates a very severe storm and is a realistic value for the North Sea basin. Hence these figures will be used.

## **Appendix 9**

*Extreme offshore wave and wind conditions*



## **Appendix 9.1**

*Monthly distribution of significant wave height*  
*(Courtesy: BMT ARGOSS)*



## **Appendix 9.2**

*Monthly distribution of wind speed*  
*(Courtesy: BMT ARGOSS)*



## **Appendix 10**

*Analysis of the UK's energy market*



## 10.1 Introduction

The long term vision of the UK Government regarding the country's energy supply is that the 2050 climate change objectives<sup>5</sup> must be achieved, while ensuring secure and affordable energy supplies. In order to achieve these goals, the current energy market, that is heavily dependent on fossil fuels, must be reformed towards a low carbon energy market. This means that renewable energy sources (solar energy, wind energy, water power, etc.), nuclear energy and fossil fuel combined with carbon capture and storage are bound to get a larger market share on the expense of traditional coal and gas fired electricity generation. Within this light the UK Government has committed that 15% of its total energy consumption comes from renewable sources by 2020, which means that approximately 30% of the UK's electricity generation should be provided by renewable energy sources [HM Treasury, 2010]. This creates opportunities for the generation of tidal energy in the UK. However, the focus of the Government seems to be more on onshore and offshore wind energy schemes.

Besides one of the most reliable supplies in Europe, the UK's energy market is also one of the most liberalised energy markets in the world. As a result of this liberalisation, the UK market is currently dominated by six large energy companies<sup>6</sup> that are acting both on the wholesale market and the retail market. These companies together dominate 99% of the retail market and 67% of the wholesale market [HM Treasury, 2010]. In other words, these companies generate a large part of the energy that they sell on the retail market themselves.

In this appendix first the historical developments of the UK's energy market will be sketched. Next the short, medium and long term objectives of the current energy policy will be treated, followed by an overview of the most important European and national policies that must enable the achievement of these objectives. Last but not least the current level of energy prices in the UK energy market is explored.

## 10.2 Short history

During the 1970s the UK was a net importer of energy, as result of the developing gas and oil production in the North Sea the UK became a net exporter of energy during the 1980s and continued to be so until 2004, when it became a net importer again [DECC, 2011].

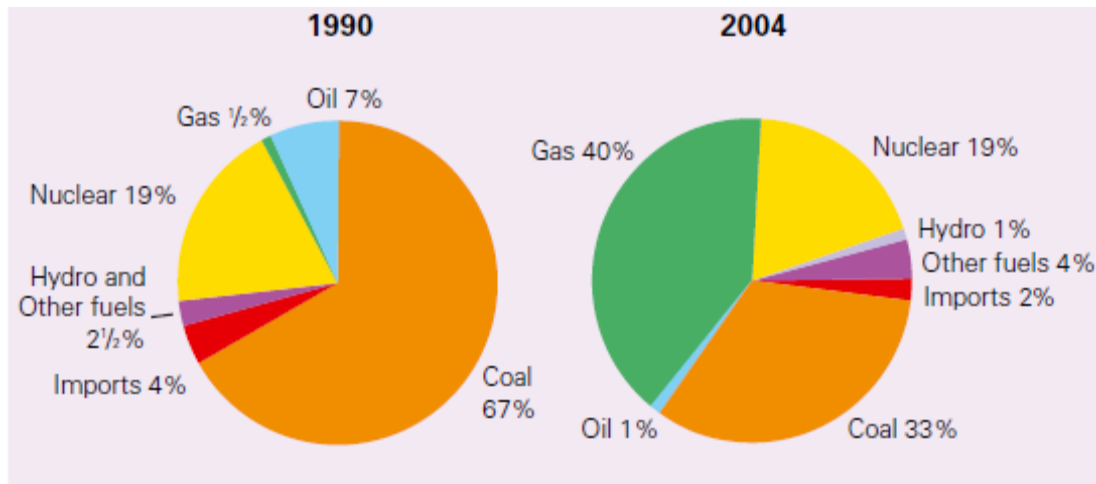
Before the 1960's 90% of the energy production in the UK was provided by coal fired energy plants, the remaining 10% was provided mostly by oil fuelled electricity production. During the 1960's the first generation nuclear power plants were built, followed by the second generation during the 1970's and 1980's. During the 1990's the market share of nuclear power increased further as a result of improved plant performance and the commissioning of a third generation nuclear power plant. By the late 1990's nuclear power plants provided 26% of the national electricity supply [Redpoint, 2010]. Since then no new nuclear power plants have been commissioned and its market share declined due to the retirement of the first generation power plants. Within the light of the Government's low carbon energy policy plans exist to build new nuclear power plants in the near future.

---

<sup>5</sup> The UK Government has committed to a legally binding target to cut greenhouse gas emissions by 80 %, from 1990 levels, by 2050 [HM Treasury, 2010].

<sup>6</sup> The six largest energy companies in the UK are: E.ON, RWE npower, SSE, EDF, Centrica and Scottish power [HM Treasury, 2010].

As a result of the liberalization of the UK energy market in 1989 the gas market was opened up [Redpoint, 2010] on the expense of the coal fired power plants. This so-called “dash for gas” started in 1993 and continued until the early 2000’s, see also figure 10.1. At the same time of the energy market liberalization a Non-Fossil Fuel Obligation was introduced, which remained the primary renewable support scheme until it was replaced by the Renewables Obligation in 2002 [Redpoint, 2010].



Source: DTI, 2005.

Figure 10.1: energy mix by fuel type, 1990 vs. 2004.

Before 1990 the only renewable energy source of some scale in the UK was hydro power, predominantly situated in Scotland. Since the mid 1990’s a steady increase in renewable energy production capacity is noticeable, mainly in the form of landfill gas and biomass fired power plants. From the mid 2000’s a significant growth can be seen with respect to wind farms, as a result of which nowadays wind energy is the second largest renewable energy source in the UK. These wind farms are for the larger part land based, however since 2009 also large offshore wind farms have been installed. The construction of offshore wind farms is expected to speed up in the coming years as onshore and offshore wind energy play a key role in reaching the 2020 target [DECC, 2010].

Marine energy in the form of wave power and tidal stream power are also a priority for the UK Government, since the UK coast has large potential and because the Government strives to develop a new world leading UK based energy sector [DECC, 2010]. In spite of the fact that already since the 1920’s the feasibility of tidal barrages is studied, no tidal range power plant was ever built. According to the Sustainable Development Commission the reasons for this are mainly the high capital costs and, more recent, environmental concerns.

As can be seen in figure 10.2; nowadays natural gas and coal are still the primary energy sources in the UK (71%), followed by nuclear energy (13%). All renewable energy sources together have a market share of only 14%.

When regarding the figure above, it is not surprisingly that in the UK electricity generation is one of the primary sources of carbon emissions. In order to reduce the emission of harmful greenhouse gasses the UK Government has decided that the domestic energy market must reform towards a low carbon energy market, through the use of renewable energy sources, nuclear power and clean fossil fuels through Carbon Capture and Storage (CCS). The

transition towards a more sustainable energy market does not only ensure a reduction in the emission of greenhouse gasses, it also results in a domestic energy market that is much less dependent on foreign energy supplies, which also benefits the long term security of energy supply in the UK.

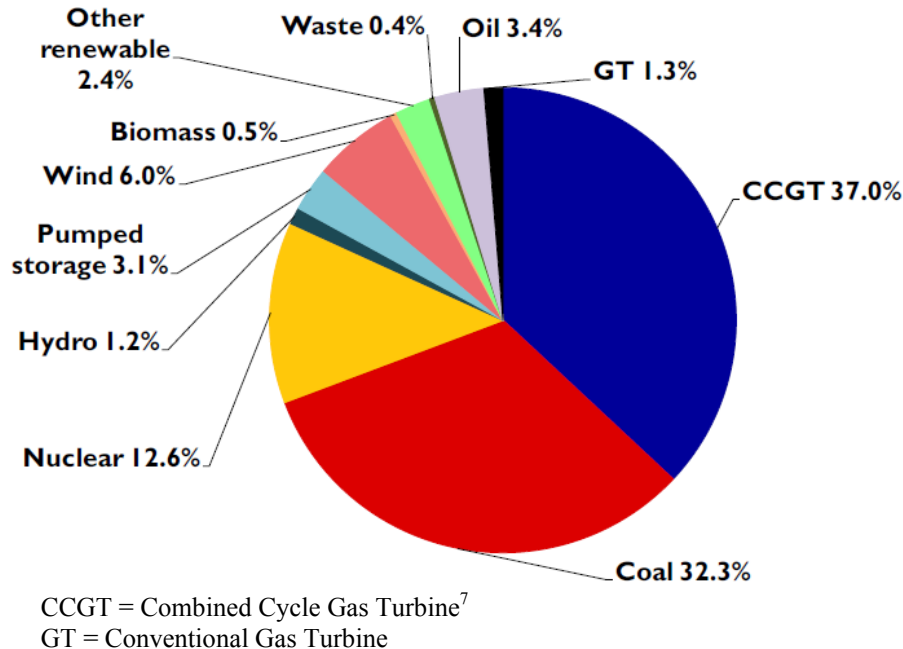


Figure 10.2: UK's electricity generation capacity (Courtesy: Redpoint estimates, 2010).

### 10.3 Objectives for energy policy

On the short term (2020) the security of energy supply is still guaranteed in the UK. But in order to meet the carbon emission reduction targets, the contribution of renewable and low carbon energy sources to the energy mix must increase considerably, see figure 10.3. In the short term this will be achieved by large investments in onshore and offshore wind energy.

On the other hand consumers need to make energy efficiency improvements to control the growth of the energy demand and better manage the impacts of the expected increase in energy price. Other spear heads of the short term energy policy are [HM Treasury, 2010]:

- become a world leader in the low carbon and environmental sector;
- create sufficient generating capacity to meet peak demand;
- increase the gas storage capacity.

On the medium term (2020-2050) efforts have to be made in order to maintain the security of energy supply. In order to do so large investments have to be made in nuclear power, fossil fuel generation with CCS and renewable energy sources (mainly wind) to replace ageing existing power plants. Also the energy sources should be diversified and further efficiency improvements must be realized. Due to the increasing energy demand both by consumers and

<sup>7</sup> Combined Cycle Gas Turbine = the turbine's generator generates electricity and heat in the exhaust is used to make steam, which in turn drives a steam turbine that generates additional electricity.  
Conventional Gas Turbine = turbine in which electricity is generated and the heated gasses are exhausted to the atmosphere. Many old gas-fired electricity plants are of this type.

as a result of the expected elimination of fossil fuels in both transport and domestic heating, the electricity production must increase markedly. This additional electricity generation capacity is to be provided by low carbon energy sources (nuclear energy, fossil fuel with CCS and renewables).

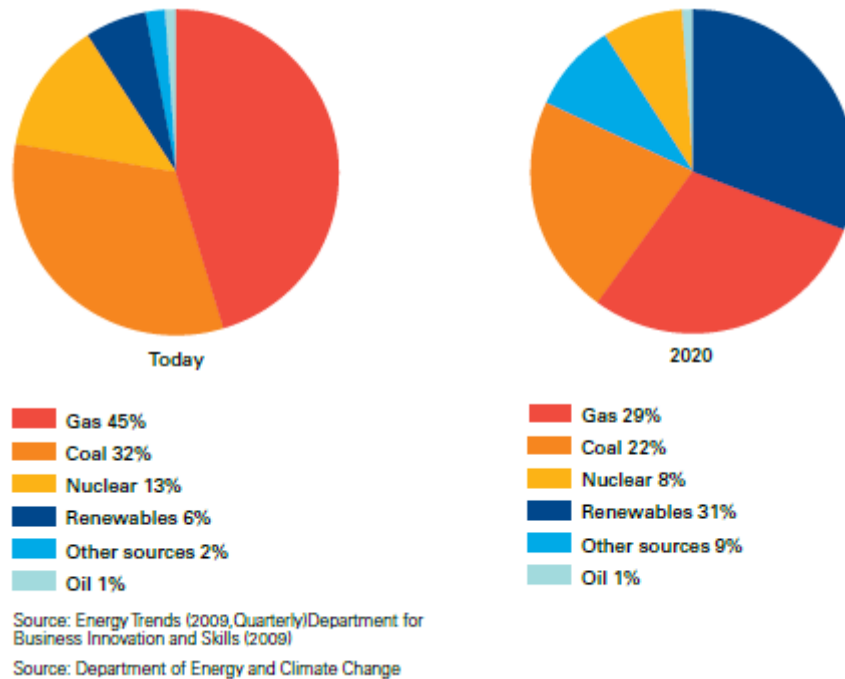


Figure 10.3: energy mix by fuel type, 2009 vs. 2020.

Because renewable energy sources are characterized by large intermittent and inflexible energy generation and because peak energy demand must be ensured, interconnection with neighbouring countries is strived for, as is the development of energy storage technologies. Additional capacity to meet energy demand when renewables are unable to deliver a constant energy supply, is provided by nuclear power plants and fossil fuel fired plants combined with CCS.

A very hard to tackle problem is the reduction in emissions from agriculture, waste, industry and (international) transport. However this must be tackled in order to be able to meet the 2050 emission target. By some point in the 2030's the electricity sector must be largely decarbonised and becoming a world leader in the low carbon and environmental sector is still aimed for.

On the long term (2050 and beyond) the ambition is to have ensured secure, clean and affordable energy supplies through a independently regulated and competitive energy market [HM Treasury, 2010]. This must be achieved by continuing the medium term objectives. The energy mix in 2050 will be characterized by large contributions from wind energy, nuclear power and fossil fuel power in combination with CCS. The use of oil will further decline, however gas will remain a important energy source. Potentially important contributions could be made from other renewable energy sources.

Regarding the policy objectives for the short, medium and long term it can be concluded that Government supported development of tidal range power plants is most likely to occur in the medium and long term, depending on the development of the global energy demand. On the

short term all effort is directed to the construction of onshore and offshore wind farms, tidal range power plants are not considered to be an option due to their environmental impacts. However this does not mean that a tidal range power plant is not technical or economical feasible. Depending on developments on the global energy market and the availability of fossil fuels, in the long term using the vast tidal range energy potential may become important in sustaining the way of life in the UK and therefore the economical benefits may be overshadowing environmental interests.

## 10.4 Current energy policy

In this section the UK's Government 's strategy to reach the 2050 climate change objectives will be treated, starting with European policy that forms one of the central pillars under the UK's energy policy. Next the national Renewable Energy Strategy will be discussed as this strategy is of importance in the framework of this thesis. Other important policies, like the Household Energy Efficiency, Climate Change Levy and Carbon Capture and Storage Incentive, though important in reaching the UK's climate change objectives, are not directly related to this thesis's subject and therefore will not be discussed.

### 10.4.1 European policy

Already in the 2001 Renewable Directive the UK was allocated a target of 10% regarding the contribution of renewable energy sources to the total electricity consumption by 2010. In March 2007 the European Commission agreed to a European wide strategy regarding both climate change and the security of energy supply in its member states. One of the targets set was ensuring that by 2020, 20% of the European energy supply comes from renewable energy sources. In the 2009 Renewable Energy Directive an agreement was reached regarding each country's share in reaching the target set for 2020. For the UK this means that by then 15% of the total energy consumption (electricity consumption, traffic, industry. etc.) should come from renewable energy sources.

One of the major pillars under the European Climate Policy is the European Union Emissions Trading System (EU ETS). In principle the system comes down to putting a price on carbon emissions. All large emitters of carbon dioxide are obliged to monitor and report their annual carbon dioxide emissions and are also obliged to return annually an amount of emission allowances equal to their emission to the Government. These emission allowances are annually allocated by the Government. In case an installation has performed well the company is allowed to sell its excess emission allowances. On the other hand if their allowances do not cover the amount of emitted carbon dioxide, allowances have to be purchased from other companies.

Year	Carbon price [£/ tonne CO <sub>2</sub> ]
2010	14.10
2020	16.30
2030	70.00
2040	135.00

Source: Mott MacDonald, 2010.

**Table 10.1:** carbon prices.

The idea behind the EU ETS system is that large sources of carbon dioxide, like heavy industry and electricity generating plants, are encouraged to reduce their emissions or trade

emissions. The trading results in a carbon price, see table 10.1, and hence ensures that throughout the system emissions cuts are made there where they are cheapest. With respect to the electricity market this ensures on the longer term that producing electricity from high carbon sources will be replaced by low carbon sources.

#### 10.4.2 National policy

The UK Government is planning to reach its 2050 climate changes objectives through a combination of regulatory and financial measures, which are:

- the Renewables Obligation Order, which requires 30% of the UK's electricity to be generated from renewable energy sources by 2020;
- Feed-in-Tariffs for small scale renewable energy generation (up to 5 MW). These are fixed prices that are not linked to the wholesale market prices and provide a high level of security for investors not traditionally involved in the production of electricity.

Also the Government intends to make the UK a world leader in the low-carbon and environmental sector. This sector includes new forms of energy including wave and tidal power, offshore wind and civil nuclear power [HM Treasury 2010]. Further the Government is looking into the possibility of a Green Investment Bank that should co-invest in major projects in the low carbon energy sector and hence help fund the introduction of renewable energy [DECC, 2010].

Electricity generation type	ROCs per MWh
Hydro-electric	1
Onshore wind	1
Offshore wind	1.5
Wave	2
Tidal stream	2
Tidal barrage	2
Tidal lagoon	2
Standard gasification	1
Advanced gasification	2
Dedicated biomass	1.5

ROCs = Renewables Obligation Certificates.

Source: DECC, 2010.

**Table 10.2:** differentiation of ROCs by technology.

#### Renewables Obligation Order

The Renewables Obligation (RO) primarily focuses on large scale renewable electricity generation by energy companies. Licensed electricity suppliers are obliged to source an increasing proportion of their annual sales from renewable energy or pay a penalty. Different electricity generators are issued Renewables Obligation Certificates (ROCs) for each MWh of eligible renewable electricity they produce [DECC, 2010]. Different technologies receive different numbers of ROCs, thus taking into account differences in technology costs. See table 10.2 for some characteristic values.

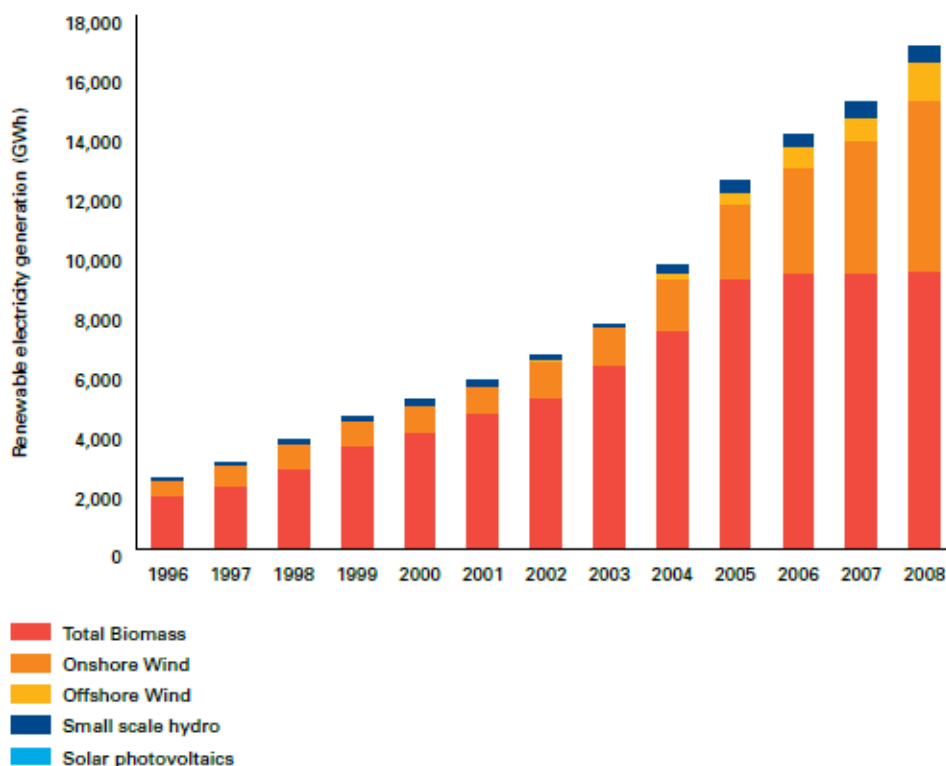
As said the RO requires electricity suppliers to source at least part of their electricity from renewable energy generators. These obligation levels are set annually by the Department of Energy and Climate Change, see table 10.3 for an overview of past and future obligation levels.

Obligation period	Obligation level [ROCs/MWh]
2002-2003	3.0
2009-2010	9.7
2010-2011	11.1
2011-2012	12.4
2012-2013	15.8

Source: website DECC.

Table 10.3: Renewables Obligation Certificates per MWh.

The electricity generators can sell their ROCs to electricity suppliers or traders in order to receive a premium on top of their electricity price. When an electricity supplier does not have acquired enough ROCs proportionate to the electricity that was sold, a penalty has to be paid, the so-called buy-out price. This price is annually updated by the Office for Gas and Electricity Markets (Ofgem), in the base year 2002-2003 the buy-out price was £30/MWh, in 2009-2010 £37.19 and it will be £36.99 in the year 2010-2011<sup>8</sup>.



Source: Digest of UK Energy Statistics; Energy Trends (2009)

Figure 10.4: growth in renewable energy generation from 1996 to 2008.

Since the introduction of the Renewables Obligation the amount of renewable energy generated had been tripled, see figure 10.4. Because the UK's main electricity network is located close to the Wash estuary and the networks ability to exploit tidal power is deemed

<sup>8</sup> Source: Ofgem information note on the Renewables Obligation buy-out price.

large, see figure 10.6, the RO may offer opportunities. Despite the fact the RO is not specifically meant for this purpose a electricity generator company may be interested in participate in a tidal range scheme in the Wash estuary.

### Feed-in-Tariffs

The Feed-in-Tariffs (FIT) are meant to support eligible small scale low carbon electricity technologies financially. The scheme supports projects up to a 5 MW limit by requiring electricity suppliers to pay generation tariffs to the owners of the scheme, based on the number of kWh they generate. In case a surplus of energy is available and this surplus is exported to the electricity network a guaranteed additional export tariff of 3 p/kWh is to be paid by the electricity supplier [Energy Trends, 2011]. The FIT support:

- new anaerobic digestion schemes;
- solar photovoltaic schemes;
- hydro schemes;
- wind schemes.

The present target groups are individual households, organisations, communities and businesses not traditionally engaged in the electricity market, but the new Government has proposed to introduce a FIT for renewable electricity schemes with a generation capacity larger than 5 MW [DECC, 2010]. So this may be an interesting development regarding the economic feasibility of a tidal power plant in the Wash estuary.

## 10.5 Current UK energy prices

The energy prices in this section are given as the average lifetime levelised energy generating costs (LEC). The LEC represents the price at which a specific source should generate energy in order to break even. As shown in the equation below the LEC is computed as the ratio of the net present value of the total of construction, operating and maintenance costs during the economic lifetime over the net present value of net electricity generation during the economic lifetime:

$$LEC = \frac{\sum_{t=1}^n \frac{I_t + M_t + F_t}{(1+r)^t}}{\sum_{t=1}^n \frac{E_t}{(1+r)^t}} \quad [10.1]$$

Were:

LEC	: average lifetime levelised electricity generation costs	[£/MWh]
$I_t$	: capital costs in year t	[£]
$M_t$	: fixed operating and maintenance costs in year t	[£]
$F_t$	: variable operating and maintenance costs in year t	[£]
$E_t$	: net electricity generation in year t	[MWh]
r	: discount rate <sup>1)</sup>	[-]
n	: economic lifetime of power plant	[yr]

<sup>1)</sup> At present a discount rate of 10% is advised by DECC, source: Mott MacDonald 2010 and Parsons Brinkerhoff 2010.

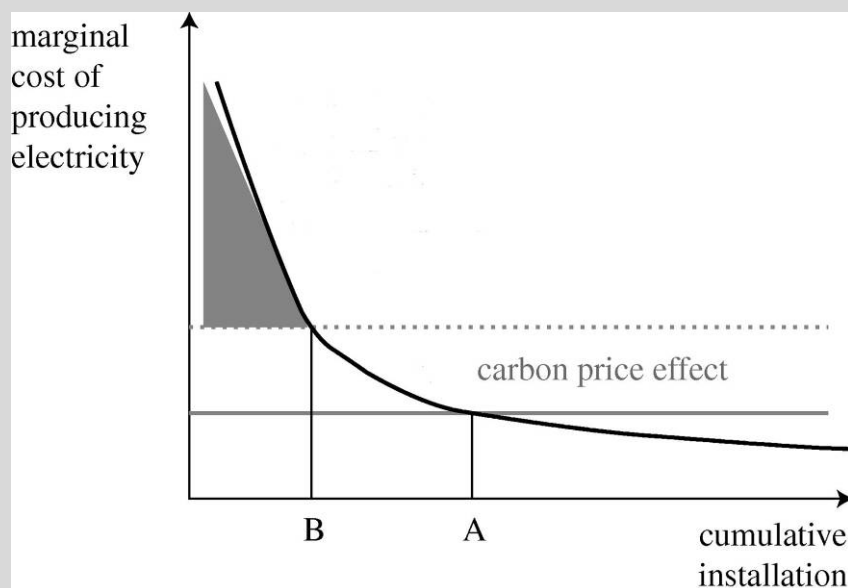
The variable operating and maintenance costs include forecasted changes in carbon and fuel prices, which are likely to increase the LEC of high carbon emission power plants in the future. On the other hand nuclear and renewable energy sources are very likely to benefit from these developments as they do not emit carbon dioxide and do not rely on fossil fuels,

hence their operational costs will be relatively low compared to those of high carbon energy schemes and thus these techniques become more competitive. However the drawbacks of renewable energy are first of all the fact that these schemes require high upfront investments and therefore tend to be more sensitive with respect to future uncertainty in the electricity prices and secondly that most of these technologies are still at the beginning of their learning curve, see the box 2.

In 2010 both Mott MacDonald and Parsons Brinkerhoff published figures on LEC in the UK. In both studies fuel and carbon emission costs are included, as is a 10% discount rate. The prices in both studies are based on cost data of recent tender contacts [Mott MacDonald 2010 and Parsons Brinkerhoff 2010]. The results of both studies need careful interpretation as they are based on cost estimates and not the actual costs after construction, but it is believed that these figures are accurate enough to determine the economic feasibility of a tidal power plant in the Wash estuary.

### Box 2: technology learning and experience curve.

Figure 10.5 shows the principle of a learning curve. A new technology is at first much more expensive than an already established technology, but in time the costs tend to decrease as a result of learning effects (R&D, increased efficiency & experience) and economies of scale. As the installed capacity increases at some point the break even point is reached (point A) and the new technology is competitive with the established technology. As a result of the European carbon pricing policy the break even point is reached in an earlier stage (point B).



Solid black line: new technology; solid grey line: established technology;  
Dotted grey line: established technology with CO<sub>2</sub> pricing

**Figure 10.5:** technology learning and experience curve (Courtesy: *Stern*, 2007).

In the table below the results of the Parsons Brinkerhoff study are presented, in this study the stated price per kWh is based on the assumption that the electricity is delivered at the power plant's high voltage grid connection. This is done in order to exclude current uncertainties concerning transmission costs due to the geographical distribution of generating types.

Because different scenarios with respect to future developments in fossil fuel and carbon prices were regarded in the study, cost ranges are defined.

Technology	LEC range [p/kWh]
Natural gas turbine, no CO <sub>2</sub> capture	5.5-11
Natural gas turbine, with CO <sub>2</sub> capture	6-13
Coal, with CO <sub>2</sub> capture	10-15.5
New nuclear energy	8-10.5
Onshore wind farm	8-11
Offshore wind farm	15-21
Tidal range power (Severn estuary)	15.5-39

Source: *Parsons & Brinkerhoff 2010.*

**Table 10.4:** UK energy LEC ranges for different generation technologies.

Table 10.5 presents the findings of the Mott MacDonald study. In this study the transmission costs are included, which may lead to a skewed comparison as at any one location the transmission costs may differ considerably. On the other hand the transmission costs are an important cost factor. The Mott MacDonald study adopts the central projections, made by DECC, for both the future fuel and carbon price developments.

Technology	LEC [p/kWh]
Natural gas turbine, no CO <sub>2</sub> capture	8
Natural gas turbine, with CO <sub>2</sub> capture	11.3
Coal, with CO <sub>2</sub> capture	14.2
New nuclear energy	9.9
Onshore wind farm	9.4
Offshore wind farm	16.1

Source: *Mott MacDonald 2010.*

**Table 10.5:** UK energy LEC for different generation technologies.

In advance it is to be expected that both studies should lead to more or less the same results as they are both based on the same data and development scenarios and also that the Mott MacDonald figures should be close to the middle of the ranges as defined by Parsons and Brinkerhoff, as Mott MacDonald used central projections for both fuel and carbon prices. Initially this seems to be the case as the Mott MacDonald results lie within the LEC ranges of the Parsons and Brinkerhoff study, but a closer inspection learns that the Mott MacDonald results lie more close to the upper boundary for energy from natural gas turbines with CCS, coal plants with CCS and nuclear power plants. For offshore wind farms the Mott MacDonald value ends up close to the lower boundary of the LEC range.

An possible explanation would be the rapidly increasing carbon prices over the coming decades, see table 10.1. However in that case the LEC of the natural gas turbine without CCS should also lie more close to the upper boundary of the LEC range and moreover, the LEC for nuclear energy should lie around the centre of the range as no carbon dioxide is produced. Therefore the most probable explanation is that this is an effect of including the transmission costs in the Mott MacDonald study.

Because the Parsons and Brinkerhoff LEC ranges includes also high and low projections and therefore express the uncertainties of future development in the global energy market it is decided to use these figures while determining the economical feasibility of a tidal range power plant in the Wash estuary. However the main reason to choose the LEC ranges as a basis for comparison is the fact that the transmission costs are excluded from the study, which makes the comparison between generation technologies more fair.

As can be seen in the figure 10.6 the UK transmission networks ability to exploit tidal power is very high, hence no exorbitant high costs are to be expected to make changes to the national grid.

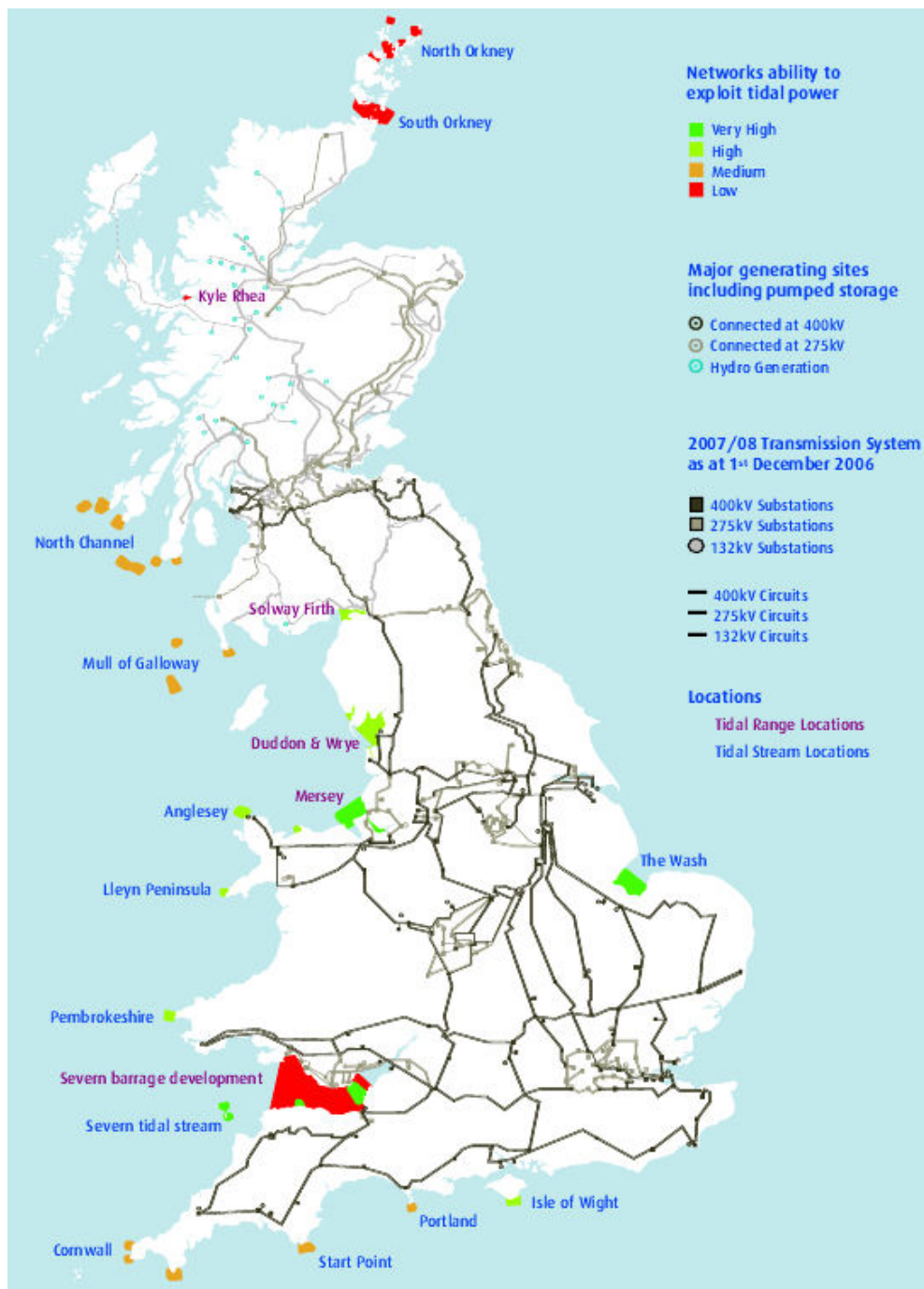


Figure 10.6: grid constraints on tidal power (Courtesy: National Grid).



## **Appendix 11**

*Top views and longitudinal cross-sections navigation locks*



## **Appendix 11.1**

### *Commercial navigation lock*



## **Appendix 11.2**

### *Recreational navigation lock*



## **Appendix 12**

*Preliminary design tidal power plant*



## 12.1 Introduction

In this appendix it will be determined whether, in case of the Wash estuary, an ebb generation scheme or a two-way generation scheme is most suited at the selected site of the storm surge barrier (see chapter 5). The decisions ultimately leading to the preliminary design of a tidal power plant are presented, as is the approach followed.

## 12.2 Density of sea water

Since several rivers discharge into the Wash estuary, the volumetric density of the sea water decreases from the mouth of the estuary towards the landward side of the basin. Salinity contours within the estuary are depicted in Figure 12.1. From this figure can be concluded that at the chosen barrier line the salt concentration is approximately 33,000 mg/l. However as a result of the construction of the barrier, the salt concentration is likely to decrease.

The combined peak discharge of the rivers into the estuary is relatively low ( $180 \text{ m}^3/\text{s}$ , see section 2.4). Hence, a conservative estimation of the future salt concentration will be 30‰. Since the average water temperature of the North Sea lies between  $15^\circ \text{C}$  in summer and  $5^\circ \text{C}$  in winter<sup>9</sup>, an yearly average of  $10^\circ \text{C}$  is assumed. Using NOAA's water density calculator<sup>10</sup> the volumetric density of the sea water in the Wash estuary is computed to be  $1023 \text{ kg/m}^3$ . In the remainder of this appendix a volumetric density of  $1025 \text{ kg/m}^3$  will be used in the computations.

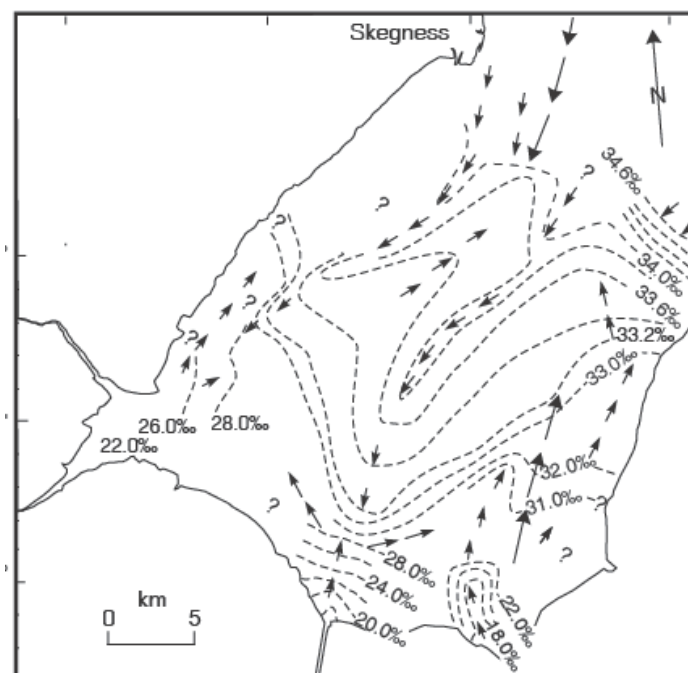


**Figure 12.1:** salinity contours within the Wash estuary.  
(Courtesy: Wingfield et al, 1978)

<sup>9</sup> Source: <http://nl.wikipedia.org/wiki/Zeeewater>.

<sup>10</sup> Source: <http://www.csgnetwork.com/h2odenscalc.html>

### 12.3 Rated head

The runner diameter and generated power of a turbine depend on the rated head<sup>11</sup>. When the head over the TPP exceeds the rated head the guide vanes are gradually closed. Thus reducing the discharge, while keeping the generator at rated capacity<sup>12</sup>. In case the head drops below the rated head the capacity of the generator reduces and as a consequence the generated power decreases.

According to Song and van Walsum the rated head is accurately estimated using equation 12.1 [Song and van Walsum, 2006]:

$$H_r = C_{TPP} \cdot R_{mean} \quad [12.1]$$

Were:

$H_r$	: rated head	[m]
$C_{TPP}$	: factor expressing the mode of operation of a TPP:	[-]
	- single effect mode of operation: $C_{TPP} = 0.66$	
	- double effect mode of operation: $C_{TPP} = 0.50$	
$R_{mean}$	: mean tidal range	[m]

In case of the Wash estuary the mean tidal range is 4.70 m. Hence, the rated head for both an ebb generation scheme and a two-way generation scheme is 3.10 m and 2.35 m respectively. In reality the head difference over the barrier is likely to vary between 65% and 125% of the rated head<sup>13</sup>. However it is not economical to design the TPP based on the mean spring tidal range, because the corresponding head difference will only occur during 20%<sup>14</sup> of the total time during one year. This would lead to the installation of too many turbines.

### 12.4 Runner diameter

The runner diameter is an important parameter in the design of a TPP because:

- the electromechanical equipment generally accounts for 45% to 55% of the direct costs of the TPP. Hence, the number of turbines needed, significantly influences the economy of the TPP scheme;
- it has a large influence on the civil engineering costs, as the dimensions of the turbine governs the dimensions of the power house, see figure 12.1;
- the turbine discharge capacity determines the number and size of the sluices.

Historically the effort to reduce unit costs has lead to an increase in turbine size. According to manufactures of turbines, a diameter of 9 to 10 m is considered to be a reasonable extension of existing knowledge and technology [Clarke, 2007]. Generally larger turbines tend to have a higher turbine and generator efficiency. Therefore it seems logical to install a limited number or turbines with a large runner diameter. It should be kept in mind however, that the required submergence in order to avoid cavitation should be available without the need for excavation.

<sup>11</sup> Rated head = lowest head for which the turbine is capable of driving the generator at its rated capacity. Hence, the turbine guide vanes are opened to their maximum.

<sup>12</sup> Rated capacity = maximum power that the generator is allowed to produce.

<sup>13</sup> Source: Indian Institute of Technology Kharagpur.

<sup>14</sup> Spring tide occurs each 14.765 days, hence 24.72 times a year. Assuming a duration of 3 days, during which the tidal range is equal to or larger than the mean spring tidal range, results in  $24.72 \cdot 3 / 365 = 0.20$ .



Runner diameter [m]	BoS ebb generation [mODN]	BoS two-way generation [mODN]
4.0	-11.00	-12.00
4.5	-12.15	-13.25
5.0	-13.25	-14.50
5.5	-14.40	-15.75
6.0	-15.50	-17.00
6.5	-16.65	-18.25
7.0	-17.75	-19.50
7.5	-18.90	-20.75
8.0	-20.00	-22.00
8.5	-21.15	-23.25
9.0	-22.25	-24.50

Table 12.1: relation between runner diameter and Bottom of Structure (BoS).

### 12.5 Turbine, generator and plant efficiency

Turbine efficiency cannot be considered to be constant, it varies with the load and is largest at the design head<sup>15</sup>. In table 12.2 an overview is given of both the turbine and generator efficiency of bulb turbines, as are the discharge coefficient in turbinning mode and the plant efficiency.

Scheme	$\eta_t$ <sup>1)</sup>	$\eta_g$ <sup>2)</sup>	$m$	$\eta$
Ebb generation	0.90	0.95	0.93	0.80
2-way generation	0.85	0.95	0.92	0.75

<sup>1)</sup> Source: Alstom Power France.

<sup>2)</sup> Source: RETScreen international.

Table 12.2: turbine, generator and plant efficiency.

The approach followed for determining the discharge coefficient is included in appendix 12.1. Note that the values included in the table above are only a crude estimation of  $m$ . The plant efficiency is computed using equation 12.2.

$$\eta = \eta_t \cdot \eta_g \cdot m \quad [12.2]$$

Were:

$\eta$	:	plant efficiency	[-]
$\eta_t$	:	turbine efficiency	[-]
$\eta_g$	:	generator efficiency	[-]
$m$	:	discharge coefficient	[-]

Despite the fact that the head difference changes in time the efficiency remains fairly constant over a large range of loads and is only expected to be lower during neap tide.

<sup>15</sup> Design head = net head for which the turbine has preferably its maximum efficiency.

## 12.6 Rated discharge

The rated discharge per turbine can be computed using the rated head and runner diameter, see equation 12.3 [Schweiger and Gregori, 1992]:

$$Q_r = \eta_t \cdot m \cdot A_t \cdot \sqrt{2 \cdot g \cdot H_r} \quad [12.3]$$

Were:

$Q_r$	: rated discharge	[m <sup>3</sup> /s]
$\eta_t$	: turbine efficiency	[-]
$m$	: discharge coefficient	[-]
$A_t$	: area of the turbine runner	[m <sup>2</sup> ]
$g$	: gravitational acceleration	[m <sup>2</sup> /s]
$H_r$	: rated head	[m]

In case of an ebb generation scheme the rated discharge per turbine amounts to:

$$Q_r = 0.90 \cdot 0.93 \cdot \frac{\pi}{4} \cdot 8^2 \cdot \sqrt{2 \cdot 9.81 \cdot 3.10} = 328 \text{ m}^3/\text{s}$$

In the same way the rated discharge for a two-way generation scheme is computed, resulting in:

$$Q_r = 0.85 \cdot 0.92 \cdot \frac{\pi}{4} \cdot 8^2 \cdot \sqrt{2 \cdot 9.81 \cdot 2.35} = 267 \text{ m}^3/\text{s}$$

As discussed in section 12.3 the maximum discharge occurs at the rated head, see figure 12.2. The discharge relation as a function of the head difference over the barrier is presented in equation 12.4.

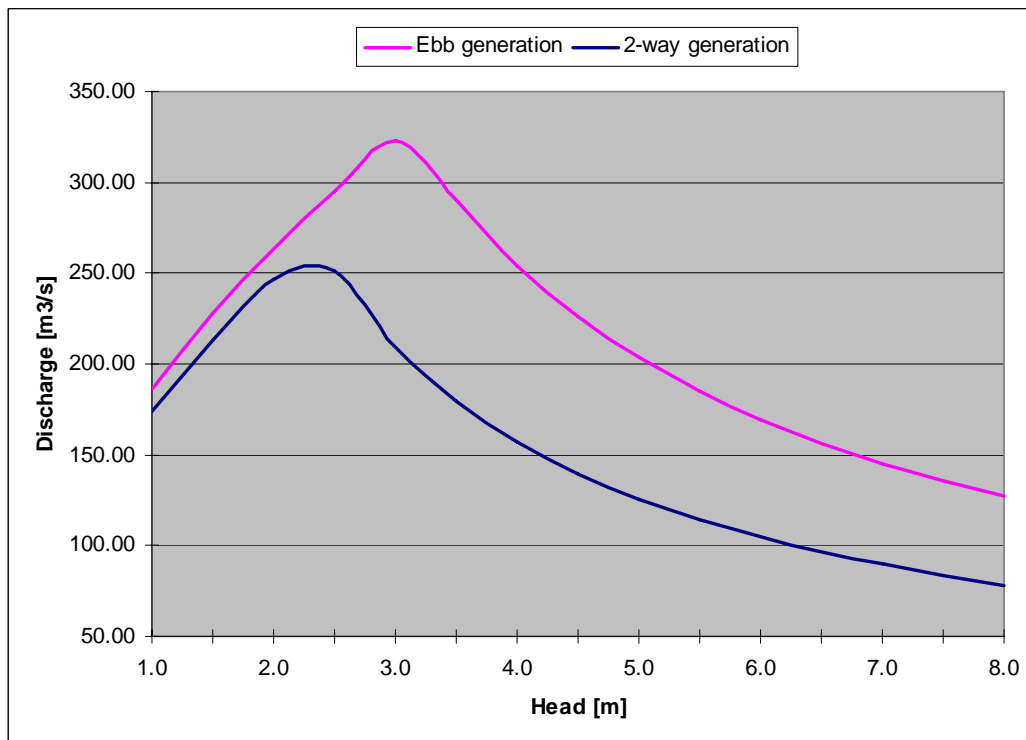


Figure 12.2: turbine discharge as a function of the head difference over the barrier.

$$f(Q) = \begin{cases} 0 \leq H \leq H_r & Q = \eta_t \cdot m \cdot \frac{\pi}{4} \cdot D^2 \cdot \sqrt{2 \cdot g \cdot H} \\ H > H_r & Q = \frac{P_{rated}}{\eta_g \cdot \rho \cdot g \cdot H} \end{cases} \quad [12.4]$$

Were:

$P_{rated}$  : rated capacity, see section 12.7 [W]  
 $\eta_g$  : generator efficiency [-]

## 12.7 Rated capacity

Figure 12.3 depicts the power output per turbine as a function of the head difference over the storm surge barrier, as described by equation 12.5.

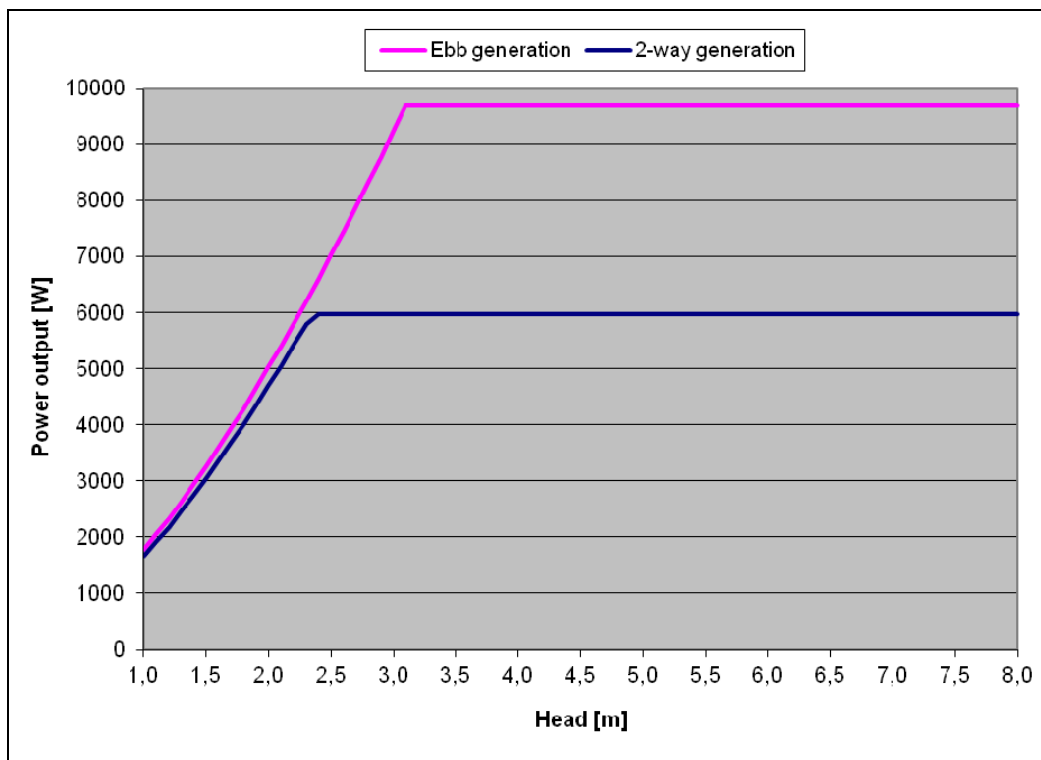


Figure 12.3: power output as a function of the head difference over the barrier.

$$f(P) = \begin{cases} 0 \leq H \leq H_r & P = \eta_g \cdot \rho \cdot g \cdot Q \cdot H \\ H > H_r & P = P_{rated} \end{cases} \quad [12.5]$$

Were:

$P$  : power [W]  
 $P_{rated}$  : rated capacity<sup>16</sup> [W]  
 $\eta_g$  : generator efficiency [-]  
 $\rho$  : volumetric density of sea water [kg/m<sup>3</sup>]  
 $g$  : gravitational acceleration [m<sup>2</sup>/s]  
 $Q$  : discharge [m<sup>3</sup>/s]  
 $H$  : head [m]

<sup>16</sup> Rated capacity = maximum power that the generator is allowed to produce.

The rated capacity for both an ebb generation scheme and a two-way generation scheme is calculated using equation 12.6 [Schweiger and Gregori, 1992].

$$P_{rated} = \eta_g \cdot \rho \cdot g \cdot Q_r \cdot H_r \quad [12.6]$$

Were:

$$\begin{aligned} Q_r & : \text{ rated discharge} & [\text{m}^3/\text{s}] \\ H_r & : \text{ rated head} & [\text{m}] \end{aligned}$$

This results in a rated capacity per turbine of 9.70 MW for an ebb generation scheme and of 6.00 MW for a two-way generation scheme.

### 12.8 Specific speed, number of pole pairs and operating speed

Because generators only operate at a predefined fixed rotational speed [Krueger, 1976] the operating speed has to be determined. In order to be able to do that, first several turbine parameters have to be determined.

Starting with the specific speed of the turbine, that depends on the rated head. The specific speed can be computed using the empirical relation presented in equation 12.7 [Schweiger and Gregori, 1992].

$$n_q = \left( \frac{920650}{H_r} \right)^{\frac{1}{2.058}} \quad [12.7]$$

Were:

$$\begin{aligned} n_q & : \text{ specific speed} & [\text{rpm}] \\ H_r & : \text{ rated head} & [\text{m}] \end{aligned}$$

With  $H_r = 3.10$  m for an ebb generation scheme and  $H_r = 2.35$  m for a two-way generation scheme, equation 12.7 results in a specific speed of 456.30 rpm and 522.04 rpm respectively.

Now a first estimate of the operation speed can be found using equation 12.8 [Schweiger and Gregori, 1992].

$$n = \frac{n_q}{\sqrt{Q_r} \cdot \sqrt[4]{H_r^{-3}}} \quad [12.8]$$

Were:

$$\begin{aligned} n & : \text{ operational speed} & [\text{rpm}] \\ n_q & : \text{ specific speed} & [\text{rpm}] \\ Q_r & : \text{ rated discharge} & [\text{m}^3/\text{s}] \\ H_r & : \text{ rated head} & [\text{m}] \end{aligned}$$

In case of an ebb generation scheme a first estimate of the operational speed is 58.86 rpm, while in case of a two-way generation scheme the first estimation amounts to 60.64 rpm.

Using equation 12.9 the number of pole pairs on the generator can be determined [Schweiger and Gregori, 1992]. A multiple of four generator pole pairs is preferred, however in practice most standard generators are available in a multiple of two pole pairs. In the United Kingdom the frequency of the national power grid is 50 Hz [National Grid].

$$N_p = \frac{120 \cdot f}{n} \quad [12.9]$$

Were:

$N_p$	:	number of generator pole pairs	[-]
$n$	:	operational speed	[rpm]
$f$	:	national grid frequency	[Hz]

In case of an ebb generation scheme the number of generator pole pairs is (multiple of two poles) :

$$N_p = \frac{120 \cdot 50}{58.86} = 101.94 \Rightarrow 102$$

While for a two-way generation scheme the number of pole pairs is:

$$N_p = \frac{120 \cdot 50}{60.64} = 98.94 \Rightarrow 100$$

The required number of generator pole pairs is rounded upwards because the variation of the head difference over the storm surge barrier is expected to vary more than 10% of the rated head, in which case the next lower operational speed is to be selected [Krueger, 1976].

For both schemes the operational speed of the turbine, and hence the generator, is computed using a rewritten form of equation 12.9 and the above determined number of generator pole pairs. For an ebb generation scheme this results in an operational speed of 58.82 rpm and for a two-way generation scheme in 60.00 rpm. Because the generator only operates with a predefined rotational speed the turbine also has to operate with a fixed operational speed. Since the head varies during the tidal cycle, which in turn varies over the lunar month, the discharge should be regulated by means of the turbine's adjustable guide and runner vanes, see equation 12.8. In order to keep the operational speed constant, the relation between head difference over the barrier and discharge is presented in figure 12.4 for the selected turbine.

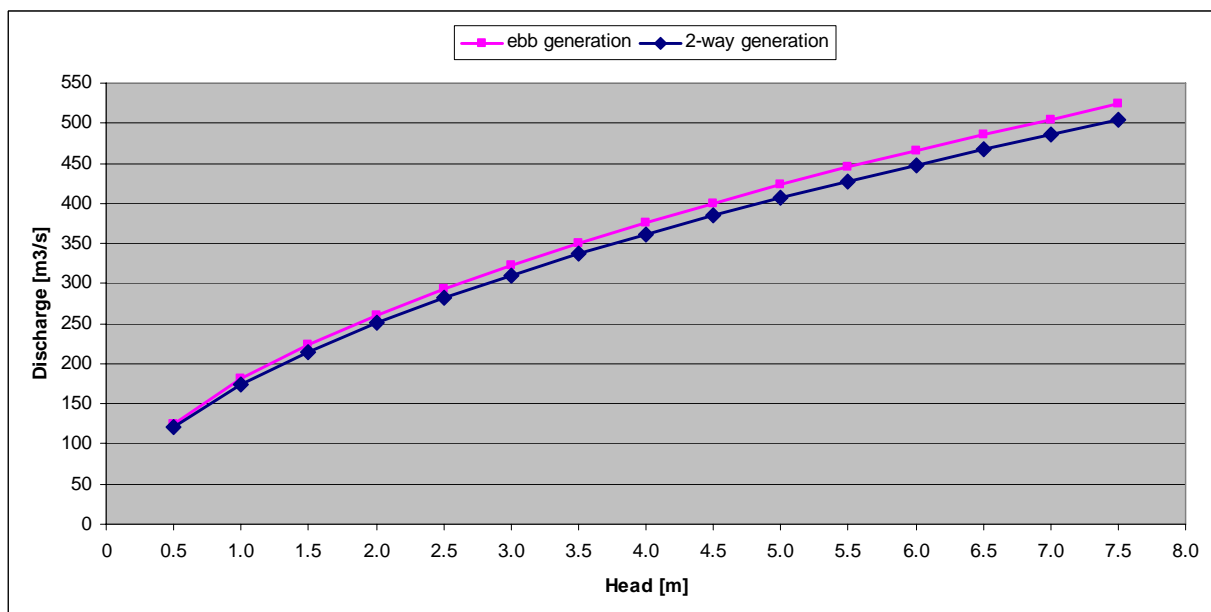


Figure 12.4: relation between head and discharge to maintain a constant operational speed.

## 12.9 Check on cavitation

Now the relevant turbine parameters are known it is time to check whether or not the turbine axis is located low enough below tailwater level to prevent cavitation<sup>17</sup>. The required distance between the minimum tailwater level and the cavitation reference point at the axis of the turbine runner can be computed using equation 12.10 [Kpordze, 1983]:

$$H_{tail} = H_a - H_v - \sigma \cdot H = \frac{P_a - P_v}{\rho_w \cdot g} - \sigma \cdot H \quad [12.10]$$

Were:

$H_{tail}$	: required difference between minimum tailwater level and the cavitation reference point <sup>18</sup>	[m]
$H_a$	: atmospheric pressure head	[m]
$H_v$	: vapour pressure head at 20° C	[m]
$\sigma$	: cavitation coefficient	[-]
$H$	: net effective head, here rated head	[m]
$P_a$	: atmospheric pressure, $101.325 \cdot 10^3$	[Pa] <sup>19</sup>
$P_v$	: vapour pressure at 20° C, $2.3 \cdot 10^3$	[Pa] <sup>20</sup>
$\rho_w$	: volumetric density of water	[kg/m <sup>3</sup> ]
$g$	: gravitational acceleration	[m/s <sup>2</sup> ]

The average temperature of the surface water layer within the North Sea is around 5° to 6° C in winter and 14° to 15° C in summer. Near the coast the temperature in summer can rise to 17° C<sup>21</sup>. Therefore it is not likely that the sea water in the Wash estuary will reach temperatures higher than 20° C. Thus the vapour pressure at 20° C is used to check for the occurrence of cavitation.

For a bulb turbine the governing equations for the specific speed and cavitation coefficient are [Kpordze, 1983]:

$$\sigma = 7.625 \cdot 10^{-5} \cdot n_q^{1.485} \quad [12.11]$$

Were:

$\sigma$	: cavitation coefficient	[-]
$n_q$	: specific speed	[rpm]

And

$$n_q = \frac{n \cdot \sqrt{P_r}}{H_r^{1.25}} \quad [12.12]$$

Were:

$n$	: operating speed	[rpm]
$P_r$	: rated capacity of the turbine	[kW]
$H_r$	: rated head	[m]

<sup>17</sup> Cavitation occurs when the absolute pressure at the axis of the turbine runner approaches the vapour pressure. In case the absolute pressure in the water flow equals the vapour pressure, vapour bubbles come into existence. These bubbles will suddenly implode when areas of higher pressure are reached, causing large temporary tension stresses in the material of the runner blades. The development and imploding of the vapour bubbles is called cavitation.

<sup>18</sup>  $H_{tail}$  is defined positive from the tailwater level in upward direction.

<sup>19</sup> Source: [http://nl.wikipedia.org/wiki/Atmosfeer\\_%28eenheid%29](http://nl.wikipedia.org/wiki/Atmosfeer_%28eenheid%29).

<sup>20</sup> Source: <http://nl.wikipedia.org/wiki/Dampdruk>.

<sup>21</sup> Source: <http://nl.wikipedia.org/wiki/Zeewater>.

Equation 12.11 represents the regression equation of an analysis performed by Kporde, based on the empirical equations for the cavitation coefficient provided by six manufacturers of bulb turbines. Note that according to Kporde the correlation coefficient is not very high [Kporde, 1983]. Since it is not known in advance which manufacturer will deliver the turbines it is in this stage considered to be sufficient to get a general impression of the cavitation coefficient. Hence, equation 12.11 will be used in this study. In case of an ebb generation scheme:

$$n_q = \frac{58.82 \cdot \sqrt{9.70 \cdot 10^3}}{3.10^{1.25}} = 1408 \text{ rpm} \quad \text{Therefore,} \quad \sigma = 7.625 \cdot 10^{-5} \cdot 1408^{1.485} = 3.61$$

$$H_{tail} = \frac{101.325 \cdot 10^3 - 2.3 \cdot 10^3}{1025 \cdot 9.81} - 3.61 \cdot 3.10 \approx -1.35 \text{ m}$$

In case of two-way generation scheme:

$$n_q = \frac{60.00 \cdot \sqrt{5.98 \cdot 10^3}}{2.35^{1.25}} = 1595 \text{ rpm} \quad \text{Therefore,} \quad \sigma = 7.625 \cdot 10^{-5} \cdot 1595^{1.485} = 4.35$$

$$H_{tail} = \frac{101.325 \cdot 10^3 - 2.3 \cdot 10^3}{1025 \cdot 9.81} - 4.35 \cdot 2.35 \approx -0.40 \text{ m}$$

In case of ebb generation scheme the tailwater level must be at least 1.35 m above the runner axis, for the two-way generation scheme this should be at least 0.40 m. Based on the turbine's specific speed it seems that this outcome is wrong, because a higher specific speed should result in a lower absolute pressure in the draft tube. The computed cavitation coefficients confirm this, as this coefficient has a larger value in case of a two-way generation scheme. However the net effective head for such a scheme is smaller compared to that of an ebb generation scheme. This explains the unexpected smaller value of  $H_{tail}$  for the two-way generation scheme.

Both the minimum water levels at the North Sea side of the storm surge barrier and within the basin occur during Low Water Spring. The lowest outside water level is taken to be Mean Low Water Spring (MLWS) and is approximately -2.00 mODN, see table 11 in section 2.1.3. The lowest basin levels are computed using the following assumptions:

- in ebb mode the two-way generation scheme will stop generating just after low water occurs, the ebb generation scheme just before reaching half the mean spring tidal range above MLWS;
- the minimum required head under which the turbine can operate is 1.00 m;
- the mean spring tidal range is 6.25 m.

This results in the following minimum basin water levels:

Ebb generation:	Two-way generation:
-2.00 mODN	-2.00 mODN
3.13 m	1.00 m
+1.13 mODN	-1.00 mODN
1.00 m	
≈ 0.00 mODN	

Hence, for both schemes the lowest tailwater level during operation occurs at the North Sea side. Taking into account the annual significant wave height on the North Sea ( $H_s = 2.80$  m), the governing lowest tailwater level with respect to cavitation is -4.80 mODN. According to Bernshtein the runner axis is located at -9.20 mODN, see figure 12.1.

Turbine parameter	Unit	Ebb generation	2-way operation
Lowest tailwater level	[mODN]	-4.80	-4.80
$H_{tail}^{1)}$	[m]	1.35	0.40
Required runner axis level	[mODN]	-6.15	-5.20
Actual runner axis level <sup>2)</sup>	[mODN]	-9.20	-9.20

<sup>1)</sup>  $H_{tail}$  = required difference between minimum tailwater level and the cavitation reference point (runner axis).

<sup>2)</sup> The runner axis is located  $0.9 \cdot D_1$  below the lowest outside water level [Bernshtein, 1996].

**Table 12.3:** check on cavitation.

Based on table 12.3 it can be concluded that no problems concerning cavitation are to be expected, because the actual runner axis level lies well below the runner axis level required to prevent cavitation. Even under storm conditions when wave heights may exceed 2.80 m no cavitation will occur.

### 12.10 Annual energy yield and power

During every one year not all tidal cycles can be used to generate energy. The main reasons for not using a tidal cycle are; maintenance, (electro) mechanic failure and severe storm conditions. According to Clarke every year 3-5% of the tidal cycles are lost to the generation of energy [Clarke, 2007]. So on average 96% of the annual tidal cycles is used to generate energy, this amounts to  $0.96 \cdot 705.50 = 677.30$  tidal cycles per annum. The annual energy yield can be estimated using equations 12.13 and 12.14 [Duivendijk, 2007].

$$E_{annum} = \frac{\eta \cdot N_{tide} \cdot \rho \cdot g \cdot H_{av} \cdot V_{av}}{3.6 \cdot 10^{12}} \quad [12.13]$$

Were:

$E_{annum}$	: annual energy yield	[GWh]
$\eta$	: plant efficiency	[-]
$N_{tide}$	: number of tides in a year generating energy	[-]
$\rho$	: volumetric density of water	[kg/m <sup>3</sup> ]
$g$	: gravitational acceleration	[m/s <sup>2</sup> ]
$H_{av}$	: average head per tidal cycle	[m]
$V_{av}$	: average volume of water per tidal cycle	[m <sup>3</sup> ]

And

$$V_{av} = \Delta\zeta_{av} \cdot A_{av} \quad [12.14]$$

Were:

$V_{av}$	: average volume of water per tidal cycle	[m <sup>3</sup> ]
$\Delta\zeta_{av}$	: average water level variation	[m]
$A_{av}$	: average basin area	[m <sup>2</sup> ]

In figures 12.5 and 12.6 a schematic representation of the operation of the TPP during a tidal cycle is presented for both an ebb generation scheme and a two-way generation scheme. The area hatched with red represents the period during which energy is generated from the tide.

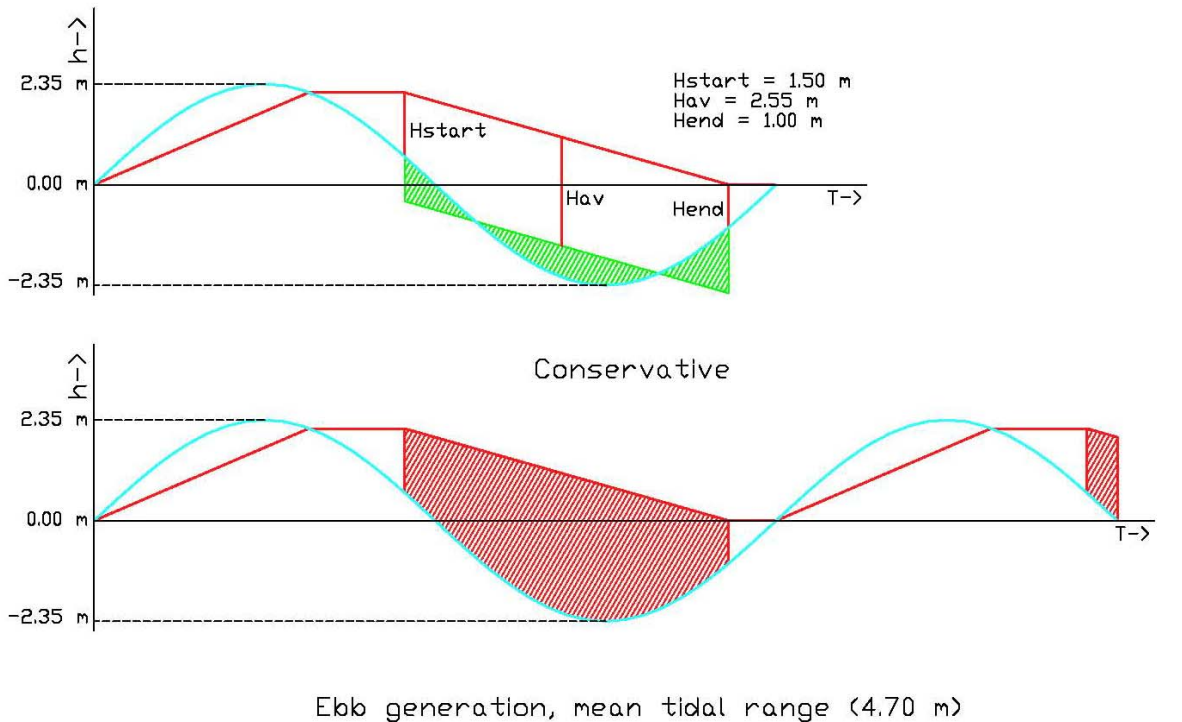


Figure 12.5: schematic representation of TPP operation in case of an ebb generation scheme (Not to scale).

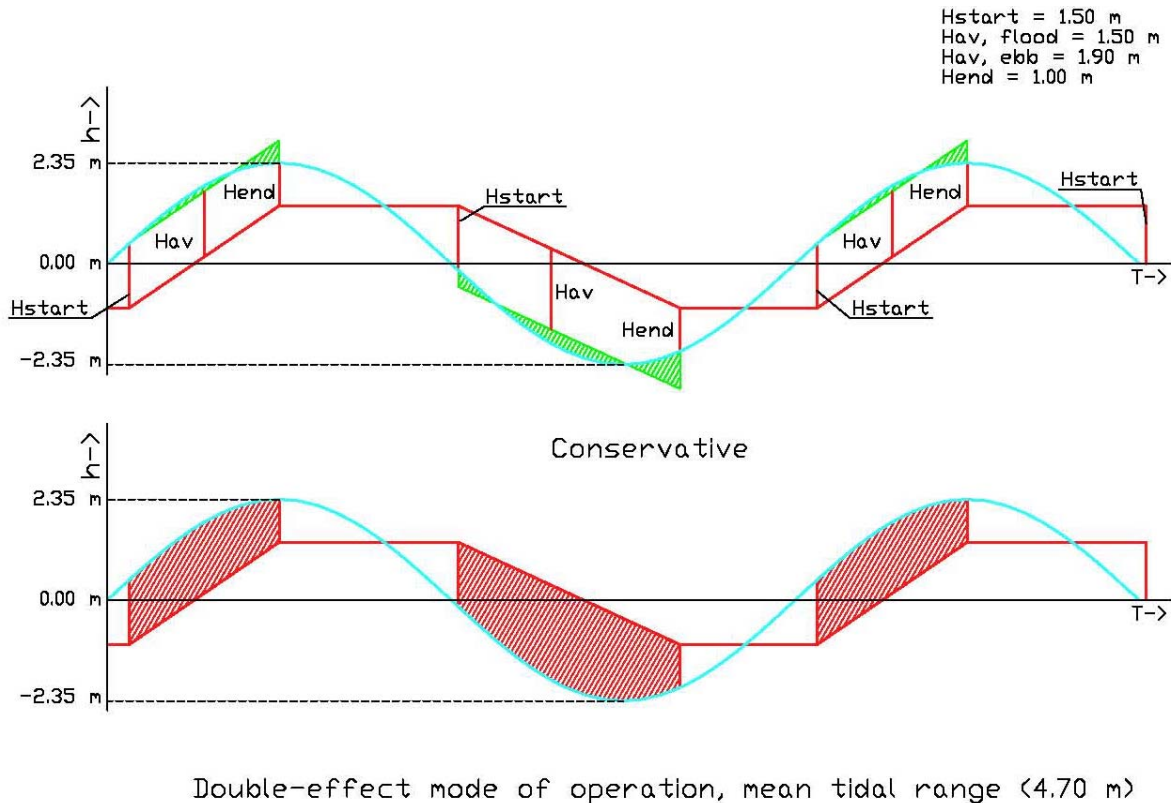


Figure 12.6: schematic representation of TPP operation in case of a two-way generation scheme (Not to scale).

In the upper images of figures 12.5 and 12.6, the green hatched area above the tidal curve equals the areas below the curve. The vertical distance between basin level (red line) and the parallel green line represents the average head during the period that the TPP is generating energy. This average head is tabulated in table 12.4 for the mean tidal range, mean neap tidal range and mean spring tidal range. In the performed schematisation the water level within the basin is assumed to change linearly during turbining and sluicing modes, in reality the water level variation in the basin will be non-linear.

Type of scheme	Neap tide		Mean tide		Spring tide	
	$H_{av, ebb}$	$H_{av, flood}$	$H_{av, ebb}$	$H_{av, flood}$	$H_{av, ebb}$	$H_{av, flood}$
	[m]	[m]	[m]	[m]	[m]	[m]
Ebb generation	1.85	-	2.55	-	3.25	-
2-way generation	1.35	1.30	1.90	1.50	2.45	1.65

**Table 12.4:** average head during TPP operation at neap, mean and spring tide.

In order to be able to determine the average volume of water that passes through the turbines during one tidal cycle, first the average basin area and water level variation must be known. The water level variation is measured from figures 12.5 and 12.6 as the distance between highest and lowest basin level. This results in 2.15 m and 2.40 m for an ebb generation scheme and a two-way generation scheme respectively.

The water covered area of the Wash estuary during high tide is approximately 615 km<sup>2</sup>, during low tide the water covered area reduces to 325 km<sup>2</sup> [Dare, 2004]. Because the Wash estuary's geometry is very complex and no numerical model of the sea bed topography is available, it is assumed that the average water covered area amounts to 470 km<sup>2</sup>, which is the mean value. As a result of the fact that the selected barrier line does not enclose the whole estuary the water covered area during high tide is determined to be 465 km<sup>2</sup>. Using the same ratio between the water covered area during high and low tide as was found by Dare, results in a water covered area during low tide of approximately 245 km<sup>2</sup>. Hence the average water covered area is established to be approximately 355 km<sup>2</sup>. However this is a very crude estimation, therefore during any future design stage a numerical model describing the relation between water level and basin area should be developed. In table 12.5 an overview is given of all basin parameters required to estimate the annual energy yield and the generated power per tidal cycle.

Basin parameter	Unit	Ebb generation	2-way operation	
			Ebb mode	Flood mode
Average head per tidal cycle	[m]	2.55	1.90	1.50
Average water level variation	[m]	2.15	2.40	2.40
Average basin area	[m <sup>2</sup> ]	355·10 <sup>6</sup>	355·10 <sup>6</sup>	355·10 <sup>6</sup>
Average volume of water per tidal cycle	[m <sup>3</sup> ]	763·10 <sup>6</sup>	852·10 <sup>6</sup>	852·10 <sup>6</sup>
fraction of tidal cycle during which TPP is operational	[-]	0.50	0.33	0.22
Average discharge per tidal cycle	[m <sup>3</sup> /s]	34.15·10 <sup>3</sup>	57.76·10 <sup>3</sup>	86.64·10 <sup>3</sup>

**Table 12.5:** overview basin parameters.

Using equations 12.13 and 12.14 results in the estimated annual energy yields, as presented in table 12.6.

Type of scheme	Ebb generation [GWh/yr]	Flood generation [GWh/yr]	Total [GWh/yr]
Ebb generation	2945	n.a.	2945
2-way generation	2300	1810 (1020) <sup>1)</sup>	4110 (3320) <sup>1)</sup>

<sup>1)</sup> As a result of the assumption made with respect to the average basin area the computed value is unrealistic, as during flood generation significantly less energy is generated than during ebb generation. Hence the values between brackets are based on the assumption that during flood mode the generated power amounts to 2/3 of the power generated during ebb generation mode, see table 12.7.

**Table 12.6:** estimation of the annual energy yield.

As was to be expected the annual energy yield of a two-way generation scheme is larger than the annual energy yield for an ebb generation scheme. However it is too early to conclude that the two-way generation scheme is the most suited TPP. The main reason for this is that a larger volume of water has to pass through the barrier in a shorter time frame, compared to an ebb generation scheme. Hence, the two-way generation scheme is most likely to require a much larger number of turbines.

Also the generated power is a more important factor than the estimated annual energy yield. The power generated per tidal cycle can be estimated by means of equations 12.15 and 12.16 [Duivendijk, 2007].

$$P = \eta \cdot \rho \cdot g \cdot H_{av} \cdot Q_{av} \quad [12.15]$$

Were:

$P$	:	power generated per tidal cycle	[W]
$\eta$	:	plant efficiency	[-]
$\rho$	:	volumetric density of water	[kg/m <sup>3</sup> ]
$g$	:	gravitational acceleration	[m/s <sup>2</sup> ]
$H_{av}$	:	average head per tidal cycle	[m]
$Q_{av}$	:	average discharge per tidal cycle	[m <sup>3</sup> /s]

And

$$Q_{av} = \frac{V_{av}}{\varepsilon \cdot T_{tide}} \quad [12.16]$$

Were:

$Q_{av}$	:	average discharge per tidal cycle	[m <sup>3</sup> /s]
$V_{av}$	:	average volume of water per tidal cycle	[m <sup>3</sup> ]
$\varepsilon$	:	fraction of tidal cycle during which TPP is operational	[-]
$T_{tide}$	:	duration of the tidal cycle, M <sub>2</sub> -tide: $T_{tide} = 44700$ s	[s]

According to literature the fraction of the tidal cycle during which a TPP is operational is 0.50 in case of an ebb generation scheme and 0.85 in case of an two-way scheme [Clarke, 2007 and Bernshtein, 1996]. From figures 12.5 and 12.6 it is determined that in case of an ebb generation scheme the operational time frame of the TPP corresponds indeed to 50% of the

tidal cycle, but in case of a two-way generation scheme the operational time frame is only 55% of the tidal cycle<sup>22</sup>.

The generated power per tidal cycle, as computed using equations 12.15 and 12.16, is presented in table 12.7.

Type of scheme	Ebb generation [MW]	Flood generation [MW]	Total [MW]
Ebb generation	700	n.a.	700
2-way generation	828	980 (552) <sup>1)</sup>	1808 (1380) <sup>1)</sup>

<sup>1)</sup> As a result of the assumption made with respect to the average basin area the computed value is unrealistic. It is assumed that the power generated during flood generation mode equals 2/3 of the power generated during ebb generation mode. These values are shown between brackets.

**Table 12.7:** estimation of the power generated per tidal cycle.

From table 12.7 can be concluded that the power generated per tidal cycle in case of a two-way generation scheme is approximately 2.5 times as large as for an ebb generation scheme. However, as will be shown in the next section, this will require a much larger number of turbines, while on the other hand no sluices will be required. Therefore a fair comparison is only possible based on the estimated cost, see section 6.6.4 of the main report.

Note that the power generated during flood generation mode is 154 MW larger than during ebb generation mode. This is a direct result of the assumption made with respect to the average basin area. In reality this will be the other way around because during flood generation the highest head occurs when the basin level is lowest and as a consequence a large part of the basin area consists of sand and mudflats that have fallen dry. Hence the water level in the basin will rise faster during the beginning of flood generation than near the end of the operation. During ebb generation mode the opposite occurs, the basin's water level will fall relatively slow during the early stages, when the largest head differences are present, compared to the end of operation when the sand and mud flats fall dry again. Therefore in case of a two-way generation scheme the power generated during ebb generation mode will be assumed governing with respect to the design of the tidal power plant.

### 12.11 Design discharge and installed power

In order to be able to determine the installed power of the tidal power plant, the required number of turbines has to be established with equation 12.17.

$$n_t = \frac{P}{P_d} \quad [12.17]$$

Were:

$n_t$	:	number of turbines	[-]
$P$	:	power generated per tidal cycle	[MW]
$P_d$	:	power per turbine during mean tidal cycle	[MW]

<sup>22</sup> During 33% of the tidal cycle, the tidal power plant is in ebb generation mode. And during 22% of the duration of the tidal cycle the tidal power plant is in flood generation mode.

With the use of equations 12.3 and 12.6 the design discharge<sup>23</sup> and power per turbine during a mean tidal cycle in case of an ebb generation scheme turn out to be:

$$Q_d = \eta_t \cdot m \cdot A_t \cdot \sqrt{2 \cdot g \cdot H_{av}} = 0.90 \cdot 0.93 \cdot \frac{\pi}{4} \cdot 8^2 \cdot \sqrt{2 \cdot 9.81 \cdot 2.55} \approx 298 \text{ m}^3/\text{s}$$

And

$$P_d = \eta_g \cdot \rho \cdot g \cdot Q_d \cdot H_{av} = 0.95 \cdot 1025 \cdot 9.81 \cdot 298 \cdot 2.55 = 7.26 \cdot 10^6 \text{ W}$$

Hence the number of turbines required for an ebb generation scheme is:

$$n_t = \frac{700}{7.26} = 96.41 \Rightarrow 97$$

For a two-way generation scheme the design discharge and power per turbine during ebb generation mode are:

$$Q_d = \eta_t \cdot m \cdot A_t \cdot \sqrt{2 \cdot g \cdot H_{av}} = 0.85 \cdot 0.92 \cdot \frac{\pi}{4} \cdot 8^2 \cdot \sqrt{2 \cdot 9.81 \cdot 1.90} = 240 \text{ m}^3/\text{s}$$

And

$$P_d = \eta_g \cdot \rho \cdot g \cdot Q_d \cdot H_{av} = 0.95 \cdot 1025 \cdot 9.81 \cdot 240 \cdot 1.90 = 4.36 \cdot 10^6 \text{ W}$$

Despite the fact that on paper the power generated during flood generation mode is larger than during ebb generation mode, the power generated during ebb generating mode is used for the calculation of the required number of turbines. The reason for this is already discussed in the previous section:

$$n_t = \frac{828}{4.36} = 189.91 \Rightarrow 190$$

Since during flood generation mode per tidal cycle the same average volume of water must be able to enter the basin as is discharged during ebb generation mode, only in a shorter period of time, it should be checked whether or not this is possible with the derived number of turbines. During flood generation mode the design discharge and power per turbine are:

$$Q_d = \eta_t \cdot m \cdot A_t \cdot \sqrt{2 \cdot g \cdot H_{av}} = 0.85 \cdot 0.92 \cdot \frac{\pi}{4} \cdot 8^2 \cdot \sqrt{2 \cdot 9.81 \cdot 1.50} = 213 \text{ m}^3/\text{s}$$

And

$$P_d = \eta_g \cdot \rho \cdot g \cdot Q_d \cdot H_{av} = 0.95 \cdot 1025 \cdot 9.81 \cdot 213 \cdot 1.50 = 3.05 \cdot 10^6 \text{ W}$$

The required number of turbines during flood generation mode is:  $n_t = \frac{550}{3.05} = 180$ .

Therefore the 190 turbines required for ebb generation mode have also sufficient capacity during flood generation mode.

<sup>23</sup> Design discharge = discharge corresponding to the average head during a mean tidal cycle.

By means of equation 12.18 the installed power can be determined.

$$P_{inst} = n_t \cdot P_{rated} \quad [12.18]$$

Were:

$P_{inst}$	:	installed power	[MW]
$n_t$	:	number of turbines	[-]
$P_{rated}$	:	rated capacity	[MW]

The installed power in case of an ebb generation scheme is:

$$P_{inst} = 97 \cdot 9.70 = 940 \text{ MW}$$

And in case of a two-way generation scheme:

$$P_{inst} = 190 \cdot 6.00 = 1140 \text{ MW}$$



## **Appendix 12.1**

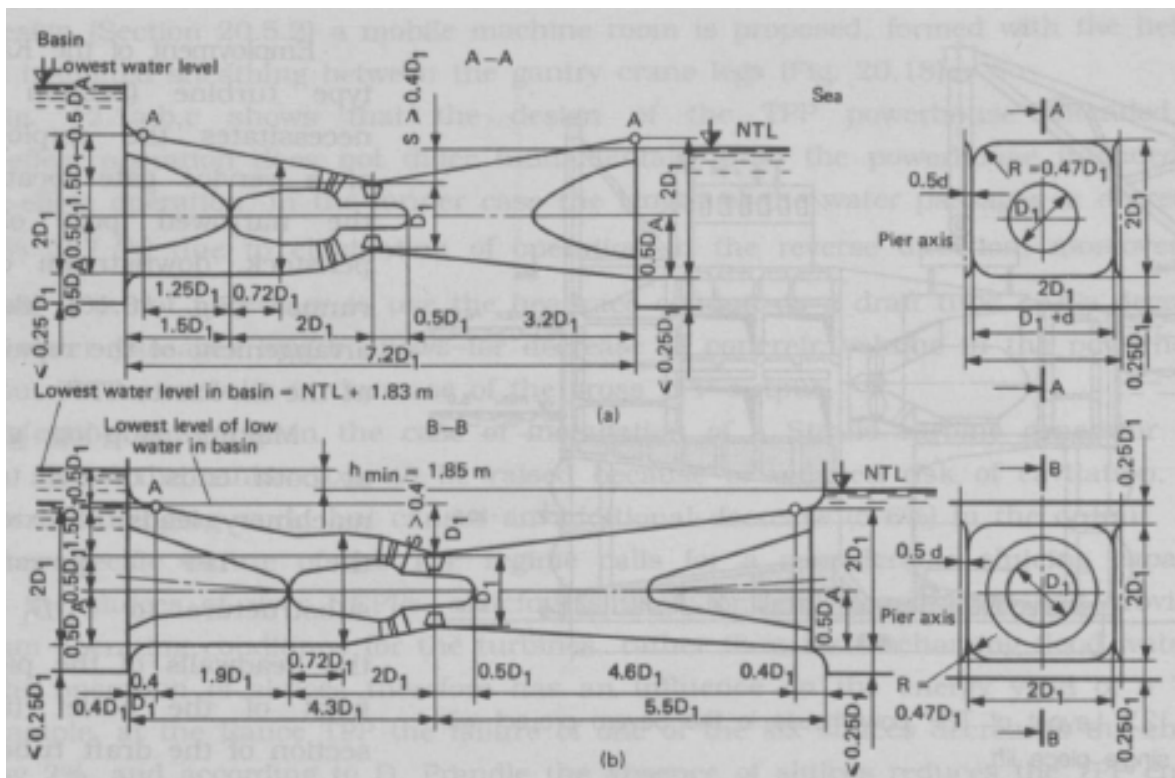
*Determination of the discharge coefficient for a single turbine*



### 12.1.1 Introduction

In this appendix a crude estimation of the discharge coefficient ( $m$ ) is made for both an ebb generation scheme and a two-way generation scheme. The following assumptions are made:

- the maximum discharge (discharge at rated head) is used, because in that case the flow velocities are largest and hence the energy losses;
- the draft tube is schematized as a square straight tube with a width and height that is the average between the runner diameter and the entree and exit of the draft tube;
- the draft tube is considered to be symmetrical;
- when sluicing the turbine capacity reduces to 70% of the capacity during turbinning [Bernshtein, 1996].



Taken from Bernshtein, 1996.

**Figure 12.1.1:** overall dimensions of the power house setting in case of a bulb unit.  
(a) single effect operation (b) double effect operation.

Using figure 1, the overall dimensions of the draft tube are determined for a runner diameter of 8.0 m. The results are listed in table 12.1.1.

Dimension of draft tube	Unit	Single effect operation	Double effect operation
Length	[m]	57.60	78.40
Height opening	[m]	16.00	16.00
Width opening	[m]	16.00	16.00
Runner diameter	[m]	8.00	8.00
Rated discharge	[m <sup>3</sup> /s]	392	341
Flow velocity	[m/s]	2.70	2.40

**Table 12.1.1:** overall dimensions of the draft tube.

### 12.1.2 Discharge coefficients

According to Nortier the discharge coefficient can be computed using equation 12.1.1 [Nortier and de Koning, 1991].

$$m = \frac{1}{\sqrt{\xi_{total}}} \quad [12.1.1]$$

Were:

$m$	:	discharge coefficient	[-]
$\xi_{tot}$	:	overall loss coefficient	[-]

Bernshtein states that when a turbine operates in sluicing mode the turbine capacity equals approximately 70% of the capacity in turbining mode [Bernshtein, 1996]. Therefore the discharge coefficient during sluicing is found by multiplying the result found with equation 12.1.1 by a factor 0.7. The computed discharge coefficients are presented in table 12.1.2.

	Single effect operation	Double effect operation
In turbine mode	0.93	0.92
In sluicing mode	0.65	0.64

Table 12.1.2: discharge coefficients ( $m$ ).

The discharge through the turbine, without taking the efficiency of both the generator and the turbine into account, is computed using equation 12.1.2 [Nortier and de Koning, 1991].

$$Q_t = m \cdot A \cdot \sqrt{2 \cdot g \cdot \Delta H} \quad [12.1.2]$$

Were:

$Q_t$	:	discharge through turbine	[m <sup>3</sup> /s]
$m$	:	discharge coefficient	[-]
$A$	:	wet area of the draft tube	[m <sup>2</sup> ]
$g$	:	gravitational acceleration	[m/s <sup>2</sup> ]
$\Delta H$	:	head over the barrier	[m]

### 12.1.3 Energy losses

The total energy loss in the draft tube is the summation of the energy losses at the entry and exit *and* the friction losses inside the draft tube. In the remainder of this section these losses will be computed for both schemes. A summary is presented in table 12.1.3 stating the computed energy losses and loss coefficients, as are the total energy loss and the overall loss coefficient ( $\xi_{total}$ ).

Type of scheme	$\xi_{in}$ [-]	$\xi_{friction}$ [-]	$\xi_{out}$ [-]	$\xi_{total}$ [-]	$\Delta H_{in}$ [m]	$\Delta H_{friction}$ [m]	$\Delta H_{out}$ [m]	$\Delta H_{total}$ [m]
Single effect operation	0.1	0.063	1.0	1.16	0.037	0.023	0.37	0.43
Double effect operation	0.1	0.085	1.0	1.19	0.029	0.025	0.29	0.34

Table 12.1.3: energy losses and loss coefficients.

### Energy loss at entry

The energy loss at entry of the turbine caisson can be computed using equation 12.1.3 [Nortier and de Koning, 1991].

$$\Delta H_{in} = \xi_{in} \cdot \frac{u^2}{2 \cdot g} \quad [12.1.3]$$

Were:

$\Delta H_{in}$	:	energy loss at entry	[m]
$\xi_{in}$	:	entrance loss	[-]
$u$	:	flow velocity in the draft tube	[m/s]
$g$	:	gravitational acceleration	[m/s <sup>2</sup> ]

And

$$\xi_{in} = \left( \frac{1}{\mu} - 1 \right)^2 \quad [12.1.4]$$

Were:

$\mu$	:	contraction coefficient	[-]
-------	---	-------------------------	-----

The edges of the turbine caissons are rounded (small radius), according to Nortier resulting in a contraction coefficient of 0.76 [Nortier and de Koning, 1991]. Hence the entrance loss ( $\xi_{in}$ ) is 0.1. Using equation 12.1.3 the energy loss at entry amounts to 0.037 m for a ebb generation scheme and 0.029 m for a two-way generation scheme.

### Energy loss due to friction

The energy loss due to friction in the turbine caisson can be computed using equation 12.1.5 [Nortier and de Koning, 1991].

$$\Delta H_{friction} = \xi_{friction} \cdot \frac{u^2}{2 \cdot g} \quad [12.1.5]$$

Were:

$\Delta H_v$	:	energy loss at entry	[m]
$\xi_{friction}$	:	friction loss	[-]
$u$	:	flow velocity in the draft tube	[m/s]
$g$	:	gravitational acceleration	[m/s <sup>2</sup> ]

And

$$\xi_{friction} = \frac{\lambda \cdot L}{4 \cdot R} \quad \text{with} \quad R = \frac{A}{O} \quad [12.1.6]$$

Were:

$\lambda$	:	friction factor	[-]
$L$	:	length of the draft tube	[m]
$R$	:	hydraulic radius	[m]
$A$	:	wet area of the draft tube	[m <sup>2</sup> ]
$O$	:	wet circumference of the draft tube	[m]

And also

$$\lambda = \frac{8 \cdot g}{C^2} \quad \text{with} \quad C = 18 \cdot \log\left(\frac{12 \cdot R}{k}\right) \quad [12.1.7]$$

Were:

$\lambda$	:	friction factor	[-]
$g$	:	gravitational acceleration	[m/s <sup>2</sup> ]
$C$	:	Chézy constant	[m <sup>0.5</sup> /s]
$R$	:	hydraulic radius	[m]
$k$	:	wall roughness, for concrete $k = 1.5 \cdot 10^{-3}$ m	[m]

The dimensions of the fictional draft tube are 12.12 m<sup>2</sup>. This results in a hydraulic radius of 3.0 m. With equation 12.1.7 the friction factor is computed to be 0.013. Combining equations 12.1.5 and 12.1.6 results for an ebb generation scheme in an energy loss due to friction of:

$$\Delta H_{friction} = \frac{\lambda \cdot L}{4 \cdot R} \cdot \frac{u^2}{2 \cdot g} = \frac{0.013 \cdot 57.8}{4 \cdot 3} \cdot \frac{2.7^2}{2 \cdot 9.81} = 0.023 \text{ m}$$

For a two-way generation scheme this becomes:

$$\Delta H_{friction} = \frac{\lambda \cdot L}{4 \cdot R} \cdot \frac{u^2}{2 \cdot g} = \frac{0.013 \cdot 78.4}{4 \cdot 3} \cdot \frac{2.4^2}{2 \cdot 9.81} = 0.025 \text{ m}$$

### Energy loss at exit

The energy loss at the exit of the turbine caisson can be computed using equation 12.1.8 [Nortier and de Koning, 1991].

$$\Delta H_{out} = \xi_{out} \cdot \frac{u^2}{2 \cdot g} \quad [12.1.8]$$

Were:

$\Delta H_{out}$	:	energy loss at entry	[m]
$\xi_{out}$	:	exit loss	[-]
$u$	:	flow velocity in the draft tube	[m/s]
$g$	:	gravitational acceleration	[m/s <sup>2</sup> ]

Because the water is discharged into a basin the total velocity head is dissipated. Hence, the exit loss ( $\xi_{out}$ ) is 1.0. Hence for an ebb generation scheme the energy loss at exit is 0.37 m and for a two-way generation scheme 0.29 m.

## **Appendix 13**

*Discharge coefficient for a single sluice*



### 13.1 Introduction

In case an ebb generation scheme is selected, sluices are required in addition to the turbines. In this appendix a crude estimation of the discharge coefficient ( $m$ ) is made for a single sluice. The following assumptions are made:

- the sluice can be regarded as a broad-crested submerged weir;
- a basin storage approach is valid in case of the Wash estuary;
- the hydraulic radius of the sluice opening is based on the average water level above the sluice's floor during the mean tidal cycle;
- the gate radius should be equal or larger than the gate height;
- the trunnion is preferably located above the maximum water level in the basin.

The overall gate dimensions presented in table 13.1 are based on figures of existing tainter gates applied by the U.S. Army Corps of Engineers [U.S.A.C.E, 2000; appendix D].

Dimension of sluice gate	Unit	Single effect operation
Width	[m]	20.00
Height	[m]	10.00
Gate radius	[m]	12.00
Height trunnion above floor level	[m]	8.00
Floor level	[mODN]	-2.00
Width sluice caisson	[m]	26.00

Table 13.1: overall dimensions of a sluice gate.

### 13.2 Discharge coefficient

In case of a broad-crested submerged weir the average discharge through one single sluice opening can be computed using equation 13.1 [Nortier and de Koning, 1991].

$$Q_{sl} = m \cdot B \cdot h_b \cdot \sqrt{2 \cdot g \cdot (h_{NS} - h_b)} \quad [13.1]$$

Were:

$Q_{sl}$	:	average discharge through sluice	[m <sup>3</sup> /s]
$m$	:	discharge coefficient	[-]
$B$	:	width of the sluice opening	[m]
$g$	:	gravitational acceleration	[m/s <sup>2</sup> ]
$h_b$	:	average water level in the basin	[m above sluice floor]
$h_{NS}$	:	average water level on the North Sea	[m above sluice floor]

The mean tidal range within the Wash estuary is 4.70 m. Therefore the maximum water level reached is 2.35 m above Mean Sea Level (0.00 mODN). Hence during rising water the average tidal level at the North Sea is approximately 1.15 mODN. This results in an average water level of 3.15 m above the sluice's floor level. Since it is assumed that a basin storage approach is valid, the average water level at the basin side will not differ much from that at the North Sea. On average a difference of 0.25 m is assumed to be present. Hence the average water level on the basin side of the sluice gate is 2.90 m above floor level.

The discharge coefficient can be computed using equation 13.2 [Nortier and de Koning, 1991].

$$m = \frac{1}{\sqrt{\xi_{total}}} \quad [13.2]$$

Were:

$m$  : discharge coefficient [-]  
 $\xi_{tot}$  : overall loss coefficient [-]

The overall loss coefficient represents the summation of entrance loss, friction loss and exit loss coefficients. In the remainder of this section these single coefficients will be determined, in order to derive the overall loss coefficient. A summary of the computed loss coefficients is presented in table 13.2.

Type of scheme	$\xi_{in}$ [-]	$\xi_{friction}$ [-]	$\xi_{out}$ [-]	$\xi_{total}$ [-]	$m$ [-]
Ebb generation	0.44	0.08	1.0	1.52	0.80

Table 13.2: loss coefficients.

With an overall loss coefficient ( $\xi_{total}$ ) of 1.56 the discharge coefficient ( $m$ ) for a single sluice is 0.80 (equation 13.2).

### 13.2.1 Entrance loss coefficient

The entrance loss coefficient of the sluice opening can be computed using equation 13.3 [Nortier and de Koning, 1991].

$$\xi_{in} = \left( \frac{1}{\mu} - 1 \right)^2 \quad [13.3]$$

Were:

$\xi_{in}$  : entrance loss [-]  
 $\mu$  : contraction coefficient [-]

Since the sluice opening has a rectangular shape and is not fully submerged, Nortier advises a contraction coefficient of 0.60 [Nortier and de Koning, 1991]. Therefore the entrance loss coefficient ( $\xi_{in}$ ) is 0.44.

### 13.2.2 Friction loss coefficient

The friction loss coefficient for the sluice is computed using equations 13.4 and 13.5 [Nortier and de Koning, 1991].

$$\xi_{friction} = \frac{\lambda \cdot L}{4 \cdot R} \quad \text{with} \quad R = \frac{A}{O} \quad [13.4]$$

Were:

$\xi_{friction}$	:	friction loss	[-]
$\lambda$	:	friction factor	[-]
$L$	:	width of the sluice caisson	[m]
$R$	:	hydraulic radius	[m]
$A$	:	wet area of the sluice opening	[m <sup>2</sup> ]
$O$	:	wet circumference of the sluice opening	[m]

And

$$\lambda = \frac{8 \cdot g}{C^2} \quad \text{with} \quad C = 18 \cdot \log\left(\frac{12 \cdot R}{k}\right) \quad [13.5]$$

Were:

$\lambda$	:	friction factor	[-]
$g$	:	gravitational acceleration	[m/s <sup>2</sup> ]
$C$	:	Chézy constant	[m <sup>0.5</sup> /s]
$R$	:	hydraulic radius	[m]
$k$	:	wall roughness, for concrete $k = 1.5 \cdot 10^{-3}$ m	[m]

As the governing average water level above the sluice floor is 2.90 m, the hydraulic radius becomes 1.27 m. Hence the friction factor is computed to be 0.015 (equation 13.5) and the friction loss coefficient 0.08 (equation 13.4).

### 13.2.3 Exit loss coefficient

Because the water is discharged into a large basin the total velocity head is dissipated. Hence, the exit loss coefficient ( $\xi_{out}$ ) is 1.0 [Nortier and de Koning, 1991].



## **Appendix 14**

*Estimation construction costs*



## **Appendix 14.1**

### *Embankment dam*



## **Appendix 14.2**

### *Caisson dam*



## **Appendix 14.3**

*Final conceptual design*



## **Appendix 15**

### *Storage basin approach*



## 15.1 Introduction

The theoretical basis for analysing and performing computations with respect to the behaviour of long waves in shallow water are the continuity equation (equation 15.1) and the equation of motion (equation 15.2), together also referred to as the St. Venant equations or shallow water equations. These equations represent a coupled system of differential equations describing the relation between water level and discharge as function of time and distance.

$$B \cdot \frac{\partial h}{\partial t} + \frac{\partial Q}{\partial x} = 0 \quad (15.1)$$

And

$$\frac{\partial Q}{\partial t} + \frac{\partial}{\partial x} \left( \frac{Q^2}{A_s} \right) + g \cdot A_s \cdot \frac{\partial h}{\partial x} + c_f \cdot \frac{|Q| \cdot Q}{A_s \cdot R} = 0 \quad (15.2)$$

Were:

$B$	: storage width	[m]
$h$	: water level	[m]
$t$	: time	[s]
$Q$	: discharge	[m <sup>3</sup> /s]
$x$	: distance	[m]
$A_s$	: current-carrying cross-section	[m <sup>2</sup> ]
$c_f$	: friction coefficient	[-]
$R$	: hydraulic radius	[m]

In this appendix this theory will be used to determine the effects of the barrier on the tidal amplitude within the Wash basin. This is relevant with respect to the optimisation of the sluicing capacity of the tidal power plant. In the approach followed the number of turbines remains fixed at 97, as was determined in chapter 6. The reason for this is that the number of turbines is based on the average head during the mean tidal cycle, where it was implicitly assumed that the average water level at the basin side will not differ much from that at the North Sea<sup>24</sup>. The purpose of the performed analysis is to see what sluicing capacity is required so that the basin level will approximately equal the maximum outside water level during the mean tidal cycle.

## 15.2 Storage basin approach

In case both the basin is closed except for a narrow opening at one side *and* if the time frame required by the tidal wave to propagate through the basin is small compared too the period of the tidal wave, the velocities are so small that resistance and inertia can be neglected. Hence, the water level within the basin may be assumed horizontal at all times, only changing in time. The precondition is checked using equation 15.3.

$$L_{basin} \leq \frac{1}{20} \cdot L_{wave} \quad (15.3)$$

Were:

$L_{basin}$	: basin length	[m]
$L_{wave}$	: length tidal wave	[m]

<sup>24</sup> On average a difference of 0.25 m is assumed to be present during the filling of the basin.

The basin length of alternative 2-3 is 18,750 m. while the length of the tidal wave corresponds too 442,733 m, assuming a depth of 10 m. Since the basin behind the future storm surge barrier is a closed basin with only a storage function<sup>25</sup>, both conditions are met. Hence the storage basin approach may be used. Integration of equation 15.1 over space results in the continuity equation applicable for a storage basin:

$$A_b \cdot \frac{dh}{dt} = Q \quad (15.4)$$

Were:

$A_b$	:	basin area	[m <sup>2</sup> ]
$h$	:	water level	[m]
$t$	:	time	[s]
$Q$	:	net discharge	[m <sup>3</sup> /s]

In the analysis the basin area is assumed to be constant in time. This is a simplification because in reality the surface area of the basin will be a function of the water level. However this relation is unknown.

### 15.3 Rigid column approach

The turbine and sluice openings form the connection between the basin and the North Sea. Since no storage is possible within the turbine openings and because the free surface area of the sluice openings is small compared too the free surface area within the basin, storage in the connection may be neglected. Therefore the connection has only a transport function. Due to the fact that the length of the connection is much smaller than the wave length of the tidal wave, the connection can be schematised as a rigid column. Integration of the equation of motion (equation 15.2) over the entire length of the connection results in the equation of motion applicable to the rigid column approach:

$$h_{NS}(t) - h_b(t) = \frac{L}{g \cdot A_s} \cdot \frac{dQ}{dt} + \chi \cdot \frac{|Q| \cdot Q}{g \cdot A_s^2} \quad (15.5)$$

Were:

$h$	:	water level	[m]
$t$	:	time	[s]
$Q$	:	discharge	[m <sup>3</sup> /s]
$h_{NS}$	:	water level on North Sea	[m]
$h_b$	:	basin water level	[m]
$L$	:	length	[m]
$g$	:	gravitational acceleration	[m/s <sup>2</sup> ]
$A_s$	:	current-carrying cross-section	[m <sup>2</sup> ]
$\chi$	:	loss coefficient	[-]

<sup>25</sup> As was already proved in chapter 2, the discharge from the tidal rivers into the estuary is small compared to the tidal prism and therefore is neglected. Also tidal locking ensures that the discharge is only present during low tide, while the analysis is used to look at the water levels within the basin during rising tide.

### 15.4 Discrete system with storage and resistance

Equations 15.4 and 15.5 form a coupled system of two first order differential equations, eliminating the discharge results in a second order differential equation:

$$h_{NS}(t) - h_b(t) = \frac{L \cdot A_b}{g \cdot A_s} \cdot \frac{d^2 h_b}{dt^2} + \frac{\chi \cdot A_b^2}{g \cdot A_s^2} \cdot \frac{|dh_b|}{dt} \cdot \frac{dh_b}{dt} \quad (15.6)$$

Were:

$h_{NS}$	:	water level on North Sea	[m]
$h_b$	:	basin water level	[m]
$t$	:	time	[s]
$L$	:	length	[m]
$g$	:	gravitational acceleration	[m/s <sup>2</sup> ]
$A_s$	:	current-carrying cross-section	[m <sup>2</sup> ]
$A_b$	:	basin area	[m <sup>2</sup> ]
$\chi$	:	loss coefficient	[-]

The resistance term is quadratic, which makes the computation more complicated. By linearization of the resistance term the effect of the resistance over the tidal period is the same as the quadratic term, only the gradient of the resistance term in time differs, see figure 15.1.

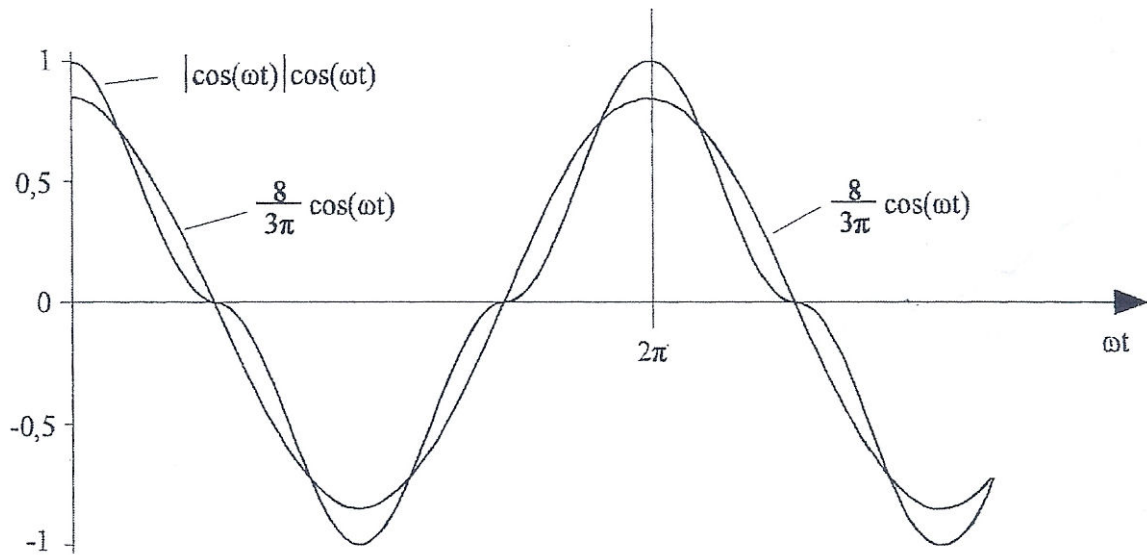


Figure 15.1: comparison quadratic and linear resistance term (Courtesy: battjes, 2002).

By introducing the linear resistance equation 15.6 reduces to:

$$h_{NS}(t) - h_b(t) = \frac{L \cdot A_b}{g \cdot A_s} \cdot \frac{d^2 h_b}{dt^2} + \tau \cdot \frac{dh_b}{dt} \quad (15.7)$$

And

$$\tau = \frac{8}{3\pi} \cdot \chi \cdot \frac{A_b}{g \cdot A_s^2} \cdot \hat{Q} \quad (15.8)$$

Were:

$h_{NS}$	:	water level on North Sea	[m]
$h_b$	:	basin water level	[m]
$t$	:	time	[s]
$L$	:	length	[m]
$g$	:	gravitational acceleration	[m/s <sup>2</sup> ]
$A_s$	:	current-carrying cross-section	[m <sup>2</sup> ]
$A_b$	:	basin area	[m <sup>2</sup> ]
$\tau$	:	relaxation time	[s]
$\chi$	:	loss coefficient	[-]
$\hat{Q}$	:	amplitude of the discharge	[m <sup>3</sup> /s]

Because the length of the connection between the North Sea and the basin behind the storm surge barrier is very small, the resistance term will be dominant over the inertia term. As a result the exit loss will dominate over the friction and  $\chi \rightarrow \frac{1}{2}$  if  $L/R \rightarrow 0$ . Hence equation 15.7 reduces to:

$$h_{NS}(t) - h_b(t) = \tau \cdot \frac{dh_b}{dt} \quad (15.9)$$

Were:

$h_{NS}$	:	water level on North Sea	[m]
$h_b$	:	basin water level	[m]
$t$	:	time	[s]
$\tau$	:	relaxation time	[s]

Neglecting the inertia term means that the extreme values of the basin water level occur when the discharge through the openings in the barrier is zero. Hence, when the outside and inside levels are equal (no head difference).

### 15.5 Computational model

A MATLAB routine is used to compute the variation of the basin water level in time, the following assumptions are made:

- the discharge from the North Sea into the basin is assumed positive;
- the water level within the basin does not affect the geometry of the cross-section. This is a simplification of the reality, as the Wash estuary's geometry changes considerably during the rising and falling of the tide;
- no river discharge is taken into account, since the discharge is small and not continuously present during time (tidal locking) and only adds a few centimetres to the head difference over the barrier during peak discharge;
- the tidal wave is composed of the four main tidal constituents ( $M_2$ ;  $S_2$ ;  $K_1$  and  $O_1$ ), see table 15.1;
- the surface area of the basin is 355 km<sup>2</sup>, the length of the connection is 26 m;
- the cross-sectional width of the estuary at the barrier line is 21586 m; the channel width of the Boston and Lynn Deeps are 1936 m and 9892 m respectively, the average depth is assumed to be 10 m;
- the roughness factor,  $cf$ , is assumed to be 0.004.

Tidal constituent	Wave period [hr]	Wave length [km]	Amplitude <sup>1)</sup> [m]
M <sub>2</sub>	12.42	443	1.596
K <sub>1</sub>	23.93	853	0.110
S <sub>2</sub>	12.00	428	0.524
O <sub>1</sub>	25.82	256	0.120

Wave celerity of all constituents is 9.9 m/s.

<sup>1)</sup> Because no data with respect to the amplitudes of the four main tidal constituents is available at the time for the tide within the Wash estuary, the data of the Immingham measuring station of the UK Tide Gauge Network is used. Per harmonic the ratio between its amplitude and the total tidal amplitude was determined, from which the amplitudes of the harmonics within the Wash estuary were determined.

**Table 15.1:** wave length and amplitude of the four major tidal constituents.

The variation of the outside water level is described by equation 15.9, using the four main harmonic constituents stated in the table above.

$$h_{NS} = \sum_{i=1}^n A_i \cdot \cos(\omega_i \cdot t) \quad (15.9)$$

Were:

$h_{NS}$	: water level on North Sea	[m]
$A_i$	: amplitude of tidal constituent i	[m]
$\omega$	: angular velocity	[rad/s]
$t$	: time	[s]

## 15.6 Outcome of the analysis

The preliminary design consists of 97 turbines and 135 sluices, the combined current-carrying cross-section amounts to  $135 \cdot (20 \cdot 2.90) + 97 \cdot (\pi/4 \cdot 8^2) = 12,706 \text{ m}^2$ . Table 15.2 presents the parameters computed by the MATLAB-routine.

Variable	Equation	Value	Unit
Relaxation time	$\tau = \frac{8}{3\pi} \cdot \chi \cdot \frac{A_b}{g \cdot A_s^2} \cdot \hat{Q}$	12770	[s]
Loss coefficient	$\chi = 0.5 + \frac{cf \cdot L}{R}$	0.5970	[-]
Discharge amplitude	$\hat{Q} = A_b \cdot \omega \cdot \hat{h}_b$	112420	[m <sup>3</sup> /s]
Response parameter	$\omega\tau = \frac{8}{3\pi} \cdot \chi \cdot \frac{A_b^2}{A_s^2} \cdot \frac{\omega^2 \cdot \hat{h}_b}{g}$	1.7950	[-]
Phase difference	$\theta = \text{atan}(\omega\tau)$	1.0625	[rad]
Gamma	$\Gamma = \frac{\omega\tau}{r} = \frac{8}{3\pi} \cdot \chi \cdot \frac{A_b^2}{A_s^2} \cdot \frac{\omega^2 \cdot \hat{h}_{NS}}{g}$	1.8723	[-]
Amplitude ratio	$r = \frac{1}{\sqrt{2} \cdot \Gamma} \cdot \sqrt{-1 + \sqrt{1 + 4\Gamma^2}}$	0.6405	[-]

**Table 15.2:** computed parameters of the preliminary design.

The amplitude ratio between the basin water level and the outside level is 0.64. In other words, as a consequence of the presence of a storm surge barrier, the amplitude of the basin water level is approximately 0.42 m lower than the amplitude of the outside water level. In figure 15.2 the blue line represents the amplitude variation of the outside water level, while the green line represents the amplitude variation of the water level within the basin.

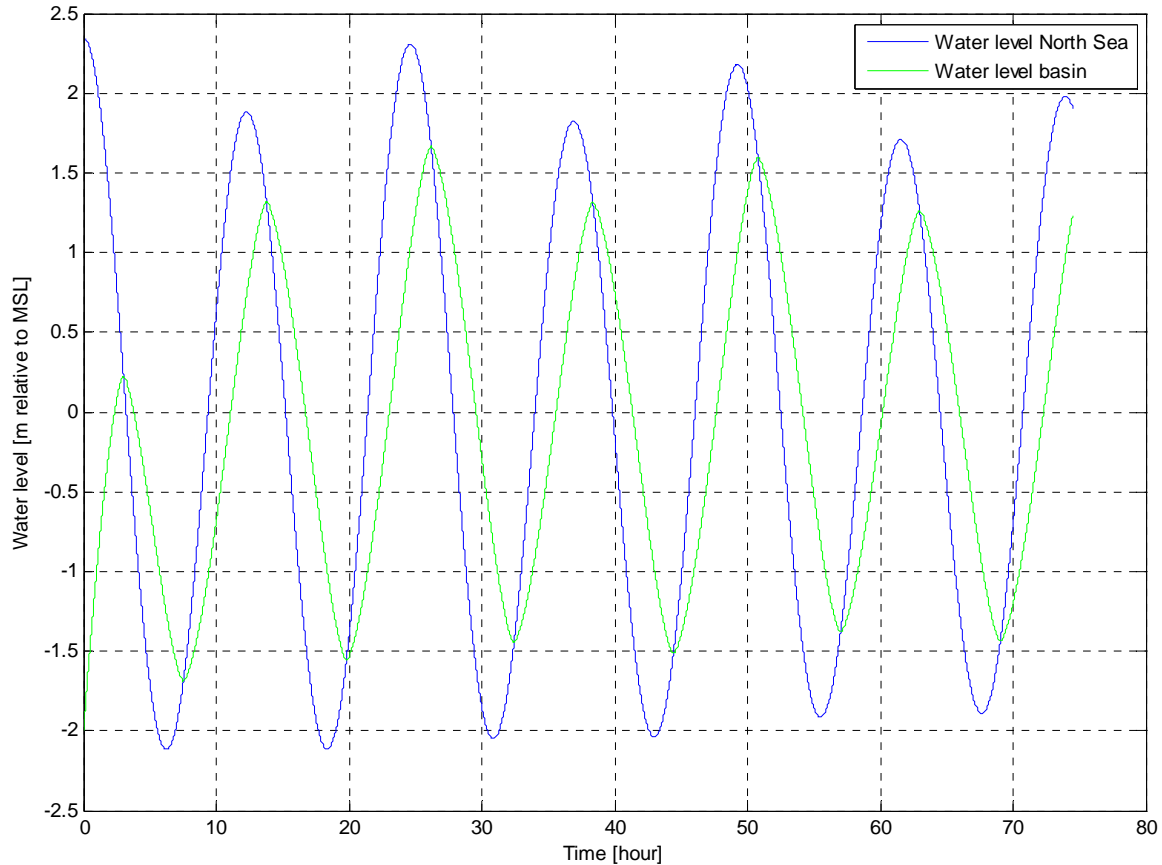


**Figure 15.2:** impact of the preliminary design on the amplitude of the water level within the basin.

Because the reduction of the amplitude of the outside water level is rather large, the current-carrying cross-section is raised in steps of  $174 \text{ m}^2$ , being the current-carrying cross-section of one sluice caisson, to determine an optimum value. The results are presented in figure 15.3.

The optimum current-carrying cross-section is found to be  $18,622 \text{ m}^2$ , corresponding to an additional 34 sluice caissons compared to the preliminary design. The computed amplitude ratio is 0.83. Hence the reduction of the amplitude of the outside water level as a result of the presence of a storm surge barrier is 0.20 m. However placing an additional 34 sluice caissons requires an extra length of 2720 m, which is not available along the barrier line without large dredging works.

Analysis learned that the available space along the barrier line allows for the placement of 30 additional sluice caissons, with a total length of 2400 m. The minimum distance between the sluices and both the commercial and recreational lock complexes is at least 140 metres at either side of the navigation locks, thus assuring that the flow conditions induced by the presence of the intake sluices does not interfere with navigation.

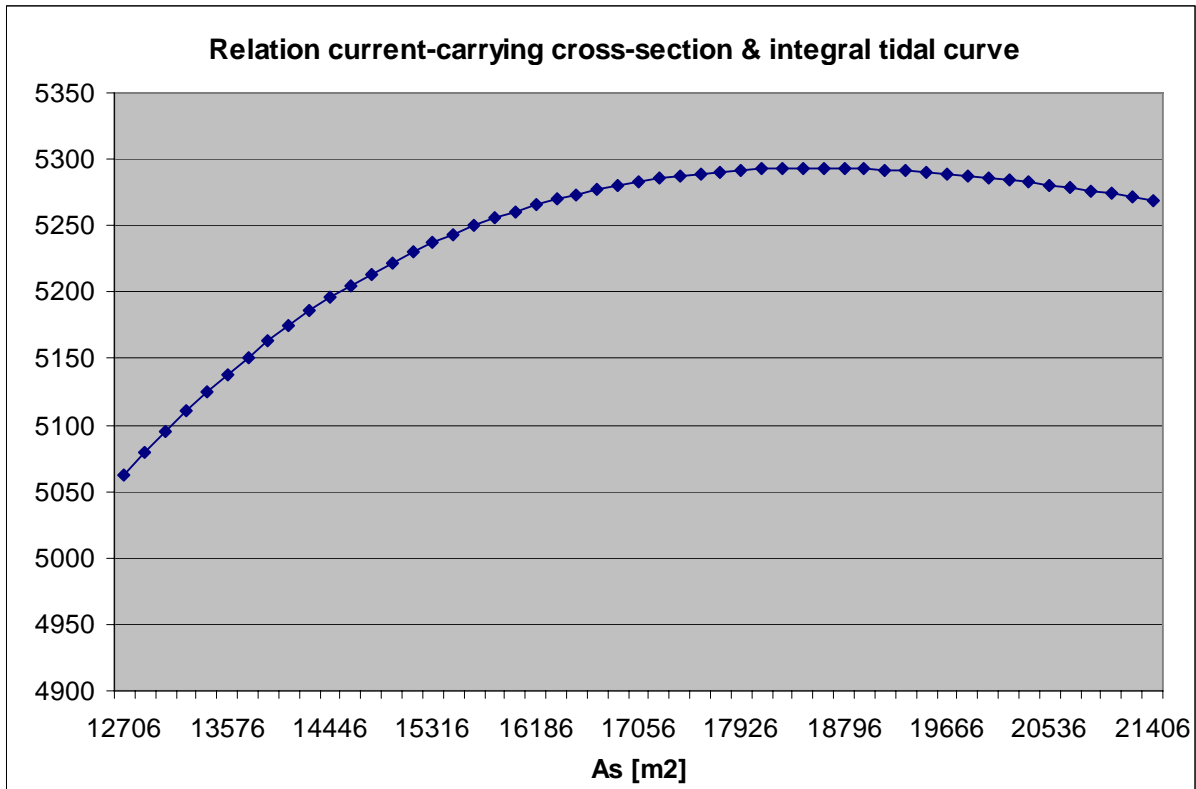


Figure 15.3: relation current-carrying cross-section and the area under the tidal curve.

As the computed amplitude ratio between outside and basin water level is approximately 0.81, the amplitude of the North Sea water level is reduced 0.22 m as a result of the presence of the storm surge barrier. This corresponds well to the 0.25 m head that was assumed during the preliminary design of the tidal power plant. Therefore the number of turbines remains the same in the final conceptual design. The variation in time of both the outside and inside water level is shown in figure 15.4 on the next page.

Variable	Equation	Value	Unit
Relaxation time	$\tau = \frac{8}{3\pi} \cdot \chi \cdot \frac{A_b}{g \cdot A_s^2} \cdot \hat{Q}$	6112	[s]
Loss coefficient	$\chi = 0.5 + \frac{cf \cdot L}{R}$	0.5687	[-]
Discharge amplitude	$\hat{Q} = A_b \cdot \omega \cdot \hat{h}_b$	112420	[m <sup>3</sup> /s]
Response parameter	$\omega\tau = \frac{8}{3\pi} \cdot \chi \cdot \frac{A_b^2}{A_s^2} \cdot \frac{\omega^2 \cdot \hat{h}_b}{g}$	0.8591	[-]
Phase difference	$\theta = \text{atan}(\omega\tau)$	0.7098	[rad]
Gamma	$\Gamma = \frac{\omega\tau}{r} = \frac{8}{3\pi} \cdot \chi \cdot \frac{A_b^2}{A_s^2} \cdot \frac{\omega^2 \cdot \hat{h}_{NS}}{g}$	0.8961	[-]
Amplitude ratio	$r = \frac{1}{\sqrt{2} \cdot \Gamma} \cdot \sqrt{-1 + \sqrt{1 + 4\Gamma^2}}$	0.8095	[-]

Table 15.3: computed parameters for the maximum current-carrying cross-sectional area.

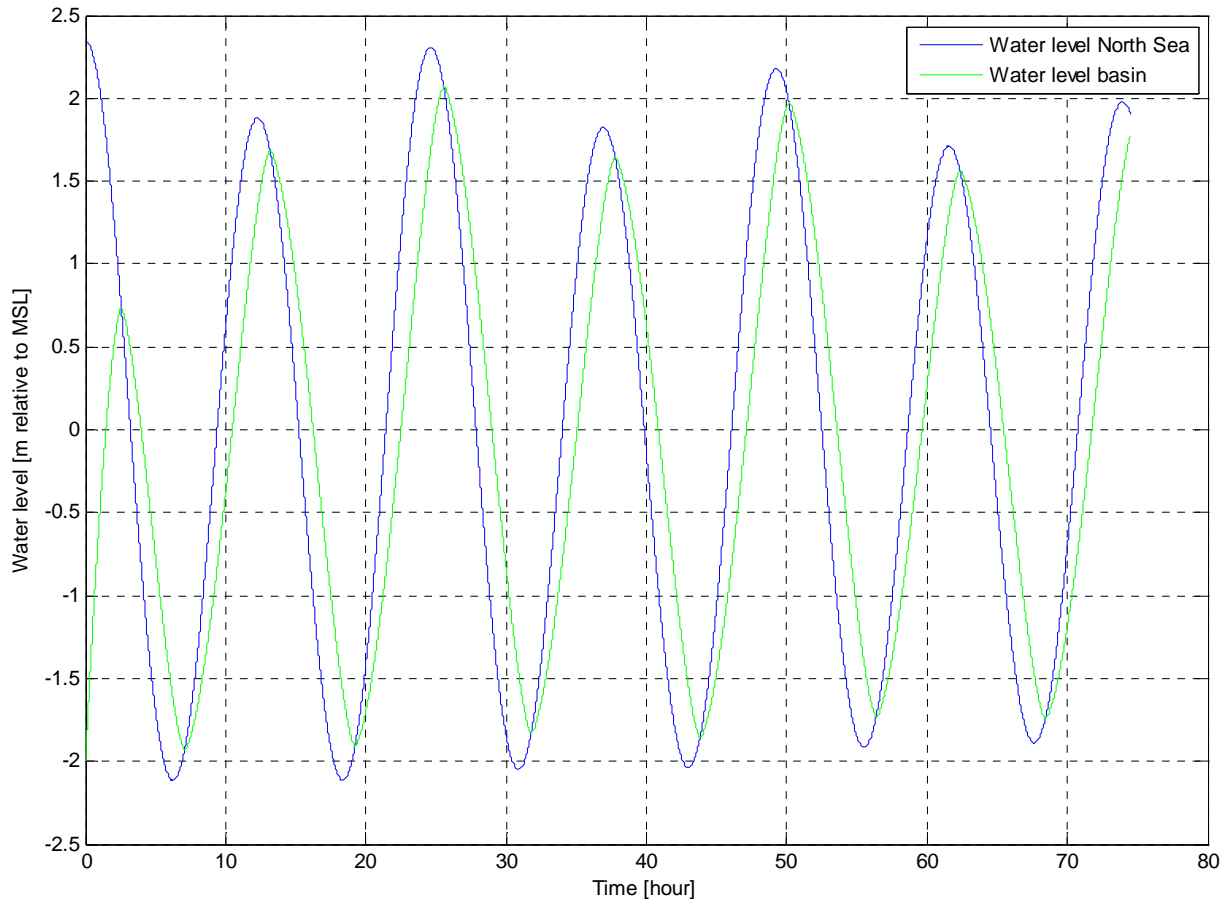


Figure 15.4: impact of the final conceptual design on the amplitude of the water level within the basin.

## **Appendix 16**

*Final conceptual design*



## **Appendix 16.1**

### *Boston Deeps*





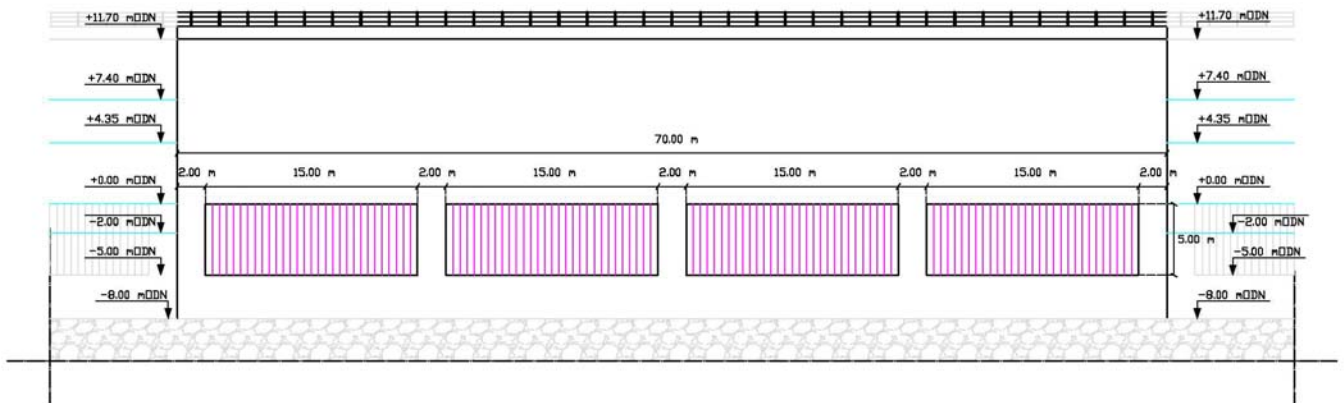


Figure 16.1.3: front view sluiced caisson Boston Deeps (not to scale).

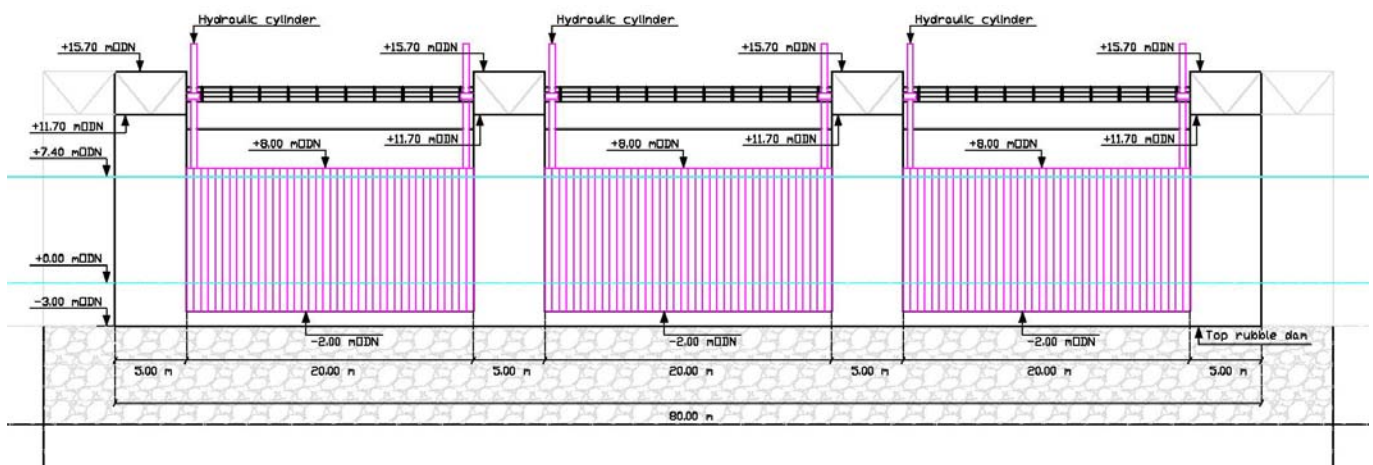


Figure 16.1.4: front view sluice caisson Boston Deeps (not to scale).

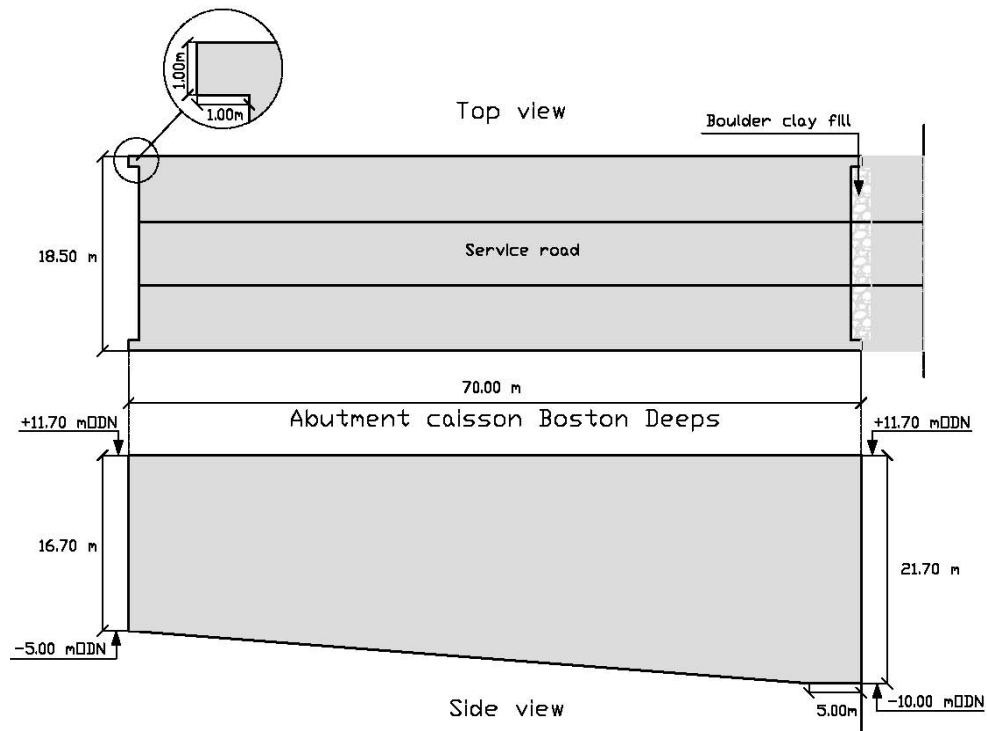


Figure 16.1.5: abutment caisson Boston Deeps (not to scale).

## **Appendix 16.2**

*Lynn Deeps*



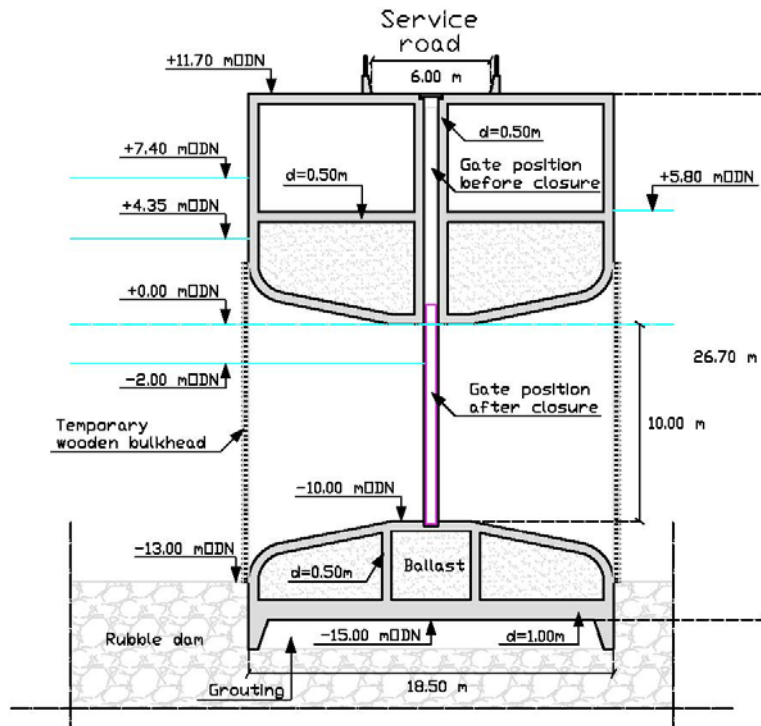


Figure 16.2.1: cross-section sluiced caisson Lynn Deeps (not to scale).

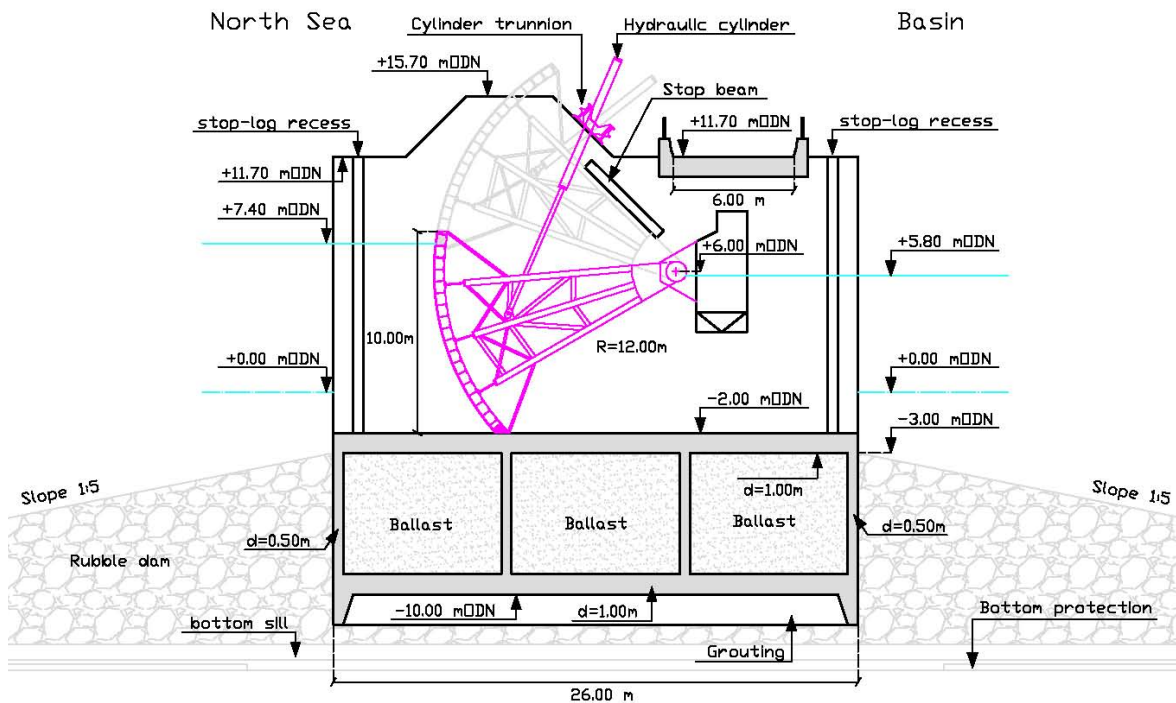


Figure 16.2.2: cross-section sluice caisson Lynn Deeps (not to scale).

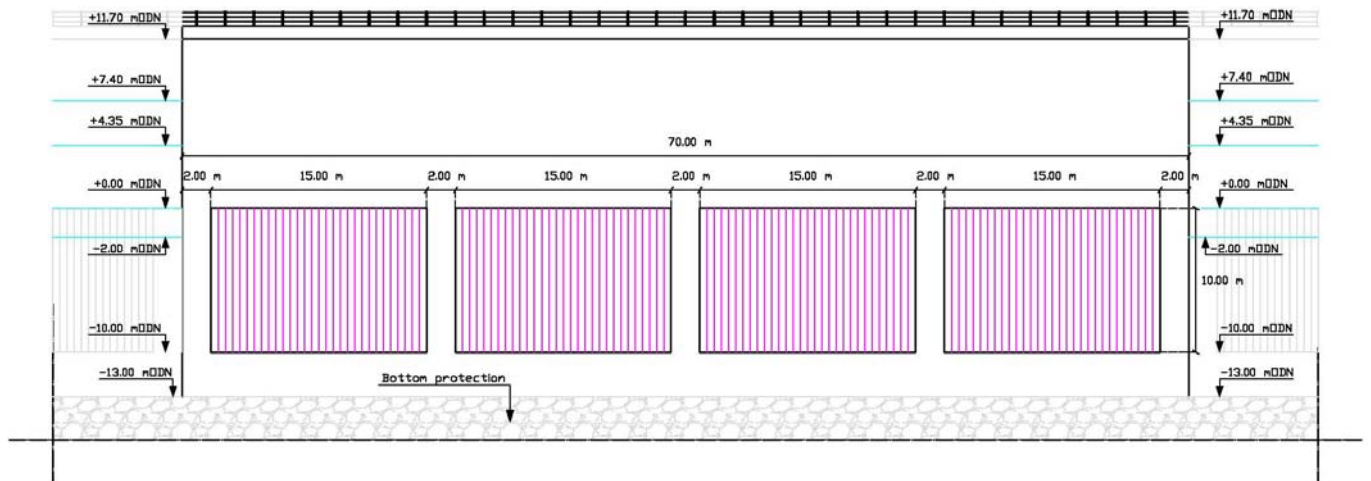


Figure 16.2.3: front view sluiced caisson Lynn Deeps (not to scale).

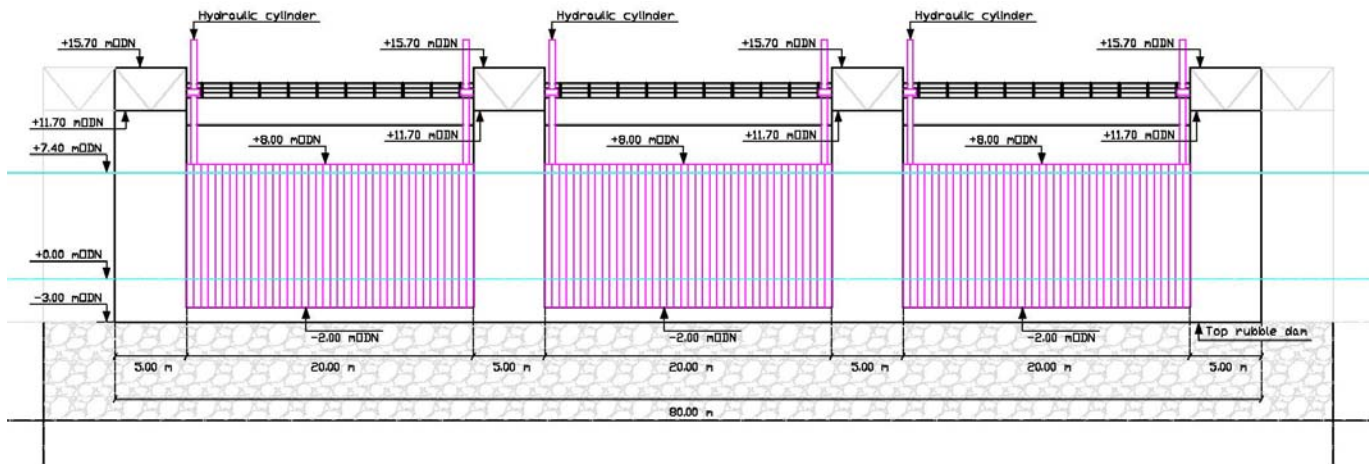


Figure 16.2.4: front view sluice caisson Lynn Deeps (not to scale).

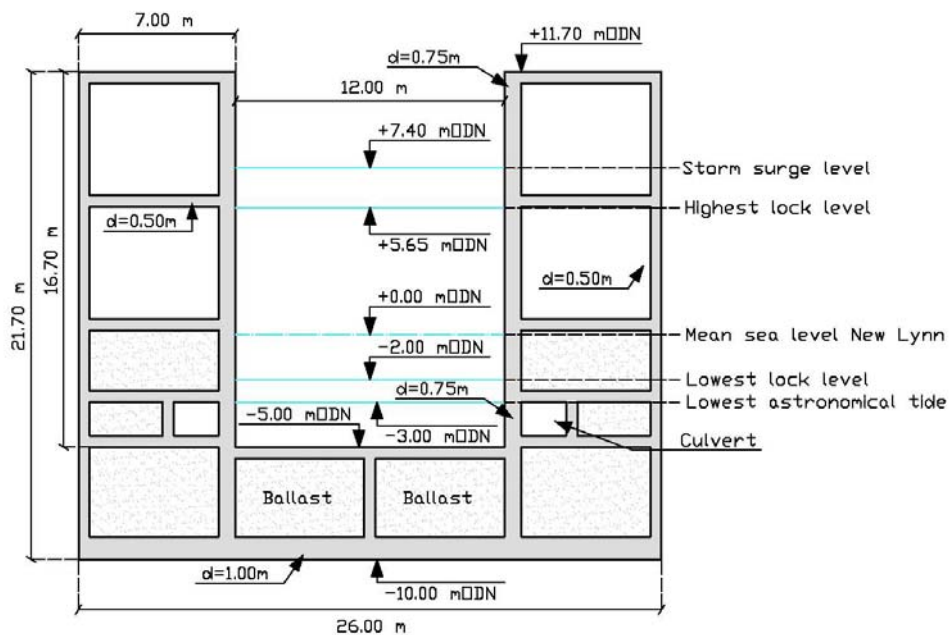


Figure 16.2.5: cross-section recreational navigation lock complex (not to scale).

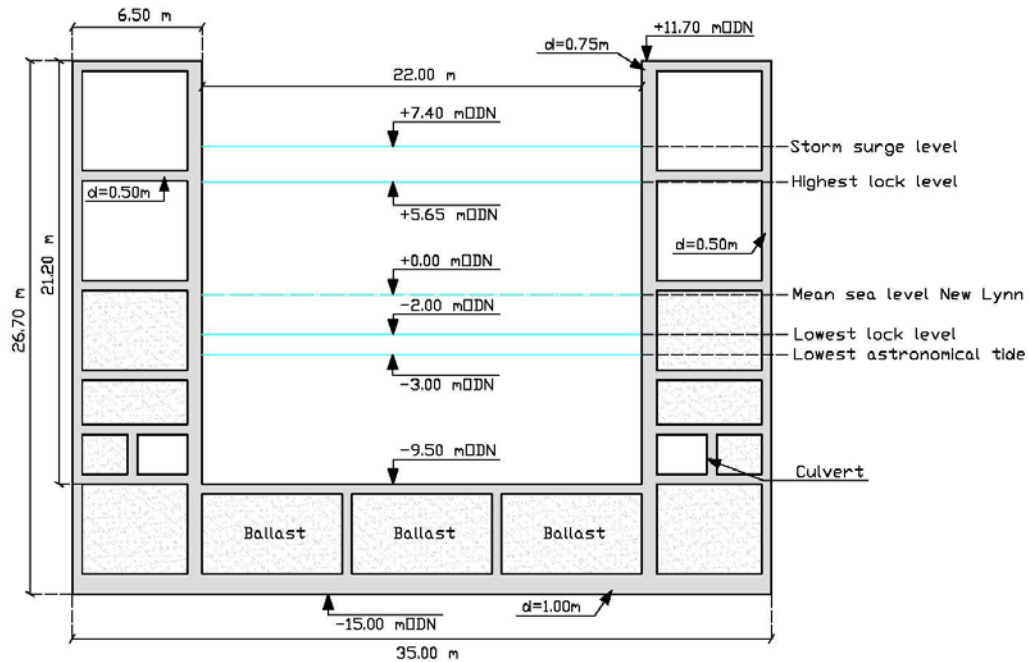


Figure 16.2.6: cross-section commercial navigation lock complex (not to scale).

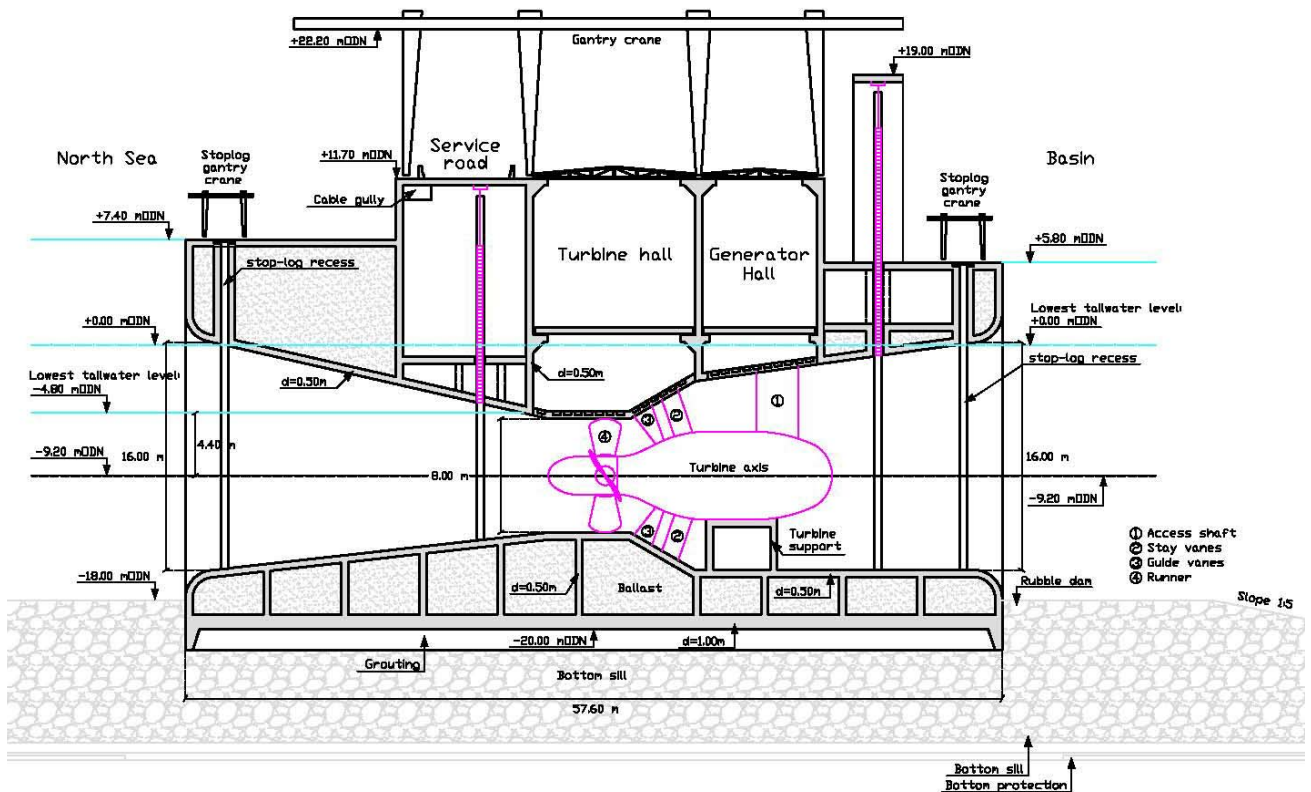


Figure 16.2.7: cross-section turbine caisson (not to scale).



## **Appendix 17**

### *Economic analysis*



## 17.1 Introduction

In this appendix the methodology and the results of the performed economic analysis are explained. In order to be able to determine the economic feasibility of the combined storm surge barrier and tidal power plant in the Wash estuary, the discounted values of all expenses and revenues are computed. After which the net present value (NPV) is determined for several energy prices (p/kWh). Also the break-even energy price will be derived. But first the preconditions and assumptions will be stated.

## 17.2 Preconditions and assumptions

The following assumptions are made with respect to the economic analysis:

- the design lifetime of the structure is 120 years;
- the construction time is estimated to be five years;
- the cost distribution of both the total investment costs and the construction costs is as follows: 55% of the cost is allocated to civil works and 45% is allocated to electromechanical equipment [Clarke, 2007];
- costs for the transmission lines is not included, see section 3.4 of the main report;
- compensation for landowners is not included;
- V.A.T. is not included in the present value (PV) computations;
- the residual value of the structure at the end of the design lifetime is not included;
- the regular maintenance and operation costs sum up to an annual sum equal to 1% of the total construction costs (direct costs only);
- transmission losses are set to be 3% of the annual energy yield.

### 17.2.1 Annual real interest rate

In view of the global economic crisis the Bank of England has lowered the official annual interest rate in March 2009 to 0.50% and has kept this rate artificially since. This measure was taken to rescue several UK banks from bankruptcy and give the banks the opportunity to rebuild their balance sheets. With the current annual inflation rate of 3.40%<sup>26</sup> (February 2012) this results in a negative annual real interest rate of -2.90%, which does not represent a sound climate for investment. However, considered over longer periods the annual real interest rate is positive, see table 17.1.

Time period	Average inflation rate	Average interest rate	Average real interest rate
1989-2010	2.72		
1971-2010		8.58	5.86

Source: [www.tradingeconomics.com/united-kingdom](http://www.tradingeconomics.com/united-kingdom).

**Table 17.1:** long term average annual interest and inflation rates.

Based on the data presented in the table above, the following rates are used in the performed economic appraisal:

- annual inflation rate: 3.00%;
- annual interest rate: 9.00%;
- annual real interest rate: 6.00%;

### 17.2.2 Allocation of the cost of electromechanical equipment

As stated before 45% of the total construction costs is allocated to electromechanical equipment, which in turn is subdivided per part or group of parts as shown in table 17.2.

<sup>26</sup> Source: [www.tradingeconomics.com/united-kingdom](http://www.tradingeconomics.com/united-kingdom)

Part	Percentage of cost electromechanical equipment
Turbines	25%
Generator	12%
Transformer	4%
Control equipment	55%
Miscellaneous equipment	4%

Source: Vrijling et al., 2008.

**Table 17.2:** subdivision costs electromechanical equipment.

Miscellaneous equipment refers to the gantry cranes and cooling and drainage equipment.

### 17.3 Discounted value expenses

The project's expenses consist of three parts, first the total investment costs, which in this case equal the value of the credit estimate before taxes, as shown in appendix 17.1. And secondly the operation and regular maintenance costs, which sum up to an annual value of 1% of the construction costs (total direct costs as presented in appendix 17.1). The last factor contributing to the expenses are the refurbishment<sup>27</sup> costs. The costs of the refurbishment are based on the schedule presented in table 17.3. The figures concerning the first three scheduled refurbishments are after Slangen [Slangen, 2008], the remaining three refurbishments are derived on the basis of an expansion of the trends present within the schedule after Slangen. Table 17.4 gives an overview of the monetary value of the refurbishments.

Time period	Refurbishment 1		Refurbishment 2		Refurbishment 3	
	Year	Percentage	Year	Percentage	Year	Percentage
Civil structures	20	3%	40	6%	60	6%
Turbines	25	10%	45	40%	70	75%
Generators	25	10%	45	40%	70	75%
Transformers	-	-	40	5%	50	100%
Control equipment	20	25%	40	50%	60	25%
Miscellaneous equipment	25	10%	50	50%	75	75%
	Refurbishment 4		Refurbishment 5		Refurbishment 6	
	Year	Percentage	Year	Percentage	Year	Percentage
Civil structures	80	6%	100	6%	120	6%
Turbines	-	-	95	10%	115	40%
Generators	-	-	95	10%	115	40%
Transformers	90	5%	100	100%	140	5%
Control equipment	80	50%	100	25%	120	50%
Miscellaneous equipment	-	-	100	10%	125	50%

Source: partly after Slangen, 2008.

Note: dates exceeding the design lifetime of 120 years are of course not included in the computation.

**Table 17.3:** refurbishment schedule.

<sup>27</sup> Refurbishment = an investment made to repair or improve existing equipment or civil works, with the purpose to restore the unit to or above its original state.

Time period	Refurbishment 1		Refurbishment 2		Refurbishment 3	
	Year	Cost [10 <sup>6</sup> £]	Year	Cost [10 <sup>6</sup> £]	Year	Cost [10 <sup>6</sup> £]
Civil structures	20	69	40	139	60	139
Turbines	25	47	45	189	70	355
Generators	25	23	45	91	70	170
Transformers	-	-	40	4	50	76
Control equipment	20	260	40	521	60	260
Miscellaneous equipment	25	8	50	38	75	57
	Refurbishment 4		Refurbishment 5		Refurbishment 6	
	Year	Cost [10 <sup>6</sup> £]	Year	Cost [10 <sup>6</sup> £]	Year	Cost [10 <sup>6</sup> £]
Civil structures	80	139	100	139	120	139
Turbines	-	-	95	47	115	189
Generators	-	-	95	23	115	91
Transformers	90	4	100	76	140	4
Control equipment	80	521	100	260	120	521
Miscellaneous equipment	-	-	100	8	125	38

Note: dates exceeding the design lifetime of 120 years are of course not included in the computation.

Table 17.4: monetary value of the scheduled refurbishments.

The discounted value of the expenses in each year is computed using equation 17.1. In appendix 17.2 the results of the computation are shown.

$$PV_{ex} = I_0 + \sum_{n=1}^N \frac{C_{ex}}{(1+r)^n} \quad [17.1]$$

Were:

$PV_{ex}$	:	summation of the discounted values of the expenses	[£]
$I_0$	:	initial investment costs	[£]
$C_{ex}$	:	monetary value of the expenses in year $n$	[£]
$r$	:	real interest rate	[-]
$n$	:	number of years from investment year ( $n = 0$ )	[-]
$N$	:	design life time storm surge barrier, 120 yr	[-]

As the construction time is estimated to be 5 years, the first five years the discounted value of the expenses equals 1/5 of the total investment costs before taxes, as presented in appendix 17.1. After that, both the annual operation and maintenance costs *and* the refurbishment costs are computed as a percentage of the construction costs (total direct costs, as presented in the credit estimation).

The discounted value of all expenses to be made within the design lifetime of 120 years amounts to £ 6704M.

## 17.4 Discounted value revenues

The revenues from the combined storm surge barrier and tidal power plant are two fold, first the revenues from the generated electricity and secondly the revenues from the reduction of the flood risk in the protected area behind the Wash barrier. Although the latter only holds when the UK Government participates in the project, as for a private investment group as the Wash Tidal Barrier Corporation plc the reduction of the potential damage does not generate additional revenues and therefore does not contribute to the profitability of the project.

### 17.4.1 Discounted value revenues from energy

In chapter 6 of the main report the annual energy yield is estimated to be 2945 GWh, this amount already includes 4% loss due to (electro)mechanical failure and severe storm conditions. Transmission losses are assumed to cause an additional loss of 3% of the amount of energy generated per annum. Since energy generation can only take place after finishing the construction work, the revenues start in the 6<sup>th</sup> year.

The discounted value of the revenues from the annual energy yield is computed by means of equation 17.2, using energy prices of 8 p/kWh, 9 p/kWh, 10 p/kWh and 11 p/kWh.

$$PV_{rev,E} = \sum_{n=1}^N \frac{C_E}{(1+r)^n} \quad [17.2]$$

Were:

$PV_{rev,E}$	: summation of the discounted values of the energy revenues	[£]
$C_E$	: monetary value of the generated energy in year n	[£]
$r$	: real interest rate	[-]
$n$	: number of years from investment year (n = 0)	[-]
$N$	: design life time storm surge barrier, 120 yr	[-]

The results of the computation are included in appendix 17.3, a summary of the results is presented in table 17.5.

Energy price [p/kWh]	Discounted value [10 <sup>6</sup> £]
8	3013
9	3390
10	3767
11	4143

Table 17.5: discounted values of revenues from energy.

### 17.4.2 Discounted value revenues from enhanced flood protection

In order to be able to determine the discounted value of the revenues gained from enhancing the present flood protection level, the current and future SoP's should be known. Also the extent of the flooding and the economic value of damages and losses have to be determined.

Assumptions made with respect to the analysis:

- the growth of the damages and losses as a result of regular economic development will be ignored;
- the coastal defences and the river defences of the four major rivers are regarded as primary flood defences, thus dividing the Fenlands into five areas, see figure 17.1;

- secondary structures, such as (rail)road embankments and former primary flood defences still present in the hinterland, that could restrict the extent of the flooding are not taken into account. Once the primary flood defences are breached it is assumed that the whole hinterland will flood;
- since the hinterland only benefits from the enhanced flood protection when the storm surge barrier is finished, the revenues start in the 6<sup>th</sup> year.

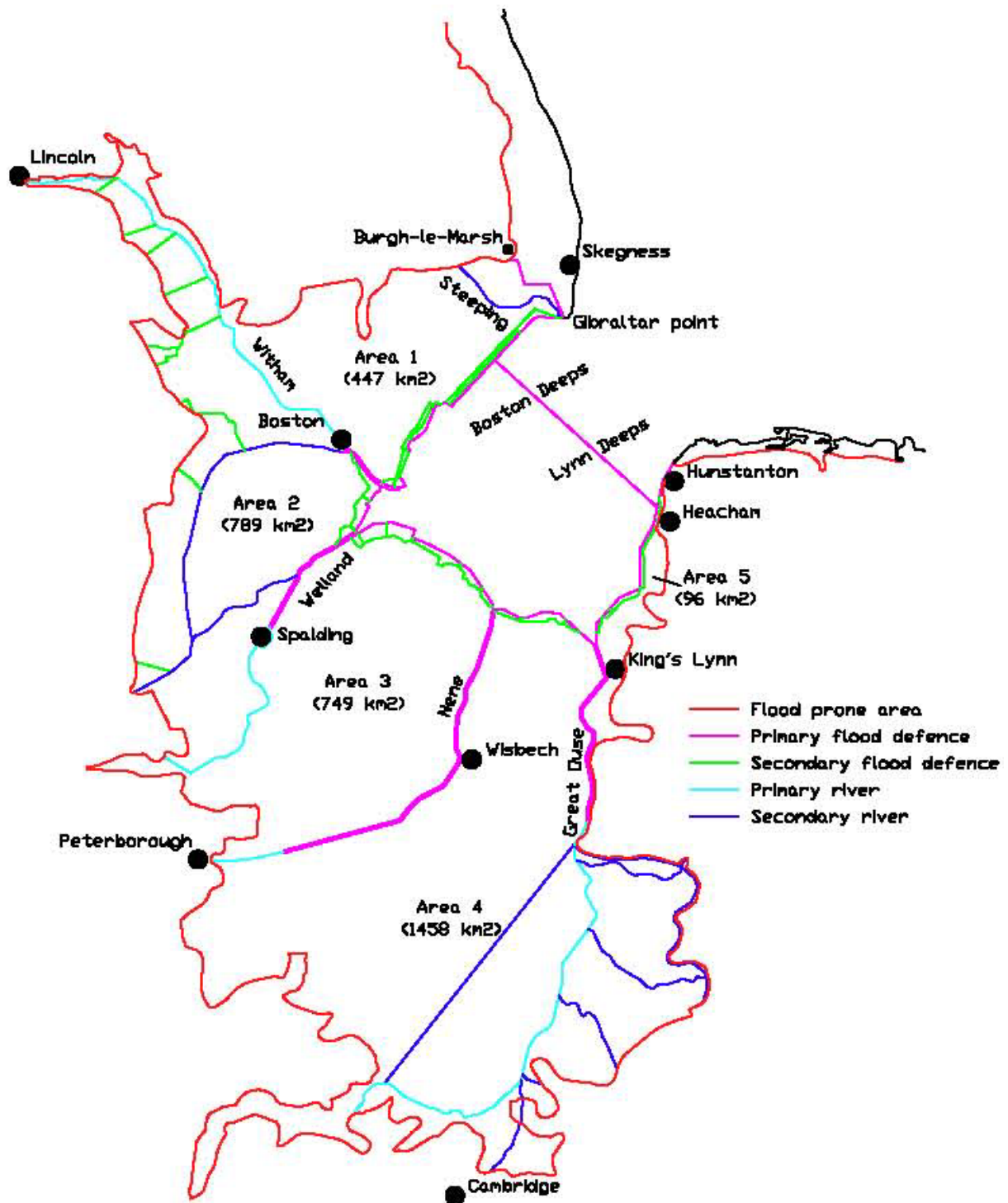


Figure 17.1: division of the Fenland's in flood prone areas (not to scale).

### Extent of the flooding

The extent of the flooding is determined on the basis of the flood maps provided by the Environment Agency<sup>28</sup>. The contours of the area that is likely to flood, either by sea or rivers, in a 1:200 flood event and in absence of flood defences were transferred to the Ordnance Survey Landranger Maps series (scale 1:50,000), from which the surface area of the flood extent has been determined. A distinction is made between rural areas and small and large cities, the outcome is presented in table 17.6. As a result of the construction of a storm surge barrier the flood protection level is raised to 1:500.

Flood prone area	SoP	Rural area [ha]	Minor city [ha]	Major city [ha]	Total area [ha]
Area 1	1:50	43,850	200	650	44,700
Area 2	1:200	77,150	1,000	750	78,900
Area 3	1:200	74,100	800	-	74,900
Area 4	1:200	144,900	100	800	145,800
Area 5	1:200	8,600	-	1000	9,600
<b>Total</b>		<b>348,600</b>	<b>2,100</b>	<b>3,200</b>	<b>353,900</b>

Table 17.6: flood prone areas.

### Economic damages and losses

The economic value of the expected damages and losses is determined using the *estimated annual average damages* figures as drawn up by Halcrow in the National Appraisal of Assets at Risk from Flooding and Coastal erosion, that was commissioned by the Department for Environment, Food and Rural Affairs in 2001 [DEFRA, 2001]. The estimated annual average damages are defined as the flood risk (probability of failure *times* damages).

The Ordnance Survey Addresspoint database<sup>29</sup> has been used to establish the number of properties within the flooded area, while their capital value is determined based on regional house price values. Limitations of the method followed by Halcrow are [Defra, 2001]:

- size and use of commercial properties is not known from private properties;
- high rise buildings are not distinguished. Hence, double-counting of losses occurs;
- accuracy concerning agricultural land values and productivity is limited to regional pricing;
- loss of life and human suffering/health is not included;
- wider impacts of flooding are not included, e.g. damage to the natural environment, impact on regional and national productivity, etc..

The values represented on the map shown in figure 17.2 should be treated as indicative for the order of magnitude of the damages and losses, not as absolute values. Current standards maintained means that maintenance and adaptation costs are only included to the extent that the current SoP continues to be provided [Defra, 2001].

The estimated annual average damages, include the following [Defra, 2001]:

- capitalised values of built property and agricultural land;
- damage and damage avoided to built property;
- damage to and loss of agricultural production;
- increased travel cost due to road traffic disruption.

<sup>28</sup> <http://maps.environment-agency.gov.uk>

<sup>29</sup> The Ordnance Survey Addresspoint database provides locations for individual postal delivery points.

In table 17.7 an overview is given of the values of the damages per hectare that are applied in the present value computations. The figures stated are based on the median values of the estimated annual average damages (AAD) ranges for a Standard of Protection of 1:200, as depicted in the legend of figure 17.2.

Category	Mean value AAD [£/ha]	Damages [£/ha]
Rural area	250	50,000
Minor city	700	140,000
Major city	3000	600,000

Table 17.7: applied value of the annual damages.

The flood risk is capitalized as the failure probability times the economic value of the sum of both damages and losses. Based on the data presented in tables 17.6 and 17.7 the present day and future flood risk are computed, see the table below.

	Failure probability [1/yr]	Total value of damages [10 <sup>6</sup> £]	Annual flood risk [10 <sup>6</sup> £/yr]
Present day	1:50 / 1:200	19,644	137.38
Future	1:500	19,644	39.29

Table 17.8: present day and future flood risk.

The discounted value of the revenues from the enhanced flood protection level is computed by means of equation 17.3. The results of the performed computations are presented in appendix 17.4.

$$PV_{rev,SoP} = \sum_{n=1}^N \frac{(P_{pd} \cdot D) - (P_{fu} \cdot D)}{(1+r)^n} \quad [17.3]$$

Were:

$PV_{rev,SoP}$	: summation of the discounted values of the revenues from raising the SoP	[£]
$P_{pd}$	: present day failure probability	[1/yr]
$P_{fu}$	: future failure probability	[1/yr]
$D$	: total damage	[£]
$r$	: real interest rate	[-]
$n$	: number of years from investment year (n = 0)	[-]
$N$	: design life time storm surge barrier, 120 yr	[-]

The discounted value of all revenues from an enhanced flood protection level within the design lifetime of 120 years amounts to £ 1293M.

### Estimated Annual Average Damages - Current Standards Maintained Eastern Area

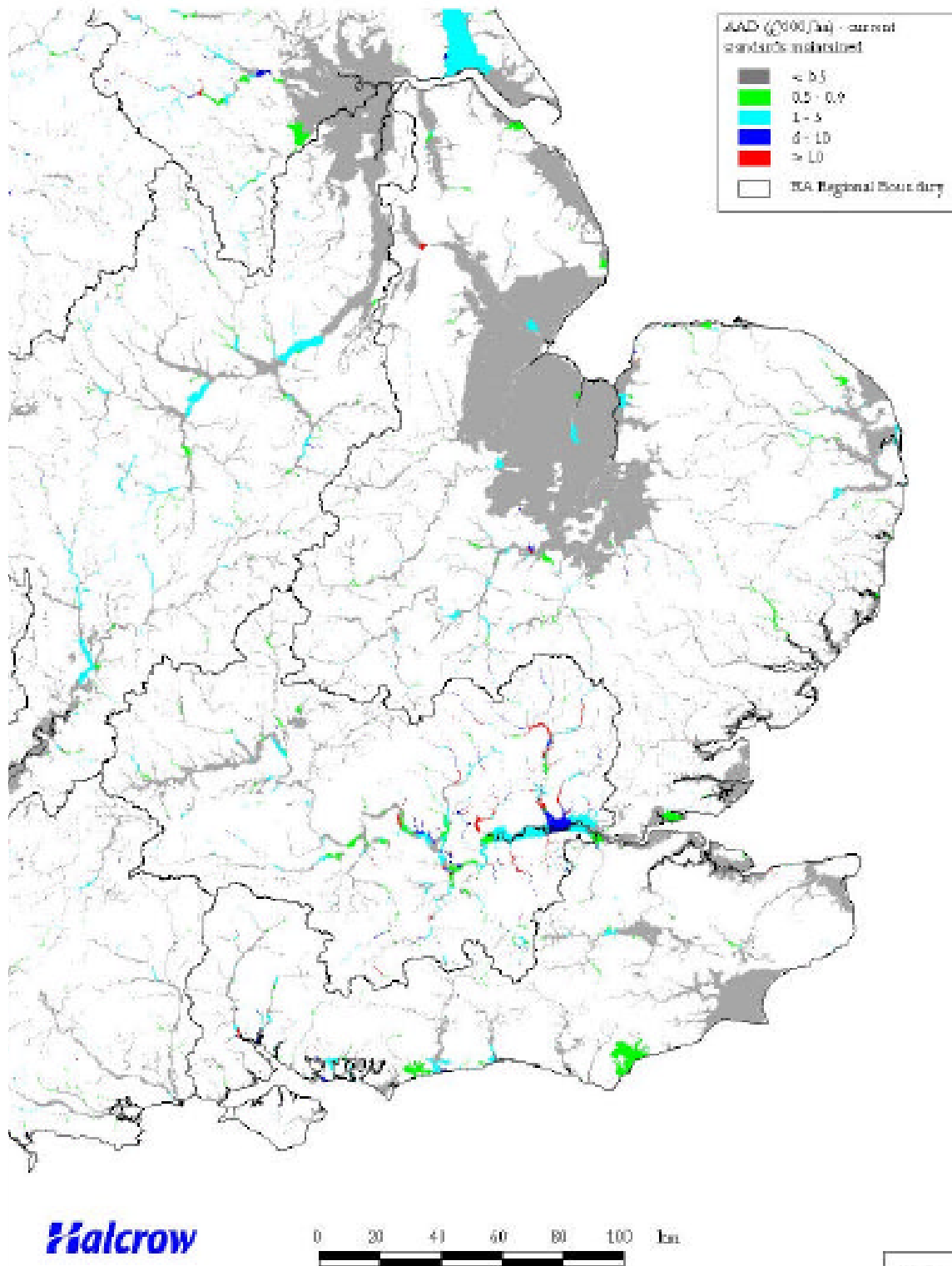


Figure 17.2

Figure 17.2: estimated annual average damages [DEFRA, 2001].

### 17.5 Net present value corresponding to several energy prices

The net present value (NPV) represents the current value of an investment by means of comparing the discounted cash flows of expenses and revenues, see equation 17.4. As long as the NPV is larger than or equal to zero an investment is considered to be feasible.

$$NPV = \left( \sum_{n=1}^N \frac{C_E}{(1+r)^n} + \sum_{n=1}^N \frac{(P_{pd} \cdot D) - (P_{fu} \cdot D)}{(1+r)^n} \right) - \left( I_0 + \sum_{n=1}^N \frac{C_{ex}}{(1+r)^n} \right) \quad [17.4]$$

Were:

$NPV$	: net present value of the investment	[£]
$C_E$	: Monetary value of the generated energy in year $n$	[£]
$P_{pd}$	: present day failure probability	[1/yr]
$P_{fu}$	: future failure probability	[1/yr]
$D$	: total damage	[£]
$I_0$	: initial investment costs	[£]
$C_{ex}$	: monetary value of the expenses in year $n$	[£]
$r$	: real interest rate	[-]
$n$	: number of years from investment year ( $n = 0$ )	[-]
$N$	: design life time storm surge barrier, 120 yr	[-]

The NPV's corresponding to several energy prices are presented in table 17.9. From the table can be concluded that the investment is economically not feasible, based on the present day preconditions and the assumptions made in the performed analysis. However possible financial incentives from the UK Government, such as the buy-out price and Feed-in-Tariffs are not included in the analysis, these may tip the scales and make the investment profitable.

Energy price [p/kWh]	Net Present Value public-private cooperation [10 <sup>6</sup> £]	Net Present Value private cooperation [10 <sup>6</sup> £]
8.00	-2398	-3691
9.00	-2021	-3314
10.00	-1644	-2938
11.00	-1268	-2561

Table 17.9: NPV corresponding to several energy prices.

### 17.6 Break-even point

The energy price corresponding to the break-even point is computed as follows:

$$BEP = \frac{PV_{ex} - PV_{SoP}}{PV_{rev,E,1p.kWh}} \quad [17.5]$$

Were:

$BEP$	: energy price corresponding to the break-even point	[£/kWh]
$PV_{ex}$	: summation of the discounted values of the expenses	[£]
$PV_{rev,SoP}$	: summation of the discounted values of the revenues from raising the SoP	[£]
$PV_{rev,E,1p.kWh}$	: summation of the discounted values of the energy revenues for a energy price of 1p/kWh	[£]

The energy price at the BEP amounts 14.4 p/kWh, including the revenues from an enhanced SoP. Without the revenues from an enhanced SoP, the energy price at the BEP amounts to 17.8 p/kWh.

## **Appendix 17.1**

*Credit estimate Wash barrier and tidal power plant*



## **Appendix 17.2**

*Discounted value of the expenses*



## **Appendix 17.3**

*Discounted value of the revenues of energy*



## **Appendix 17.4**

*Discounted value of the revenues of improved flood protection*



Monthly distribution of wave height (m)

lower	upper	Jan	Feb	Mar	Apr	May	Jun	Jul	Aug	Sep	Oct	Nov	Dec	Total
0.0	0.2	85	123	291	370	412	461	622	402	257	169	36	95	3323
0.2	0.4	150	167	336	513	490	483	824	574	325	245	74	147	4328
0.4	0.6	359	536	936	1237	1365	1625	1891	1648	1095	686	421	588	12387
0.6	0.8	624	720	1004	1396	1540	1668	1796	1488	1124	803	498	636	13297
0.8	1.0	953	1090	1233	1670	1944	2062	1867	1866	1518	1319	949	1133	17604
1.0	1.2	1056	1082	1150	1429	1677	1463	1271	1476	1493	1190	1055	1151	15493
1.2	1.4	1845	1495	1693	1733	1982	1727	1417	1715	2058	2045	1760	1847	21317
1.4	1.6	629	524	499	477	515	382	366	469	568	630	646	504	6209
1.6	1.8	1061	814	830	793	739	495	490	735	772	929	1209	972	9839
1.8	2.0	1007	832	875	724	541	372	365	581	660	876	1105	992	8930
2.0	2.2	825	609	695	431	352	247	190	391	442	628	808	805	6423
2.2	2.4	901	546	555	262	245	182	172	277	384	562	736	679	5501
2.4	2.6	547	388	366	162	128	104	101	158	267	481	475	379	3556
2.6	2.8	729	547	510	233	163	128	163	192	338	736	706	592	5037
2.8	3.0	192	146	94	59	36	41	26	28	94	191	148	206	1261
3.0	3.2	331	261	162	77	55	39	74	39	128	272	222	370	2030
3.2	3.4	225	163	120	58	41	32	57	34	98	201	185	275	1489
3.4	3.6	178	115	117	26	30	27	53	32	80	145	146	205	1154
3.6	3.8	164	103	105	30	11	24	27	17	72	125	161	170	1009
3.8	4.0	57	46	46	8	1	10	10	4	32	46	44	42	346
4.0	4.2	56	82	63	13	3	16	5	3	50	72	92	78	533
4.2	4.4	43	56	33	11	0	12	7	2	73	36	59	62	394
4.4	4.6	38	52	26	5	0	14	6	0	40	29	52	50	312
4.6	4.8	28	44	29	4	0	5	4	1	23	23	57	40	258
4.8	5.0	23	41	20	1	0	1	1	0	18	17	46	22	190
5.0	5.2	14	22	18	1	0	0	0	1	11	16	37	35	155
5.2	5.4	5	26	5	0	0	0	0	0	4	8	29	23	100
5.4	5.6	8	20	1	0	0	0	0	0	2	4	17	16	68
5.6	5.8	0	18	0	1	0	0	0	0	1	4	14	14	52
5.8	6.0	2	18	0	2	0	0	0	0	0	0	8	12	42
6.0	6.2	5	8	0	0	0	0	0	0	0	0	8	7	28
6.2	6.4	2	15	0	2	0	0	0	0	1	0	9	6	35
6.4	6.6	1	12	0	0	0	0	0	0	1	0	4	2	20
6.6	6.8	0	3	0	1	0	0	0	0	1	0	3	1	9
6.8	7.0	0	4	0	0	0	0	0	0	3	0	1	0	8
7.0	7.2	0	3	0	0	0	0	0	0	1	0	0	0	4
7.2	7.4	0	3	0	0	0	0	0	0	0	0	0	0	3
7.4	7.6	2	1	0	0	0	0	0	0	0	0	0	0	3
7.6	7.8	1	1	0	0	0	0	0	0	1	0	0	0	3
7.8	8.0	0	2	0	0	0	0	0	0	0	0	0	0	2
8.0	8.2	0	0	0	0	0	0	0	0	0	0	0	0	0
<b>total</b>		12146	10738	11812	11729	12270	11620	11805	12133	12035	12488	11820	12156	142752

Monthly distribution of wind speed (m/s)

lower	upper	Jan	Feb	Mar	Apr	May	Jun	Jul	Aug	Sep	Oct	Nov	Dec	Total
0	1	25	93	98	185	352	313	408	281	182	126	39	43	2145
1	2	163	237	470	824	782	931	913	687	486	237	181	216	6127
2	3	243	316	597	995	873	1127	1119	942	667	455	274	370	7978
3	4	375	520	894	1098	1111	1280	1375	1153	820	603	377	515	10121
4	5	570	664	1132	1316	1526	1551	1730	1375	1054	854	534	723	13029
5	6	701	876	1248	1410	1545	1808	1698	1686	1326	1141	777	1035	15251
6	7	882	1050	1268	1214	1469	1394	1238	1517	1392	1369	1039	1113	14945
7	8	1097	1093	1110	997	1197	928	971	1460	1402	1429	1174	1121	13979
8	9	1334	1192	978	896	1033	509	682	1019	1335	1386	1335	1150	12849
9	10	1454	894	925	830	764	304	400	666	942	1180	1394	1083	10836
10	11	1196	705	693	486	363	176	185	307	512	838	1226	928	7615
11	12	984	616	525	296	164	153	151	148	454	787	853	795	5926
12	13	811	557	378	155	72	96	55	77	238	555	691	773	4458
13	14	614	470	277	129	38	41	92	46	165	451	565	633	3521
14	15	371	337	178	40	17	30	34	24	138	304	332	414	2219
15	16	160	182	60	13	1	9	21	8	77	164	191	234	1120
16	17	189	164	79	8	0	3	9	4	77	151	160	125	969
17	18	87	76	36	1	0	0	3	1	32	62	66	48	412
18	19	5	60	17	0	0	0	5	0	3	9	36	16	151
19	20	1	20	0	0	0	0	2	0	0	4	27	4	58
20	21	1	0	0	0	0	0	0	0	0	0	1	0	2
21	22	0	0	0	0	0	0	0	0	0	0	0	0	0
<b>total</b>		11263	10122	10963	10893	11307	10653	11091	11401	11302	12105	11272	11339	133711

Copyright ARGOSS, August 2011





Description	L [m]	L_cumm [m]	h [mODN]	Volume [m3/m1]	Total volume soil [m3]	Total volume rubble [m3]	Total volume [m3]	Costs [10*6 £]
<b>Land connection western shoreline</b>								
Embankment dam (new)	10,000	-	3.00	270	2,700,000		2,700,000	40.50
Embankment dam (addapted)	8,200	-	6.80	180	1,476,000		1,476,000	22.14
<b>Friskney Flats</b>								
Embankment dam	350	350	3.70	443	155,050		155,050	4.65
Embankment dam	4,113	4,463	0.00	854	3,512,502		3,512,502	105.38
Embankment dam	26	4,489	-3.90	1418	36,868		36,868	1.11
Embankment dam	11	4,500	-5.00	1795	19,745		19,745	0.59
<b>Boston Deepes</b>								
Embankment dam	50	4,550	-6.10	1519	71,378	4,590	75,968	4.64
Embankment dam	61	4,611	-9.40	2119	123,775	5,490	129,265	8.61
Embankment dam	28	4,639	-15.20	3488	88,785	8,882	97,667	5.32
Sluices tidal power plant	583	5,222	-15.20	-		655,525	655,525	110.05
Sluices tidal power plant	71	5,293	-8.90	-		49,842	49,842	11.45
Sluices tidal power plant	222	5,515	-7.70	-		155,844	155,844	35.81
Sluices tidal power plant	166	5,681	-8.90	-		116,532	116,532	26.78
Sluices tidal power plant	463	6,144	-14.10	-		448,022	448,022	82.68
Sluices tidal power plant	96	6,240	-10.90	-		55,723	55,723	14.73
Embankment dam	50	6,290	-10.90	2491	118,512	6,056	124,568	6.15
Embankment dam	20	6,310	-6.50	1592	31,254	593	31,847	1.86
<b>Long Sand</b>								
Embankment dam	20	6,330	-5.00	1868	37,360		37,360	1.12
Embankment dam	69	6,399	-3.90	1418	97,842		97,842	2.94
Embankment dam	1,463	7,862	0.00	854	1,249,402		1,249,402	37.48
Embankment dam	333	8,195	-3.70	1385	461,205		461,205	13.84
Embankment dam	204	8,399	-6.15	1804	368,016		368,016	11.04
Embankment dam	136	8,535	-10.50	2678	364,208		364,208	10.93
<b>Lynn Deepes</b>								
Embankment dam	197	8,732	-10.50	2301	435,488	17,730	453,218	30.51
Embankment dam	153	8,885	-14.10	3150	475,073	6,816	481,889	27.35
Commercial lock complex	35	8,920	-14.10	-		31,938	31,938	41.58
Embankment dam	368	9,288	-14.10	3113	1,112,317	33,120	1,145,437	76.36
Embankment dam	203	9,491	-18.90	4424	854,843	43,148	897,991	50.98
Embankment dam	809	10,300	-25.00	6383	4,475,873	687,650	5,163,523	268.75
Turbines tidal power plant	877	11,177	-25.00	-		670,905	670,905	900.31
Turbines tidal power plant	222	11,399	-21.40	-		57,942	57,942	220.63
Turbines tidal power plant	630	12,029	-24.50	-		432,968	432,968	643.56
Turbines tidal power plant	211	12,240	-21.40	-		55,071	55,071	209.70
Embankment dam	630	12,870	-21.40	5187	2,997,414	270,144	3,267,558	177.39
Sluices tidal power plant	196	13,066	-21.40	-		437,903	437,903	51.14
Sluices tidal power plant	685	13,751	-17.10	-		975,200	975,200	142.63
Sluices tidal power plant	1,119	14,870	-16.70	-		1,519,210	1,519,210	228.19
Embankment dam	492	15,362	-16.70	3890	1,688,126	225,803	1,913,929	101.90
Embankment dam	138	15,500	-11.30	2535	342,399	7,445	349,844	21.02
Recreational lock complex	26	15,526	-11.30	-		11,868	11,868	17.67
Embankment dam	96	15,622	-11.30	2535	238,191	5,179	243,370	14.62
Embankment dam	113	15,735	-7.00	1640	175,161	10,170	185,331	14.32
<b>Stubborn Sands</b>								
Embankment dam	1,276	17,011	-7.00	1962	2,503,512		2,503,512	75.11
Embankment dam	741	17,752	-4.60	1533	1,135,953		1,135,953	34.08
Embankment dam	3,834	21,586	0.00	854	3,274,236		3,274,236	98.23
<b>Land connection eastern shoreline</b>								
Embankment dam (addapted)	2,000	-	4.50	165	330,000		330,000	5.42
<b>Total</b>	<b>41,786</b>						<b>37,957,796</b>	<b>4011</b>

Description	L [m]	L_cumm [m]	h [mODN]	Sill level [m]	Crest width sill [m]	Sill height [mODN]	Volume/m1 [m3/m1]	Total volume sill [m3]	Height rubble [m]	Width rubble [m]	Volume/m1 [m3/m1]	Total volume rubble [m3]	Total Volume [m3]	Costs [10 <sup>6</sup> £]
<b>Land connection western shoreline</b>														
Embankment dam (new)	10,000	-	3.00				270						2,700,000	40.50
Embankment dam (addapted)	8,200	-	6.80				180						1,476,000	22.14
<b>Friskney Flats</b>														
Embankment dam	350	350	3.70				443						155,050	4.65
Embankment dam	4,113	4,463	0.00				854						3,512,502	105.38
Embankment dam	26	4,489	-3.90				1418						36,868	1.11
Embankment dam	11	4,500	-5.00				1795						19,745	0.59
<b>Boston Deepes</b>														
Abutment caisson	50	4,550	-6.10	-7.00	35.00	2.00	90	4,500	0.00	0.00	0	0	4,500	2.49
Small sluiced caisson & abutment caisson	61	4,611	-9.40	-9.90	35.00	2.00	90	5,490	2.00	10.00	80	4,880	10,370	4.63
Small sluiced caisson	28	4,639	-15.20	-10.00	35.00	5.20	317	8,882	2.00	10.00	80	2,240	11,122	2.80
Sluices tidal power plant	583	5,222	-15.20	-10.00	96.00	5.20	634	369,855	7.00	0.00	490	285,670	655,525	110.05
Sluices tidal power plant	71	5,293	-8.90	-10.00	96.00	2.00	212	15,052	7.00	0.00	490	34,790	49,842	11.45
Sluices tidal power plant	222	5,515	-7.70	-10.00	96.00	2.00	212	47,064	7.00	0.00	490	108,780	155,844	35.81
Sluices tidal power plant	166	5,681	-8.90	-10.00	96.00	2.00	212	35,192	7.00	0.00	490	81,340	116,532	26.78
Sluices tidal power plant	463	6,144	-14.10	-10.00	96.00	4.10	478	221,152	7.00	0.00	490	226,870	448,022	82.68
Sluices tidal power plant	96	6,240	-10.90	-10.00	96.00	0.90	90	6,683	7.00	0.00	490	47,040	55,723	14.73
Abutment caisson	50	6,290	-10.90	-8.40	35.00	2.50	119	5,938	0.00	0.00	0	0	5,938	2.58
Abutment caisson	20	6,310	-6.50	-5.70	35.00	0.80	31	624	0.00	0.00	0	0	624	0.92
<b>Long Sand</b>														
Embankment dam	20	6,330	-5.00				1868						37,360	1.12
Embankment dam	69	6,399	-3.90				1418						97,842	2.94
Embankment dam	1,463	7,862	0.00				854						1,249,402	37.48
Embankment dam	333	8,195	-3.70				1385						461,205	13.84
Embankment dam	204	8,399	-6.15				1804						368,016	11.04
Embankment dam	136	8,535	-10.00				2678						364,208	10.93
<b>Lynn Deepes</b>														
Medium sluiced caisson	197	8,732	-10.50	-13.00	35.00	2.00	90	17,730	2.00	10.00	80	15,760	33,490	18.47
Medium sluiced caisson	153	8,885	-14.10	-13.00	35.00	1.10	45	6,816	2.00	10.00	80	12,240	19,056	13.89
Commercial lock complex	35	8,920	-14.10	-15.00	300.00	2.00	620	21,700	4.50	10.00	293	10,238	31,938	41.58
Large sluiced caisson	368	9,288	-14.10	-15.00	35.00	2.00	90	33,120	2.00	10.00	80	29,440	62,560	44.90
Large sluiced caisson	203	9,491	-18.90	-15.00	35.00	3.90	213	43,148	2.00	10.00	80	16,240	59,388	26.39
Large sluiced caisson	809	10,300	-25.00	-15.00	35.00	10.00	850	687,650	2.00	10.00	80	64,720	752,370	138.68
Turbines tidal power plant	877	11,177	-25.00	-20.00	108.00	5.00	665	583,205	2.00	15.00	100	87,700	670,905	900.31
Turbines tidal power plant	222	11,399	-21.40	-20.00	108.00	1.40	161	35,742	2.00	15.00	100	22,200	57,942	220.63
Turbines tidal power plant	630	12,029	-24.50	-20.00	108.00	4.50	587	369,968	2.00	15.00	100	63,000	432,968	643.56
Turbines tidal power plant	211	12,240	-21.40	-20.00	108.00	1.40	161	33,971	2.00	15.00	100	21,100	55,071	209.70
Large sluiced caisson	630	12,870	-21.40	-15.00	35.00	6.40	429	270,144	2.00	10.00	80	50,400	320,544	90.75
Sluices tidal power plant	196	13,066	-21.40	-10.00	96.00	11.40	1744	341,863	7.00	0.00	490	96,040	437,903	51.14
Sluices tidal power plant	685	13,751	-17.10	-10.00	96.00	7.10	934	639,550	7.00	0.00	490	335,650	975,200	142.63
Sluices tidal power plant	1,119	14,870	-16.70	-10.00	96.00	6.70	868	970,900	7.00	0.00	490	548,310	1,519,210	228.19
Small sluiced caisson	492	15,362	-16.70	-10.00	35.00	6.70	459	225,803	2.00	10.00	80	39,360	265,163	53.81
Small sluiced caisson	138	15,500	-11.30	-10.00	35.00	1.30	54	7,445	2.00	10.00	80	11,040	18,485	11.46
Recreational lock complex	26	15,526	-11.30	-10.00	160.00	1.30	216	5,628	4.00	10.00	240	6,240	11,868	17.67
Small sluiced caisson	96	15,622	-11.30	-10.00	35.00	1.30	54	5,179	2.00	10.00	80	7,680	12,859	7.97
Small sluiced caisson	113	15,735	-7.00	-10.00	35.00	2.00	90	10,170	2.00	10.00	80	9,040	19,210	9.65
<b>Stubborn Sands</b>														
Embankment dam	1,276	17,011	-7.00				1962						2,503,512	75.11
Embankment dam	741	17,752	-4.60				1533						1,135,953	34.08
Embankment dam	3,834	21,586	0.00				854						3,274,236	98.23
<b>Land connection eastern shoreline</b>														
Embankment dam (addapted)	2,000	-	4.50				165						330,000	5.42

Total 41,786

24,992,070 3,631

Description	L [m]	L_cumm [m]	h [mODN]	Sill level [m]	Crest width sill [m]	Sill height [mODN]	Volume/m1 [m3/m1]	Total volume sill [m3]	Height rubble [m]	Width rubble [m]	Volume/m1 [m3/m1]	Total volume rubble [m3]	Total Volume [m3]	Costs [10^6 £]
<b>Land connection western shoreline</b>														
Embankment dam (new)	10,000	-	3.00				270						2,700,000	40.50
Embankment dam (addapted)	8,200	-	6.80				180						1,476,000	22.14
<b>Friskney Flats</b>														
Embankment dam	350	350	3.70				443						155,050	4.65
Embankment dam	4,113	4,463	0.00				854						3,512,502	105.38
Embankment dam	26	4,489	-3.90				1418						36,868	1.11
Embankment dam	11	4,500	-5.00				1795						19,745	0.59
<b>Boston Deepes</b>														
Abutment caisson	50	4,550	-6.10	-7.00	35.00	2.00	90	4,500	0.00	0.00	0	0	4,500	2.49
Small sluiced caisson & abutment caisson	61	4,611	-9.40	-9.90	35.00	2.00	90	5,490	2.00	10.00	80	4,880	10,370	4.63
Small sluiced caisson	28	4,639	-15.20	-10.00	35.00	5.20	317	8,882	2.00	10.00	80	2,240	11,122	2.80
Sluices tidal power plant	583	5,222	-15.20	-10.00	96.00	5.20	634	369,855	7.00	0.00	490	285,670	655,525	110.05
Sluices tidal power plant	71	5,293	-8.90	-10.00	96.00	2.00	212	15,052	7.00	0.00	490	34,790	49,842	11.45
Sluices tidal power plant	222	5,515	-7.70	-10.00	96.00	2.00	212	47,064	7.00	0.00	490	108,780	155,844	35.81
Sluices tidal power plant	166	5,681	-8.90	-10.00	96.00	2.00	212	35,192	7.00	0.00	490	81,340	116,532	26.78
Sluices tidal power plant	463	6,144	-14.10	-10.00	96.00	4.10	478	221,152	7.00	0.00	490	226,870	448,022	82.68
Sluices tidal power plant	96	6,240	-10.90	-10.00	96.00	0.90	90	8,683	7.00	0.00	490	47,040	55,723	14.73
Abutment caisson	50	6,290	-10.90	-8.40	35.00	2.50	119	5,938	0.00	0.00	0	0	5,938	2.58
Abutment caisson	20	6,310	-6.50	-5.70	35.00	0.80	31	624	0.00	0.00	0	0	624	0.92
<b>Long Sand</b>														
Embankment dam	20	6,330	-5.00				1868						37,360	1.12
Embankment dam	69	6,399	-3.90				1418						97,842	2.94
Embankment dam	1,463	7,862	0.00				854						1,249,402	37.48
Embankment dam	333	8,195	-3.70				1385						461,205	13.84
Embankment dam	204	8,399	-6.15				1804						368,016	11.04
Embankment dam	136	8,535	-10.00				2678						364,208	10.93
<b>Lynn Deepes</b>														
Medium sluiced caisson	197	8,732	-10.50	-13.00	35.00	2.00	90	17,730	2.00	10.00	80	15,760	33,490	18.47
Medium sluiced caisson	83	8,815	-14.10	-13.00	35.00	1.10	45	3,698	2.00	10.00	80	6,640	10,338	7.54
Commercial lock complex	35	8,850	-14.10	-15.00	300.00	2.00	620	21,700	4.50	10.00	293	10,238	31,938	41.58
Large sluiced caisson	70	8,920	-14.10	-15.00	35.00	2.00	90	6,300	2.00	10.00	80	5,600	11,900	8.54
Sluices tidal power plant	368	9,288	-14.10	-15.00	96.00	2.00	212	78,016	7.00	0.00	490	180,320	258,336	59.36
Sluices tidal power plant	203	9,491	-18.90	-15.00	96.00	3.90	450	91,441	7.00	0.00	490	99,470	190,911	35.89
Sluices tidal power plant	709	10,200	-25.00	-15.00	96.00	10.00	1460	1,035,140	7.00	0.00	490	347,410	1,382,550	171.88
Large sluiced caisson	100	10,300	-25.00	-15.00	35.00	10.00	850	85,000	2.00	10.00	80	8,000	93,000	17.14
Turbines tidal power plant	877	11,177	-25.00	-20.00	108.00	5.00	665	583,205	2.00	15.00	100	87,700	670,905	900.31
Turbines tidal power plant	222	11,399	-21.40	-20.00	108.00	1.40	161	35,742	2.00	15.00	100	22,200	57,942	220.63
Turbines tidal power plant	630	12,029	-24.50	-20.00	108.00	4.50	587	369,968	2.00	15.00	100	63,000	432,968	643.56
Turbines tidal power plant	211	12,240	-21.40	-20.00	108.00	1.40	161	33,971	2.00	15.00	100	21,100	55,071	209.70
Large sluiced caisson	70	12,310	-21.40	-15.00	35.00	6.40	429	30,016	2.00	10.00	80	5,600	35,616	10.08
Sluices tidal power plant	560	12,870	-21.40	-10.00	96.00	11.40	1744	976,752	7.00	0.00	490	274,400	1,251,152	146.10
Sluices tidal power plant	196	13,066	-21.40	-10.00	96.00	11.40	1744	341,863	7.00	0.00	490	96,040	437,903	51.14
Sluices tidal power plant	685	13,751	-17.10	-10.00	96.00	7.10	934	639,550	7.00	0.00	490	335,650	975,200	142.63
Sluices tidal power plant	1,119	14,870	-16.70	-10.00	96.00	6.70	868	970,900	7.00	0.00	490	548,310	1,519,210	228.19
Sluices tidal power plant	492	15,362	-16.70	-10.00	96.00	6.70	868	426,884	7.00	0.00	490	241,080	667,964	100.33
Sluices tidal power plant	67	15,429	-11.30	-10.00	96.00	1.30	133	8,928	7.00	0.00	490	32,830	41,758	10.46
Small sluiced caisson	140	15,569	-11.30	-10.00	35.00	1.30	54	7,553	2.00	10.00	80	11,200	18,753	11.63
Recreational lock complex	26	15,595	-11.30	-10.00	160.00	1.30	216	5,628	4.00	10.00	240	6,240	11,868	17.67
Small sluiced caisson	27	15,622	-11.30	-10.00	35.00	1.30	54	1,457	2.00	10.00	80	2,160	3,617	2.24
Small sluiced caisson	113	15,735	-7.00	-10.00	35.00	2.00	90	10,170	2.00	10.00	80	9,040	19,210	9.65
<b>Stubborn Sands</b>														
Embankment dam	1,276	17,011	-7.00				1962						2,503,512	75.11
Embankment dam	741	17,752	-4.60				1533						1,135,953	34.08
Embankment dam	3,834	21,586	0.00				854						3,274,236	98.23
<b>Land connection eastern shoreline</b>														
Embankment dam (addapted)	2,000	-	4.50				165						330,000	5.42
<b>Total</b>	<b>41,786</b>												<b>27,447,539</b>	<b>3,824</b>

## Credit estimate Wash barrier and Tidal Power Plant

### Direct costs

Estimated construction costs £ 3,824,000,000.00

**Subtotal direct costs** £ 3,824,000,000

To be detailed 10% £ 3,824,000,000.00 £ 382,400,000.00

**Total direct costs** £ 4,206,400,000

### Indirect costs

General construction site costs 13% £ 4,206,400,000.00 £ 546,832,000.00

**Subtotal indirect costs** 546,832,000

**Subtotal including direct costs** £ 4,753,232,000

General costs 7% £ 4,753,232,000.00 £ 332,726,240.00

Profit and risk 4% £ 5,085,958,240.00 £ 203,438,329.60

**Subtotal indirect costs** £ 1,082,996,570

To be detailed 10% £ 1,082,996,569.60 £ 108,299,656.96

**Total indirect costs** 0.28 £ 1,191,296,227

**Total direct and indirect costs** £ 5,397,696,227

Contingency 10% £ 5,397,696,226.56 £ 539,769,622.66

**Total construction costs** £ 5,937,465,849

### Engineering costs

Engineering, administration & survey costs 20% £ 5,937,465,849.22 £ 11,874,931.70

Contingency 5% £ 11,874,931.70 £ 2,374,986.34

**Total engineering costs** £ 14,249,918

**Total credit estimate** 5,951,715,767

### Project contingency

Political influences *Prob.* 50% £ 1,000,000,000 £ *Prob.\* Cons.* 500,000,000.00

Scope changes 5% £ 1,000,000,000 £ 50,000,000.00

Mitigation measures 75% £ 500,000,000 £ 375,000,000.00

**Total project contingency** £ 925,000,000

**Total investment costs** 6,876,715,767

V.A.T. 20% 1,375,343,153

**Total investment costs incl. V.A.T.** 8,252,058,921

Year	Civil work	PV_Civil work	Electromechanical	PV_Electromechanical	Year	Civil work	PV_Civil work	Electromechanical	PV_Electromechanical	Year	Civil work	PV_Civil work	Electromechanical	PV_Electromechanical	Summary: NPV_Investment :	6704	10^6 £
1	756.44	756.44	618.90	618.90	41	23.14	2.25	0.00	0.00	81	23.14	0.22	0.00	0.00			
2	756.44	713.62	618.90	583.87	42	23.14	2.12	0.00	0.00	82	23.14	0.21	0.00	0.00			
3	756.44	673.23	618.90	550.82	43	23.14	2.00	0.00	0.00	83	23.14	0.19	0.00	0.00			
4	756.44	635.12	618.90	519.64	44	23.14	1.89	0.00	0.00	84	23.14	0.18	0.00	0.00			
5	756.44	599.17	618.90	490.23	45	23.14	1.78	280.15	21.57	85	23.14	0.17	0.00	0.00			
6	23.14	17.29	0.00	0.00	46	23.14	1.68	0.00	0.00	86	23.14	0.16	0.00	0.00			
7	23.14	16.31	0.00	0.00	47	23.14	1.59	0.00	0.00	87	23.14	0.15	0.00	0.00			
8	23.14	15.39	0.00	0.00	48	23.14	1.50	0.00	0.00	88	23.14	0.15	0.00	0.00			
9	23.14	14.52	0.00	0.00	49	23.14	1.41	0.00	0.00	89	23.14	0.14	0.00	0.00			
10	23.14	13.69	0.00	0.00	50	23.14	1.33	113.57	6.54	90	23.14	0.13	3.79	0.02			
11	23.14	12.92	0.00	0.00	51	23.14	1.26	0.00	0.00	91	23.14	0.12	0.00	0.00			
12	23.14	12.19	0.00	0.00	52	23.14	1.18	0.00	0.00	92	23.14	0.12	0.00	0.00			
13	23.14	11.50	0.00	0.00	53	23.14	1.12	0.00	0.00	93	23.14	0.11	0.00	0.00			
14	23.14	10.85	0.00	0.00	54	23.14	1.05	0.00	0.00	94	23.14	0.10	0.00	0.00			
15	23.14	10.23	0.00	0.00	55	23.14	0.99	0.00	0.00	95	23.14	0.10	70.04	0.29			
16	23.14	9.65	0.00	0.00	56	23.14	0.94	0.00	0.00	96	23.14	0.09	0.00	0.00			
17	23.14	9.11	0.00	0.00	57	23.14	0.89	0.00	0.00	97	23.14	0.09	0.00	0.00			
18	23.14	8.59	0.00	0.00	58	23.14	0.84	260.27	9.40	98	23.14	0.08	0.00	0.00			
19	23.14	8.11	0.00	0.00	59	23.14	0.79	0.00	0.00	99	23.14	0.08	0.00	0.00			
20	92.54	30.59	260.27	86.02	60	161.95	5.20	0.00	0.00	100	161.95	0.51	343.56	1.07			
21	23.14	7.21	0.00	0.00	61	23.14	0.70	0.00	0.00	101	23.14	0.07	0.00	0.00			
22	23.14	6.81	0.00	0.00	62	23.14	0.66	0.00	0.00	102	23.14	0.06	0.00	0.00			
23	23.14	6.42	0.00	0.00	63	23.14	0.62	0.00	0.00	103	23.14	0.06	0.00	0.00			
24	23.14	6.06	0.00	0.00	64	23.14	0.59	0.00	0.00	104	23.14	0.06	0.00	0.00			
25	23.14	5.71	77.61	19.17	65	23.14	0.56	0.00	0.00	105	23.14	0.05	0.00	0.00			
26	23.14	5.39	0.00	0.00	66	23.14	0.52	0.00	0.00	106	23.14	0.05	0.00	0.00			
27	23.14	5.09	0.00	0.00	67	23.14	0.49	0.00	0.00	107	23.14	0.05	0.00	0.00			
28	23.14	4.80	0.00	0.00	68	23.14	0.47	0.00	0.00	108	23.14	0.05	0.00	0.00			
29	23.14	4.53	0.00	0.00	69	23.14	0.44	0.00	0.00	109	23.14	0.04	0.00	0.00			
30	23.14	4.27	0.00	0.00	70	23.14	0.42	525.27	9.43	110	23.14	0.04	0.00	0.00			
31	23.14	4.03	0.00	0.00	71	23.14	0.39	0.00	0.00	111	23.14	0.04	0.00	0.00			
32	23.14	3.80	0.00	0.00	72	23.14	0.37	0.00	0.00	112	23.14	0.04	0.00	0.00			
33	23.14	3.58	0.00	0.00	73	23.14	0.35	0.00	0.00	113	23.14	0.03	0.00	0.00			
34	23.14	3.38	0.00	0.00	74	23.14	0.33	0.00	0.00	114	23.14	0.03	0.00	0.00			
35	23.14	3.19	0.00	0.00	75	23.14	0.31	56.79	0.76	115	23.14	0.03	280.15	0.37			
36	23.14	3.01	0.00	0.00	76	23.14	0.29	0.00	0.00	116	23.14	0.03	0.00	0.00			
37	23.14	2.84	0.00	0.00	77	23.14	0.28	0.00	0.00	117	23.14	0.03	0.00	0.00			
38	23.14	2.68	0.00	0.00	78	23.14	0.26	0.00	0.00	118	23.14	0.03	0.00	0.00			
39	23.14	2.53	0.00	0.00	79	23.14	0.25	0.00	0.00	119	23.14	0.02	0.00	0.00			
40	161.95	16.69	524.33	54.03	80	161.95	1.62	520.54	5.22	120	161.95	0.16	558.40	0.54			
	<b>4800.14</b>	<b>3680.51</b>	<b>3956.73</b>	<b>2922.70</b>		<b>1203.03</b>	<b>41.72</b>	<b>1756.59</b>	<b>52.91</b>		<b>1203.03</b>	<b>4.06</b>	<b>1255.93</b>	<b>2.30</b>			

Year	PV_8p/kWh	PV_9p/kWh	PV_10p/kWh	PV_11p/kWh	Year	PV_8p/kWh	PV_9p/kWh	PV_10p/kWh	PV_11p/kWh	Year	PV_8p/kWh	PV_9p/kWh	PV_10p/kWh	PV_11p/kWh
1	0.0000	0.0000	0.0000	0.0000	41	22.2184	24.9957	27.7730	30.5503	81	2.1601	2.4301	2.7001	2.9702
2	0.0000	0.0000	0.0000	0.0000	42	20.9607	23.5808	26.2009	28.8210	82	2.0378	2.2926	2.5473	2.8020
3	0.0000	0.0000	0.0000	0.0000	43	19.7743	22.2461	24.7178	27.1896	83	1.9225	2.1628	2.4031	2.6434
4	0.0000	0.0000	0.0000	0.0000	44	18.6550	20.9869	23.3187	25.6506	84	1.8137	2.0404	2.2671	2.4938
5	0.0000	0.0000	0.0000	0.0000	45	17.5990	19.7989	21.9988	24.1987	85	1.7110	1.9249	2.1388	2.3526
6	170.7724	192.1190	213.4655	234.8121	46	16.6029	18.6782	20.7536	22.8289	86	1.6142	1.8159	2.0177	2.2195
7	161.1060	181.2443	201.3826	221.5208	47	15.6631	17.6210	19.5789	21.5367	87	1.5228	1.7131	1.9035	2.0938
8	151.9868	170.9852	189.9835	208.9819	48	14.7765	16.6236	18.4706	20.3177	88	1.4366	1.6162	1.7958	1.9753
9	143.3838	161.3068	179.2298	197.1527	49	13.9401	15.6826	17.4251	19.1676	89	1.3553	1.5247	1.6941	1.8635
10	135.2677	152.1762	169.0847	185.9931	50	13.1510	14.7949	16.4388	18.0827	90	1.2786	1.4384	1.5982	1.7580
11	127.6111	143.5625	159.5138	175.4652	51	12.4066	13.9575	15.5083	17.0591	91	1.2062	1.3570	1.5077	1.6585
12	120.3878	135.4363	150.4848	165.5332	52	11.7044	13.1674	14.6305	16.0935	92	1.1379	1.2802	1.4224	1.5646
13	113.5734	127.7701	141.9668	156.1634	53	11.0419	12.4221	13.8023	15.1826	93	1.0735	1.2077	1.3419	1.4761
14	107.1447	120.5378	133.9309	147.3240	54	10.4168	11.7189	13.0211	14.3232	94	1.0127	1.1393	1.2659	1.3925
15	101.0799	113.7149	126.3499	138.9849	55	9.8272	11.0556	12.2840	13.5124	95	0.9554	1.0749	1.1943	1.3137
16	95.3584	107.2782	119.1980	131.1178	56	9.2710	10.4298	11.5887	12.7476	96	0.9013	1.0140	1.1267	1.2393
17	89.9608	101.2059	112.4510	123.6961	57	8.7462	9.8395	10.9327	12.0260	97	0.8503	0.9566	1.0629	1.1692
18	84.8687	95.4772	106.0858	116.6944	58	8.2511	9.2825	10.3139	11.3453	98	0.8022	0.9025	1.0027	1.1030
19	80.0648	90.0729	100.0810	110.0891	59	7.7841	8.7571	9.7301	10.7031	99	0.7568	0.8514	0.9460	1.0406
20	75.5328	84.9744	94.4160	103.8576	60	7.3435	8.2614	9.1793	10.0973	100	0.7139	0.8032	0.8924	0.9817
21	71.2574	80.1645	89.0717	97.9789	61	6.9278	7.7938	8.6597	9.5257	101	0.6735	0.7577	0.8419	0.9261
22	67.2239	75.6269	84.0299	92.4329	62	6.5357	7.3526	8.1696	8.9865	102	0.6354	0.7148	0.7943	0.8737
23	63.4188	71.3461	79.2735	87.2008	63	6.1657	6.9364	7.7071	8.4779	103	0.5994	0.6744	0.7493	0.8242
24	59.8291	67.3077	74.7863	82.2649	64	5.8167	6.5438	7.2709	7.9980	104	0.5655	0.6362	0.7069	0.7776
25	56.4425	63.4978	70.5531	77.6084	65	5.4875	6.1734	6.8593	7.5453	105	0.5335	0.6002	0.6669	0.7336
26	53.2476	59.9036	66.5596	73.2155	66	5.1769	5.8240	6.4711	7.1182	106	0.5033	0.5662	0.6291	0.6920
27	50.2336	56.5128	62.7920	69.0712	67	4.8838	5.4943	6.1048	6.7153	107	0.4748	0.5342	0.5935	0.6529
28	47.3902	53.3140	59.2378	65.1615	68	4.6074	5.1833	5.7592	6.3351	108	0.4479	0.5039	0.5599	0.6159
29	44.7077	50.2962	55.8847	61.4732	69	4.3466	4.8899	5.4332	5.9766	109	0.4226	0.4754	0.5282	0.5811
30	42.1771	47.4493	52.7214	57.9935	70	4.1006	4.6131	5.1257	5.6383	110	0.3987	0.4485	0.4983	0.5482
31	39.7897	44.7635	49.7372	54.7109	71	3.8684	4.3520	4.8356	5.3191	111	0.3761	0.4231	0.4701	0.5171
32	37.5375	42.2297	46.9219	51.6140	72	3.6495	4.1057	4.5618	5.0180	112	0.3548	0.3992	0.4435	0.4879
33	35.4127	39.8393	44.2659	48.6925	73	3.4429	3.8733	4.3036	4.7340	113	0.3347	0.3766	0.4184	0.4602
34	33.4082	37.5843	41.7603	45.9363	74	3.2480	3.6540	4.0600	4.4660	114	0.3158	0.3553	0.3947	0.4342
35	31.5172	35.4568	39.3965	43.3361	75	3.0642	3.4472	3.8302	4.2132	115	0.2979	0.3351	0.3724	0.4096
36	29.7332	33.4499	37.1665	40.8832	76	2.8907	3.2521	3.6134	3.9748	116	0.2810	0.3162	0.3513	0.3864
37	28.0502	31.5565	35.0627	38.5690	77	2.7271	3.0680	3.4089	3.7498	117	0.2651	0.2983	0.3314	0.3646
38	26.4624	29.7703	33.0781	36.3859	78	2.5727	2.8943	3.2159	3.5375	118	0.2501	0.2814	0.3127	0.3439
39	24.9646	28.0851	31.2057	34.3263	79	2.4271	2.7305	3.0339	3.3373	119	0.2360	0.2655	0.2950	0.3245
40	23.5515	26.4954	29.4394	32.3833	80	2.2897	2.5759	2.8622	3.1484	120	0.2226	0.2504	0.2783	0.3061
	<b>2624.4544</b>	<b>2952.5112</b>	<b>3280.5680</b>	<b>3608.6248</b>		<b>354.3626</b>	<b>398.6579</b>	<b>442.9533</b>	<b>487.2486</b>		<b>34.4519</b>	<b>38.7584</b>	<b>43.0649</b>	<b>47.3714</b>

Summary: NPV\_8p/kWh : 3013 10^6 £  
NPV\_9p/kWh : 3390 10^6 £  
NPV\_10p/kWh : 3767 10^6 £  
NPV\_11p/kWh : 4143 10^6 £  
BEP (NPV=0) : 14.37 p/kWh

Year	PV_present day	PV_1:500	PV_ΔD	Year	PV_present day	PV_1:500	PV_ΔD	Year	PV_present day	PV_1:500	PV_ΔD
1	0.0000	0.0000	0.0000	41	13.3561	3.8197	9.5365	81	1.2985	0.3714	0.9272
2	0.0000	0.0000	0.0000	42	12.6001	3.6035	8.9967	82	1.2250	0.3503	0.8747
3	0.0000	0.0000	0.0000	43	11.8869	3.3995	8.4874	83	1.1557	0.3305	0.8252
4	0.0000	0.0000	0.0000	44	11.2141	3.2071	8.0070	84	1.0903	0.3118	0.7785
5	0.0000	0.0000	0.0000	45	10.5793	3.0255	7.5538	85	1.0285	0.2941	0.7344
6	102.6565	29.3583	73.2982	46	9.9805	2.8543	7.1262	86	0.9703	0.2775	0.6928
7	96.8457	27.6965	69.1492	47	9.4156	2.6927	6.7228	87	0.9154	0.2618	0.6536
8	91.3639	26.1288	65.2351	48	8.8826	2.5403	6.3423	88	0.8636	0.2470	0.6166
9	86.1923	24.6498	61.5426	49	8.3798	2.3965	5.9833	89	0.8147	0.2330	0.5817
10	81.3135	23.2545	58.0590	50	7.9055	2.2609	5.6446	90	0.7686	0.2198	0.5488
11	76.7109	21.9382	54.7727	51	7.4580	2.1329	5.3251	91	0.7251	0.2074	0.5177
12	72.3688	20.6964	51.6723	52	7.0358	2.0122	5.0237	92	0.6840	0.1956	0.4884
13	68.2724	19.5249	48.7475	53	6.6376	1.8983	4.7393	93	0.6453	0.1846	0.4608
14	64.4079	18.4197	45.9882	54	6.2619	1.7908	4.4711	94	0.6088	0.1741	0.4347
15	60.7622	17.3771	43.3851	55	5.9074	1.6894	4.2180	95	0.5743	0.1643	0.4101
16	57.3228	16.3935	40.9293	56	5.5731	1.5938	3.9792	96	0.5418	0.1550	0.3869
17	54.0781	15.4656	38.6126	57	5.2576	1.5036	3.7540	97	0.5112	0.1462	0.3650
18	51.0171	14.5902	36.4270	58	4.9600	1.4185	3.5415	98	0.4822	0.1379	0.3443
19	48.1294	13.7643	34.3650	59	4.6792	1.3382	3.3410	99	0.4549	0.1301	0.3248
20	45.4051	12.9852	32.4199	60	4.4144	1.2624	3.1519	100	0.4292	0.1227	0.3064
21	42.8350	12.2502	30.5848	61	4.1645	1.1910	2.9735	101	0.4049	0.1158	0.2891
22	40.4103	11.5568	28.8536	62	3.9288	1.1236	2.8052	102	0.3820	0.1092	0.2727
23	38.1230	10.9026	27.2203	63	3.7064	1.0600	2.6464	103	0.3603	0.1031	0.2573
24	35.9651	10.2855	25.6796	64	3.4966	1.0000	2.4966	104	0.3399	0.0972	0.2427
25	33.9293	9.7033	24.2260	65	3.2987	0.9434	2.3553	105	0.3207	0.0917	0.2290
26	32.0088	9.1541	22.8547	66	3.1120	0.8900	2.2220	106	0.3026	0.0865	0.2160
27	30.1970	8.6359	21.5611	67	2.9358	0.8396	2.0962	107	0.2854	0.0816	0.2038
28	28.4877	8.1471	20.3406	68	2.7696	0.7921	1.9776	108	0.2693	0.0770	0.1923
29	26.8752	7.6859	19.1893	69	2.6129	0.7472	1.8656	109	0.2540	0.0726	0.1814
30	25.3539	7.2509	18.1031	70	2.4650	0.7049	1.7600	110	0.2396	0.0685	0.1711
31	23.9188	6.8404	17.0784	71	2.3254	0.6650	1.6604	111	0.2261	0.0647	0.1614
32	22.5649	6.4532	16.1117	72	2.1938	0.6274	1.5664	112	0.2133	0.0610	0.1523
33	21.2877	6.0880	15.1997	73	2.0696	0.5919	1.4777	113	0.2012	0.0575	0.1437
34	20.0827	5.7434	14.3393	74	1.9525	0.5584	1.3941	114	0.1898	0.0543	0.1355
35	18.9459	5.4183	13.5277	75	1.8420	0.5268	1.3152	115	0.1791	0.0512	0.1279
36	17.8735	5.1116	12.7620	76	1.7377	0.4970	1.2407	116	0.1689	0.0483	0.1206
37	16.8618	4.8222	12.0396	77	1.6393	0.4688	1.1705	117	0.1594	0.0456	0.1138
38	15.9074	4.5493	11.3581	78	1.5466	0.4423	1.1043	118	0.1504	0.0430	0.1074
39	15.0070	4.2918	10.7152	79	1.4590	0.4173	1.0418	119	0.1418	0.0406	0.1013
40	14.1575	4.0488	10.1087	80	1.3764	0.3936	0.9828	120	0.1338	0.0383	0.0955
	<b>1577.6390</b>	<b>451.1822</b>	<b>1126.4568</b>		<b>213.0181</b>	<b>60.9201</b>	<b>152.0980</b>		<b>20.7101</b>	<b>5.9228</b>	<b>14.7873</b>

Summary: NPV\_present day : 1811.37 10^6 £  
NPV\_1:500 : 518.03 10^6 £  
NPV\_ΔD : 1293.34 10^6 £